

Aus dem Institut für Physiologie und Pathophysiologie
des Fachbereichs Medizin der Philipps-Universität Marburg
Geschäftsführender Direktor: Prof. Dr. med. Dr. phil. J. Daut

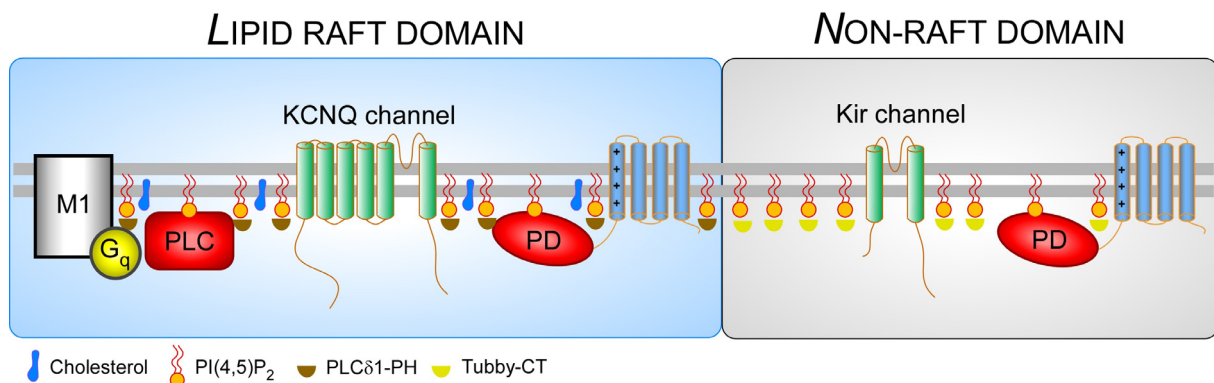
Philipps



Universität
Marburg

In Zusammenarbeit mit dem Physiologischen Institut II
des Fachbereichs Medizin der Albert-Ludwigs-Universität Freiburg
Geschäftsführender Direktor: Prof. med B. Fakler

Quantification of the in-vivo affinity of PI(4,5)P₂ effectors and sensors with the phosphoinositide phosphatase Ci-VSP



Inaugural-Dissertation zur Erlangung des Doktorgrades der Naturwissenschaften
dem Fachbereich Medizin der Philipps-Universität Marburg

vorgelegt von

Alexandra Rjasanow

aus Karl-Marx-Stadt
Marburg, 2011

Aus dem Institut für Physiologie und Pathophysiologie
des Fachbereichs Medizin der Philipps-Universität Marburg
Geschäftsführender Direktor: Prof. Dr. med. Dr. phil. J. Daut

Philipps



Universität
Marburg

In Zusammenarbeit mit dem Physiologischen Institut II
des Fachbereichs Medizin der Albert-Ludwigs-Universität Freiburg
Geschäftsführender Direktor: Prof. med B. Fakler

Quantification of the in-vivo affinity of PI(4,5)P₂ effectors and sensors with the phosphoinositide phosphatase Ci-VSP

Inaugural-Dissertation zur Erlangung des Doktorgrades der Naturwissenschaften
dem Fachbereich Medizin der Philipps-Universität Marburg

vorgelegt von

Alexandra Rjasanow
aus Karl-Marx-Stadt
Marburg, 2011

Angenommen vom Fachbereich Medizin der Philipps-Universität Marburg am:
13.05.2011

Gedruckt mit Genehmigung des Fachbereichs

Dekan: Prof. Dr. med. Matthias Rothmund
Referent: Prof. Dr. rer. nat. Dominik Oliver
1. Korreferent: Prof. Dr. med Robert Grosse

„Was du in anderen entzünden willst, muss in dir selbst brennen.“

Aurelius Augustinus

Denjenigen, die mir am nächsten sind und die mich lieben
in tiefster Dankbarkeit.

Summary

Quantification of the in-vivo affinity of PI(4,5)P₂ effectors and sensors with the phosphoinositide phosphatase Ci-VSP

Phosphoinositides (PIs) constitute a family of membrane phospholipids which play important roles in many eukaryotic signal transduction pathways. The PI phosphatidylinositol(4,5)biphosphate (PI(4,5)P₂) is predominantly located in the plasma membrane and regulates many cellular functions including protein activation (e.g. ion channels). PI(4,5)P₂-mediated signalling usually occurs via dynamic changes in the PI(4,5)P₂ concentration. Given the multitude of cellular functions that depend on PI(4,5)P₂, it is not fully understood how specificity of signalling is achieved, i.e. how only a subset of potential effector proteins can respond to a given change in the PI(4,5)P₂ concentration. One major factor determining signalling specificity may be the PI(4,5)P₂ affinity of these effectors. Thus, to understand the impact of dynamic PI(4,5)P₂ concentration changes on effector proteins it is necessary to know their PI(4,5)P₂ affinity. However, methods to define PI(4,5)P₂ affinities used so far have serious limitations in their potential to assess the affinities of PI(4,5)P₂ effectors (e.g. ion channels) under physiological conditions, i.e. in the living cell. Therefore, the PI(4,5)P₂ affinity of many proteins has yet to be established.

In this study, the voltage sensor-containing PI(4,5)P₂ 5' phosphatase of *Ciona intestinalis* (Ci-VSP) was established as a novel tool to quantify the PI(4,5)P₂ affinity of effector and sensor proteins. Ion channels are a physiologically relevant class of cellular PI(4,5)P₂ effectors with various PI(4,5)P₂ affinities, and their regulation by PIs has been the subject of wide-ranging investigation. The activity of inwardly rectifying potassium (Kir) channels, for example, is controlled by PI(4,5)P₂ binding. Thus, Kir channels were used as a model system to establish the potential of Ci-VSP for estimating PI(4,5)P₂ affinities. Kir currents were recorded during Ci-VSP activity using whole-cell patch-clamp recordings on CHO cells or two-electrode voltage clamp recordings on *Xenopus laevis* oocytes. Kir currents declined upon depolarization due to PI(4,5)P₂ depletion by Ci-VSP activity, and recovered upon repolarization as a result of endogenous PI(4,5)P₂ resynthesis. Steady state channel deactivation upon gradual Ci-VSP activation served as a readout for the level of channel-PI(4,5)P₂

affinity. Different degrees of Ci-VSP activity were required for channel deactivation, consistent with their different PI(4,5)P₂ affinities. Kir2.1WT channels were found to have a high PI(4,5)P₂ affinity, Kir1.1WT channels an intermediate one, and Kir3 channels a low one. The reduced channel-PI(4,5)P₂ affinity occurring as a result of amino acid mutations (e.g. R228Q in Kir2.1) that lead to severe diseases such as Andersen's syndrome was reliably detected with Ci-VSP. Similarly, using Ci-VSP allowed to track successfully a change in the PI(4,5)P₂ affinity of Kir3 channels modulated by G_{βγ}. These data revealed that Ci-VSP allowed, in contrast to earlier established approaches, the reversible and gradual titration of endogenous PI(4,5)P₂ in intact cells.

The reliability of Ci-VSP was confirmed by comparison of these results with those obtained with an independent approach to deplete PI(4,5)P₂. PI(4,5)P₂ depletion was achieved by chemically triggered recruitment of the PI(4,5)P₂ 5' phosphatase, Inp54p, to the plasma membrane. Kir currents of all channels investigated declined upon Inp54p-induced PI(4,5)P₂ depletion similar to the results obtained with Ci-VSP.

Finally, Ci-VSP was used to resolve the controversial PI(4,5)P₂ affinities of two PI(4,5)P₂ sensor proteins, PLCδ1-PH domain and tubby-CT, with the purpose of assessing their usefulness for monitoring PI(4,5)P₂ dynamics in intact cells in future studies. Total internal reflection fluorescence (TIRF) microscopy on CHO cells showed that the PI(4,5)P₂ affinity of tubby-CT is lower than that of PLCδ1-PH domain. The dynamic range of the tubby-CT sensor corresponded to the physiological range of PI(4,5)P₂ concentration, as indicated by KCNQ2 channel activity recorded simultaneously by patch-clamp.

In conclusion, the results establish Ci-VSP as a novel experimental tool for rapid, reversible and gradual manipulation of PI(4,5)P₂ in living cells. Ci-VSP allows for the quantitative examination of PI(4,5)P₂ sensitivities of cellular effectors and genetically encoded fluorescent sensors of PI(4,5)P₂ signaling.

Zusammenfassung

Quantifizierung der in-vivo Affinität von PI(4,5)P₂- Effektoren und Sensoren mit der Phosphoinositidphosphatase Ci-VSP

Phosphoinositide (PI) sind Mitglieder einer Familie kleiner Membranphospholipide, die wichtige Aufgaben in vielen eukaryotischen Signaltransduktionswegen übernehmen. Das PI Phosphoinositid(4,5)biphosphat (PI(4,5)P₂) z.B. ist vorwiegend in Plasmamembranen lokalisiert und reguliert viele zelluläre Funktionen, wie z.B. die Aktivierung von Proteinen (z.B. Ionenkanäle). In Anbetracht der Vielfalt zellulärer PI(4,5)P₂ abhängiger Funktionen ist es unklar, wie eine Spezifität dieser Signalwege erzielt werden kann, so dass z.B. nur ein Teil potentieller Effektorproteine auf eine gegebene PI(4,5)P₂ Konzentrationsänderung antwortet. Ein wichtiger Faktor, der die Spezifität der PI(4,5)P₂-Signalwege in Bezug auf die verschiedenen Zielproteine bestimmt, ist die PI(4,5)P₂-Affinität dieser Effektoren. Um den Einfluss dynamischer PI(4,5)P₂ Konzentrationsänderungen auf Effektorproteine zu verstehen, ist es notwendig die PI(4,5)P₂-Affinitäten dieser Proteine zu kennen. Jedoch fehlte den bisherigen Methoden das Potential, die PI(4,5)P₂-Affinität der Effektoren (z.B. Ionenkanälen) unter physiologischen Bedingungen, wie z.B. in der lebenden Zelle, zu untersuchen. Deshalb müssen die PI(4,5)P₂-Affinitäten vieler Proteine immer noch bestimmt werden.

In dieser Studie wurde eine spannungsgesteuerte 5' Phosphatase des Ascids *Ciona intestinalis* (Ci-VSP) als neues Werkzeug verwendet um die PI(4,5)P₂-Affinitäten von Effektoren und Sensoren zu quantifizieren. Ionenkanäle stellen eine Klasse physiologisch relevanter PI(4,5)P₂-Effektoren mit verschiedenen PI(4,5)P₂-Affinitäten dar und ihre Regulation durch PIs war Gegenstand weitreichender Untersuchungen. Die Aktivität von einwärts rektifizierenden Kalium-(Kir) Kanälen wird z.B. durch die Bindung von PI(4,5)P₂ reguliert. Deshalb wurden Kir-Kanäle als Modellsystem verwendet um abzuschätzen, wie gut Ci-VSP geeignet ist, die PI(4,5)P₂-Affinität dieser Kanäle festzustellen. Kir-Ströme wurden während der Ci-VSP-Aktivität mit Hilfe von Whole-cell Patch-Clamp an CHO-Zellen und mit Hilfe von Zwei-Elektroden Voltage-Clamp an *Xenopus laevis* Oocyten abgeleitet. Die Kir-Ströme nahmen bei Depolarisation aufgrund der Ci-VSP-vermittelten PI(4,5)P₂-

Depletion ab und nahmen bei Repolarisation aufgrund der endogenen PI(4,5)P₂-Resynthese wieder zu. Der Gleichgewichtszustand der Kanaldeaktivierung bei gradueller Ci-VSP-Aktivierung diente dem Auslesen des Grades der PI(4,5)P₂-Affinität. Aufgrund ihrer verschiedenen Affinitäten musste die Ci-VSP unterschiedlich stark aktiviert werden um die untersuchten Kir-Kanäle zu deaktivieren. In Übereinstimmung mit früheren Studien wurde ermittelt, dass Kir2.1WT-Kanäle eine hohe, Kir1.1WT-Kanäle eine mittlere und Kir3-Kanäle eine niedrige PI(4,5)P₂-Affinität haben. Ebenfalls wurde die reduzierte PI(4,5)P₂-Affinität von Mutanten (z.B. R228Q in Kir2.1), die zu schweren Erkrankungen wie das Anderson Syndrom führen können, erfolgreich mit Hilfe der Ci-VSP detektiert. Genauso konnte erfolgreich die sich ändernde PI(4,5)P₂-Affinität von Kir3-Kanälen bei Modulation durch G_{βγ} nachvollzogen werden. Diese Ergebnisse zeigten, dass die Verwendung der Ci-VSP, verglichen mit früheren Methoden PI(4,5)P₂-Level zu manipulieren und Protein-PI(4,5)P₂-Affinitäten zu quantifizieren, eine graduelle und reversible Titration des endogenen PI(4,5)P₂ in intakten Zellen erlaubt.

Die Reliabilität der Ci-VSP wurde bekräftigt durch den Vergleich der erhaltenen Resultate mit einer unabhängigen Methode PI(4,5)P₂ zu depletieren. Die Depletion wurde durch eine chemisch gesteuerte Membranrekrutierung einer 5' Phosphatase, der Inp54p, erzielt. Die Ströme aller untersuchten Kir-Kanäle nahmen infolge der Inp54p-induzierten PI(4,5)P₂-Depletion, ähnlich wie bei Ci-VSP-Aktivierung beobachtet, ab.

Zuletzt wurde die Ci-VSP dazu verwendet die kontroversen PI(4,5)P₂-Affinitäten zweier PI(4,5)P₂-Bindungsdomänen (PLCδ1-PH-Domäne und tubby-CT) aufzulösen um ihre Tauglichkeit in Bezug auf die Visualisierung von PI(4,5)P₂-Dynamiken in künftigen Studien abzuschätzen. Der dynamische Bereich des tubby-CT-Sensors stimmte mit dem physiologischen PI(4,5)P₂-Konzentrationsbereich überein, welcher durch die Aktivität von KCNQ2-Kanälen in simultanen Messungen mit Patch-Clamp angezeigt wurde.

Zusammengefasst zeigen die Resultate, dass Ci-VSP als neues Werkzeug geeignet ist zuverlässig PI(4,5)P₂-Level in lebenden Zellen reversibel und graduell zu manipulieren. Ci-VSP erlaubt die quantitative Ermittlung von PI(4,5)P₂-Sensitivitäten zellulärer Effektoren und genetisch kodierter fluoreszierender Sensoren von PI(4,5)P₂-Signalwegen.

Table of Contents

1	Abbreviations.....	ix
1.1	Abbreviations of amino acids	xi
2	Introduction.....	1
2.1	Phosphoinositides – Cellular function and dynamic regulation.....	1
2.1.1	Structure and synthesis of PIs.....	1
2.1.2	Cellular functions of PIs and PI concentration dynamics.....	3
2.2	Principles that govern intracellular PI signalling	5
2.2.1	The PI affinity of effector proteins.....	5
2.2.2	Dynamic regulation of the PI affinity	6
2.2.3	Spatially segregated PI signalling	7
2.2.4	Regulation of ion channels by PI(4,5)P ₂	8
2.3	Experimental approaches for examining the interaction of PI(4,5)P ₂ with ion channels.....	12
2.3.1	Methods for the quantification of the PI(4,5)P ₂ affinity of ion channels	12
2.3.2	Genetically encoded sensors for measuring PI dynamics	14
2.3.3	Ci-VSP as a potential novel tool to control cellular PI(4,5)P ₂ levels	16
2.4	Aims of this study	18
3	Experimental procedures.....	20
3.1	Cell culture and transfection	20
3.2	Electrophysiology on CHO cells	21
3.3	<i>Xenopus laevis</i> oocyte preparation	23
3.4	Electrophysiology on oocytes	24
3.4.1	Two-electrode voltage clamp recordings.....	24
3.4.2	Inside-out giant patch recordings	25
3.5	Fluorescence microscopy.....	27
3.6	Data analysis and statistics	27
4	Results	28
4.1	Quantification of the PI(4,5)P ₂ affinities of K ⁺ channels using Ci-VSP.....	28
4.1.1	Effects of Ci-VSP activity on Kir2.1WT channels	28
4.1.2	Quantification of the PI(4,5)P ₂ affinities of Kir2.1WT and Kir2.1R228Q channels	31
4.1.3	Quantification of KCNQ channel-PI(4,5)P ₂ affinity	34
4.1.4	Quantification of Kir1.1WT channel-PI(4,5)P ₂ affinity	34
4.1.5	Quantification of Kir1.1K80M channel-PI(4,5)P ₂ affinities	36
4.1.6	Quantification of Kir3.1/3.2 channel-PI(4,5)P ₂ affinity	37
4.1.7	Quantification of the dynamically altered PI(4,5)P ₂ affinities of modulated Kir3.1/3.2 channels using Ci-VSP	38
4.2	Comparison of the Kir channel sensitivities to Ci-VSP-induced PI(4,5)P ₂ depletion	41
4.2.1	Effects of substrates and products of Ci-VSP on Kir channel family members	43
4.2.2	Effects of PIs on Kir2.1WT channels.....	43
4.2.3	Effects of PIs on Kir6.2/SUR1 channels.....	45
4.2.4	Effects of PIs on Kir1.1WT channels.....	48
4.2.5	Effects of PIs on Kir1.1K80M channels	50
4.2.6	Summary of the PI effects on Kir channels	51
4.3	Verification of the usefulness of Ci-VSP with an independent approach	53
4.3.1	PI(4,5)P ₂ depletion by inducible Inp54p membrane translocation	53

4.3.2	Modulation of Kir channels by physiologically occurring dynamic PI(4,5)P ₂ changes	55
4.4	Characterization of two fluorescent PI(4,5)P ₂ sensors	56
4.4.1	Quantification of the PI(4,5)P ₂ affinities of fluorescent sensors using Ci-VSP	56
4.4.2	Estimation of the dynamic range and the PI(4,5)P ₂ affinity of fluorescence sensors.....	58
4.4.3	Biosensor fluorescence signals during PLC-mediated cellular PI(4,5)P ₂ dynamics	60
5	Discussion	62
5.1	Efficiency of Ci-VSP in quantification of the PI(4,5)P ₂ affinities of ion channels.....	62
5.1.1	Parameters that describe the apparent PI(4,5)P ₂ affinity of Kir channels- reversibility, gradual activation, and velocity.....	62
5.1.2	Usefulness of Ci-VSP in comparison to alternative approaches for controlling PI(4,5)P ₂ levels	65
5.1.3	Quantification of the PI(4,5)P ₂ affinities of K ⁺ channels.....	67
5.2	Does sensitivity to Ci-VSP predict the regulation of channels by physiological PI(4,5)P ₂ dynamics?	68
5.3	PLCδ1-PH and tubby-CT may detect distinct PI(4,5)P ₂ pools.....	71
5.4	Future prospects	74
6	References	76
7	Attachments	89

Index of Tables and Figures

Table 1: Kir channel properties and modulators	9
Table 2: Vector constructs	20
Table 3: Solutions for whole-cell recordings in CHO cells	22
Table 4: Solution for storage and incubation of oocytes	24
Table 5: Solutions for two-electrode voltage clamp recordings from oocytes	24
Table 6: Solutions for inside-out patch-clamp recordings in oocytes	25
Table 7: Overview of PI effects on open and deactivated Kir channel family members	52
Figure 1: Chemical structure of phosphatidyl-inositol(4,5)bisphosphate (PI(4,5)P ₂)... ..	2
Figure 2: Phosphoinositide metabolism.....	3
Figure 3: Interaction sites of Kir2.1, Kir1.1, Kir3.1/3.2 and Kir6.2/SUR1 channels. ...	11
Figure 4: PI(4,5)P ₂ depletion by Inp54p membrane translocation.	13
Figure 5: PLC-triggered PI(4,5)P ₂ hydrolysis leads to the translocation of PI(4,5)P ₂ sensor domains towards the cytoplasm.....	15
Figure 6: Ci-VSP is a voltage-dependent 5' phosphatase.	17
Figure 7: Reversible decline of membrane localized PLCδ1-PH-GFP fluorescence upon gradual Ci-VSP activation.....	18
Figure 8: Step protocols for Kir and KCNQ current whole-cell recordings in CHO cells.	23
Figure 9: Ramp protocol for measuring Kir currents by two-electrode voltage clamp.	25
Figure 10: Ramp protocol for measuring Kir currents in inside-out giant patches.....	26
Figure 11: Deactivation of Kir2.1WT channels upon Ci-VSP activation.....	29
Figure 12: Kir2.1 channel deactivation upon activation of Ci-VSP measured in CHO cells.	30
Figure 13: Kir2.1 channel deactivation upon activation of Ci-VSP measured in <i>Xenopus laevis</i> oocytes.....	33
Figure 14: KCNQ channel deactivation upon activation of Ci-VSP in CHO cells.	34
Figure 15: Kir1.1 channel deactivation upon activation of Ci-VSP measured in CHO cells.	35
Figure 16: Kir3.1/3.2 channel deactivation and stabilizing effects of G _{βγ} upon activation of Ci-VSP measured in <i>Xenopus laevis</i> oocytes.	40
Figure 17: Comparison of current decline and dose-response properties of Kir channels with different PI(4,5)P ₂ affinities after Ci-VSP activation.	42
Figure 18: Open Kir2.1WT channels are not inhibited by any of the PI investigated.	44
Figure 19: Deactivated Kir2.1WT channels after Mg ²⁺ application are activated by PI(4,5)P ₂	45
Figure 20: Effects of PI(4,5)P ₂ , PI(4)P, PI(3,4,5)P ₃ and PI(3,4)P ₂ on open Kir6.2/SUR1 channels.	46
Figure 21: Deactivated Kir6.2/SUR1 channels after Mg ²⁺ application are activated by all PIs investigated.....	47
Figure 22: Kir1.1WT channel re-opening depends on the extracellular K ⁺ concentration.....	48
Figure 23: Open Kir1.1WT channels are inhibited by PI(4)P, PI(3,4,5)P ₃ and PI(3,4)P ₂	49
Figure 24: Open Kir1.1K80M channels are not inhibited by any PI investigated.	50
Figure 25: Deactivated Kir1.1K80M channels after Mg ²⁺ application are activated by PI(4,5)P ₂ , PI(4)P and PI(3,4)P ₂	51

Figure 26: Deactivation of Kir channels upon Inp54p-induced PI(4,5)P ₂ depletion...	54
Figure 27: PLC induced PI(4,5)P ₂ hydrolysis is ineffective on Kir2.1 and Kir1.1 channels.	56
Figure 28: Translocation of PLCδ1-PH domain and tubby-CT upon Ci-VSP activation.	58
Figure 29: Simultaneous KCNQ2 channel deactivation and PLCδ1-PH or tubby-CT translocation upon Ci-VSP activation.	60
Figure 30: Translocation of PLCδ1-PH domain upon PLC-triggered PI(4,5)P ₂ depletion.	61
Figure 31: Correlation of the K ⁺ channel-PI(4,5)P ₂ affinities measured with diC8-PI(4,5)P ₂ and Ci-VSP.	68
Figure 32: Hypothetical model for the distribution of ion channels, M1 receptors and Ci-VSP in lipid raft domains or non-lipid raft domains.	71
Figure 33: Hypothetical model for the distribution of the sensors PLCδ1-PH domain and tubby-CT in lipid raft domains or non-raft domains.	74

1 Abbreviations

ATP	Adenosine triphosphate
BIR channel	Basal inward rectifying potassium channel
Cav channel	Voltage-gated Ca ²⁺ channel
CFP	Cyano fluorescent protein
CHO	Chinese hamster ovary cells
Ci-VSP	<i>Ciona intestinalis</i> voltage sensor-containing phosphatase
C-terminal	Carboxy-terminal
DAG	Diacylglycerol
diC8-PI(4,5)P ₂	Water soluble PI(4,5)P ₂ analogue
EC50	Concentration for half-maximal channel activation
EGFP	Enhanced green fluorescent protein
ER	Endoplasmic reticulum
FKBP	FK506 binding protein
FRAP	Fluorescence recovery after photobleaching
FRB	Protein domain of mammalian target of rapamycin
G _α	G protein subunit alpha
GABA	Gamma amino butyric acid
GABA _B	GABA receptor type B
G _{βγ}	G protein subunit beta and gamma
GFP	Green fluorescent protein
GIRK channel	G protein activated potassium channel
GPCR	G protein coupled receptor
G protein	Guanine nucleotide-binding proteins
H	Hydrogen
H5	Pore-forming loop
I(1,4,5)P ₃	Inositol(1,4,5)trisphosphate
Inp54p	PI(4,5)P ₂ specific 5' phosphatase in yeast
IRK channel	Inwardly rectifying potassium channel
K2P channel	Two-pore-domain potassium channel
K _{ATP} channel	ATP-sensitive potassium channel
Kir channel	Inwardly rectifying potassium channel
Kir6.2/SUR1	K _{ATP} channels composed of Kir6.2 channel and SUR1 units
Kv channel	Voltage-gated K ⁺ channel

M1 receptor	Muscarinic acetylcholine receptor type 1
MARCKS	Myristoylated alanine-rich C kinase substrate
NB	Nucleotide binding domain
NDP	Nucleotide diphosphate
N-terminal	Amino-terminal
P ₀	Open probability
PH	Pleckstrin homology
PI	Phosphoinositide
PI3K	Phosphatidylinositol 3' kinase
PI4K	Phosphatidylinositol 4' kinase
PI5K	Phosphatidylinositol 5' kinase
PI(3)P	Phosphatidylinositol(3)monophosphate
PI(3,4)P ₂	Phosphatidylinositol(3,4)bisphosphate
PI(3,4,5)P ₃	Phosphatidylinositol(3,4,5)trisphosphate
PI(4)P	Phosphatidylinositol(4)monophosphate
PI(4,5)P ₂	Phosphatidylinositol(4,5)bisphosphate
PI(5)P	Phosphatidylinositol(5)monophosphate
PIP4K	Phosphatidylinositolphosphate 4' kinase
PIP5K	Phosphatidylinositolphosphate 5' kinase
PKA	Protein kinase A
PKC	Protein kinase C
PLC	Phospholipase C
PLCδ1-PH domain	PH domain of PLCδ1
PTEN	Phosphatase and tensin homolog
ROMK channel	Renal outer medullary potassium channel
SEM	Standard error of the mean
SHIP	Src homology 2 domain-containing inositol polyphosphate 5' phosphatase
SUR1	Sulfunylurea receptor type 1
τ	Time constant
TRP channel	Transient receptor potential channel
TIRF	Total internal reflection fluorescence
TM	Transmembrane spanning helix

Tubby-CT	C-terminally localized binding module of the transcription factor tubby protein
$V_{1/2}$	Voltage for half-maximal current inhibition
V_{hold}	Holding potential
WT	Wild type

1.1 Abbreviations of amino acids

A	Alanine
K	Lysine
M	Methionine
Q	Glutamine
R	Arginine

2 Introduction

2.1 Phosphoinositides – Cellular function and dynamic regulation

Phosphoinositides (PIs) are minor components of all eukaryotic cellular membranes. Besides a structural function as a fraction of the overall phospholipid mixture that makes up the membranes their major role is to act as genuine signalling molecules that control a wide variety of pivotal cellular processes including trafficking, differentiation and proliferation, endo- and exocytosis, and the activity of transporters and ion channels (Botelho et al., 2000, Hilgemann et al., 2001, Toker, 2002). Consistent with this signalling role, their concentrations are subject to do dynamic changes on various time scales. In the 1950s, Hokin and Hokin found changes in the turnover of phospholipids upon activation of membrane receptors, the so-called 'phospholipid effect' (Hokin, 1985). This work pioneered many fundamental discoveries within PI signalling, which has become a dynamic and extensive field of research within cell biological, biochemical and biomedical research in the last ten years. The 'phospholipid effect' was primarily detected after stimulation of exocrine tissues but was subsequently found in essentially any cellular system studied (Odorizzi et al., 2000, Czech, 2003, Di Paolo and De Camilli, 2006, Andrews et al., 2007, Coburn, 2009). It was proposed by Hokin that the effect was due to changes in the turnover of phosphatidylinositol and its phosphorylated products, the PIs (Hokin, 1985). Today, it is accepted that a large number of physiological processes utilize some form of signal transduction which is PI-dependent.

2.1.1 Structure and synthesis of PIs

Phosphatidylinositol is the precursor molecule of PIs. The molecule is a canonical glycerophospholipid that contains a phosphatidic acid backbone with two hydrophobic fatty acid tails, and a phosphate group substituted to a hydrophilic inositol head group (Figure 1) making the lipid an amphiphile (Kuksis, 2003). The synthesis of phosphatidylinositol takes place primarily in the endoplasmic reticulum (ER), where it is delivered to the plasma membrane either by vesicular transport or via cytosolic phosphatidylinositol transfer proteins (Di Paolo and De Camilli, 2006). Phosphatidylinositol represents less than 15% of the total phospholipids found in the

eukaryotic cells plasma membranes, and its phosphorylated products, the PIs, are less abundant by one order of magnitude (Toker, 2002, Di Paolo and De Camilli, 2006).

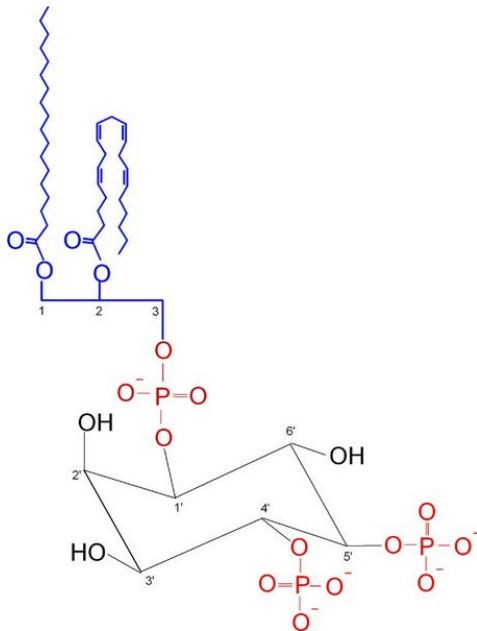


Figure 1: Chemical structure of phosphatidylinositol(4,5)bisphosphate (PI(4,5)P₂).

The PI(4,5)P₂ molecule. Black: inositol ring, upper red: phosphate group, blue: glycerol backbone with two fatty acid groups, lower red: phosphate groups at positions 4 and 5. The IUPAC name is 1,2-Diacyl-sn-glycero-3-phospho-(1-D-myo-inositol 4,5-bisphosphate) (<http://en.wikipedia.org/wiki/PIP2>).

PI kinases phosphorylate phosphatidylinositol at the inositol ring in a stereospecific manner, either at 3', 4' or 5' position, resulting in the generation of seven PI species which are phosphorylated at one (monophosphate), two (bisphosphate) or three (trisphosphate) positions (Figure 2). During the first step for the generation of PIs, phosphatidylinositol is phosphorylated by phosphatidylinositol 3-kinase (PI3K), PI4K or PI5K. In a second step, the monophosphate species phosphatidylinositol(3)monophosphate (PI(3)P), PI(4)P, and PI(5)P are phosphorylated by phosphatidylinositolphosphate 5' kinase (PIP5K), PI3K and PIP4K, giving rise to the bisphosphates PI(3,5)P₂, PI(3,4)P₂ and PI(4,5)P₂. Finally, PIP5K and PI3K convert PI(3,4)P₂ and PI(4,5)P₂ into PI(3,4,5)P₃, respectively – the only trisphosphate. All phosphorylations by kinases have been shown to be reversed by distinct phosphatases. Well characterized examples are the 3' phosphatase “phosphatase and tensin homolog” (PTEN) and the “Src homology 2 domain-containing inositol polyphosphate 5' phosphatase” (SHIP) (Damen et al., 1996, Vanhaesebroeck et al., 2001).

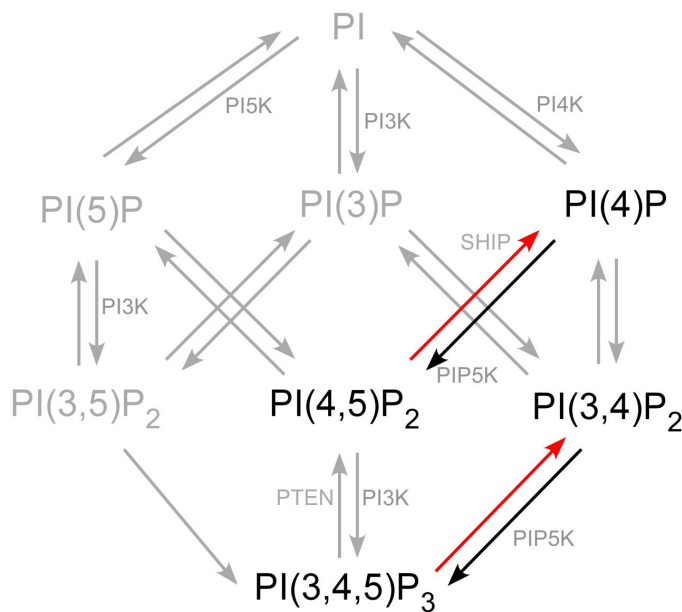


Figure 2: Phosphoinositide metabolism.

PI is phosphorylated by distinct kinases into PI(x)P monophosphate. Monophosphates are phosphorylated into bisphosphates and PI(3,4)P₂ and PI(4,5)P₂ are converted into the trisphosphate PI(3,4,5)P₃. Phosphorylation by kinases is reversed by distinct phosphatases such as PTEN and SHIP. Black PIs are involved in 5' phosphatase activity indicated by coloured arrows and described in paragraphs 2.3.1 and 2.3.3.

2.1.2 Cellular functions of PIs and PI concentration dynamics

Many cellular functions have been shown to depend on the abundance of particular PIs or the dynamic regulation of their concentration. Physiological processes that are regulated by PI(4,5)P₂ signalling are actin remodelling during cell motility, trafficking, phagocytosis, pinocytosis, exocytosis and endocytosis, cell adhesion and microtubule capture (Terebiznik et al., 2002, Di Paolo et al., 2004, Pizarro-Cerda and Cossart, 2004, Golub and Caroni, 2005, Haucke, 2005, Milosevic et al., 2005, Catimel et al., 2008).

Furthermore, PIs, and PI(4,5)P₂ in particular, have been shown to regulate the activity of many ion channels, e.g. inwardly rectifying potassium (Kir) channels (Logothetis et al., 2007a), and transporters (Hilgemann et al., 2001). PI(4,5)P₂ is considered to be an indispensable co-factor of Kir channels as no activity can be observed in its absence (Logothetis et al., 2007b). Their main functions are the stabilization of the membrane potential and the maintenance of the K⁺ homeostasis. Mutations in Kir channels affecting the channel-PI(4,5)P₂ interaction result in severe diseases such as Andersen's syndrome (mutations in Kir2.1 channels: (Lopes et al., 2002)) and Bartter's syndromes (Kir1.1: (Lopes et al., 2002)) and hyperinsulinaemias (Kir6.2: (Lin et al., 2006)). Other PIs which have been found to influence Kir channel properties are PI(4)P, PI(3,4)P₂, PI(3,5)P₂ and PI(3,4,5)P₃ (Rohacs et al., 1999, Zeng et al., 2002, Rohacs et al., 2003). Another type of K⁺ channels whose PI(4,5)P₂ sensitivity is well characterized is the KCNQ channel family. KCNQ channels are

expressed in the heart (Attali, 1996, Yang et al., 1998), in hair cells of the inner ear (Kubisch et al., 1999) and in the central and peripheral nervous system (Wang et al., 1998, Kubista et al., 2009), where they mediate voltage-dependent outwardly rectifying potassium currents. Heterotetrameric KCNQ2/3 channels control the excitability in many neurons (Jones et al., 1995, Wang et al., 1998).

PI concentrations are regulated dynamically in response to many physiological stimuli such as growth factor receptor stimulation or after the activation of guanine nucleotide-binding protein (G protein) coupled receptors (GPCR). The membrane abundance of PI(3,4,5)P₃ e.g. is low at rest but the number dramatically increases due to extracellular stimulation by a variety of ligands including growth factors and hormones (Toker, 2002). Its accumulation typically results in the recruitment of proteins or the activation of enzymes that directly interact with PI(3,4,5)P₃ (Vanhaesebroeck et al., 2001). Thus, cellular processes controlled by PI(3,4,5)P₃ and PI(3,4)P₂ are mostly initiated by a concentration increase of these PIs. Such processes include, proliferation, differentiation, and cell survival, immune as well as responses to insulin secretion, cell responses against apoptosis or responses to oxidative stress (Traynor-Kaplan et al., 1989, Franke et al., 1997, Frech et al., 1997, Aman et al., 1998, Lee et al., 2000, Kimber et al., 2002, Rajala and Anderson, 2003, Ahn et al., 2004, Andrews et al., 2007, Aoki et al., 2007).

The membrane concentration of PI(4,5)P₂, however, is high at rest (Czech, 2003) and the activation of GPCRs by agonist stimulation leads to phospholipase C (PLC)-triggered hydrolysis of PI(4,5)P₂ to inositol(1,4,5)trisphosphate (I(1,4,5)P₃) and diacylglycerol (DAG) (Suh and Hille, 2002). The resulting decrease of PI(4,5)P₂ levels typically leads to the deactivation of ion channels and transporters. In neurons, for example, KCNQ channel activity is modulated by GPCRs such as the muscarinic acetylcholine receptor type 1 (M1). The channel deactivation induced by receptor activation and subsequent PI(4,5)P₂ hydrolysis leads to enhanced neuronal excitability (Suh and Hille, 2002).

Other ion channels and transporters whose activity depends on the presence of PI(4,5)P₂ are voltage-gated Ca²⁺ channels, hyperpolarization-activated cyclic-nucleotide-gated (HCN) channels, EAG/ERG family channels, transient receptor potential (TRP) channels, P2X purinoreceptor channels, Ca²⁺ pumps, and Na⁺/Ca²⁺-, Na⁺/H⁺-, and Na⁺/Mg²⁺ exchangers (Aharonovitz et al., 2000, Rasgado-Flores and Gonzalez-Serratos, 2000, Bian et al., 2001, Beauge et al., 2002, Zolles et al., 2006,

Bernier et al., 2008). However, it still remains to be investigated for most of these channels and transporters whether their activity is controlled by dynamic PI concentration changes. Further reviews summarize the effects of PIs on proteins and their dynamic concentration regulations during physiological processes: (He et al., 2000, Hilgemann et al., 2001, Halstead et al., 2005, Di Paolo and De Camilli, 2006, Gamper and Shapiro, 2007, Tucker and Baukrowitz, 2008).

In summary, dynamic concentration changes of PIs are of particular importance in PI signalling.

2.2 Principles that govern intracellular PI signalling

Since many cellular functions and proteins within a single cell including ion channels and transporters depend on a single PI messenger (e.g. the regulation of their activity by PI(4,5)P₂ depletion), the question arises, how intracellular signalling can be specific in terms of the activation, recruitment or regulation of distinct sets of proteins.

2.2.1 The PI affinity of effector proteins

The most obvious factor that contributes to the specificity of PI signalling with respect to different target proteins is the PI affinity of these effectors.

Thus, a given change in PI levels can differentially regulate effector proteins if they display different PI affinities. Effectors that exhibit a low PI affinity are easily modulated by small PI concentration changes whereas strong concentration changes are required to affect proteins with high PI affinity, that are saturated with PI under resting conditions. Moderate PI(4,5)P₂ depletion, for example, leads to a closure of ion channels with low PI(4,5)P₂ affinity, while strong depletion is necessary to deactivate channels that exhibit a high PI(4,5)P₂ affinity.

Direct actions of PIs on proteins may fall into two categories (Gamper and Shapiro, 2007). PI-protein interactions, belonging to the first category have a permissive role, which means that the protein's function requires the presence of the particular PI. PI-protein interactions that have a signalling role, meaning that the protein is dynamically regulated by the changing abundance of the PI, fall into the second category. It has been suggested that for proteins which exhibit a high affinity, the PI-protein interaction probably has a permissive role, whereas proteins that exhibit a low affinity are expected to be sensitive to dynamic changes in PI levels.

2.2.2 Dynamic regulation of the PI affinity

An additional layer of signalling specificity may be achieved by dynamic regulation of the PI affinity of effectors by other cellular signalling pathways. By such a mechanism, the signalling status of a cell may determine which of the potential effectors of PI dynamics actually respond to a given change in PI concentration. So far, evidence for the modulation of the PI affinity has been obtained for Kir3 channels whose activity depends on the presence of both, the G protein subunit $G_{\beta\gamma}$ and PI(4,5)P₂ (Huang et al., 1998, Dascal, 2001, Rubinstein et al., 2009). In inside-out patches excised from *Xenopus laevis* oocytes, Kir3 channels were less sensitive to depletion of PI(4,5)P₂ when $G_{\beta\gamma}$ was co-expressed, suggesting that $G_{\beta\gamma}$ stabilized the interaction with PI(4,5)P₂ (Huang et al., 1998). It has been suggested that the degree of Kir3 channel activity results from the balanced impact of two antagonistic pathways: first, a stimulatory pathway where signalling through $G_{\beta\gamma}$ subunits stabilizes the channel interaction with PI(4,5)P₂ and promotes activation. The second, inhibitory pathway mediated by GPCRs, involves activation of PLC and subsequent hydrolysis of PI(4,5)P₂, thus limiting channel opening by $G_{\beta\gamma}$ (Kobrinisky et al., 2000).

The PI(4,5)P₂ affinity of KCNQ1 channels which form one of the main repolarizing cardiac K⁺ currents is regulated by β -adrenergic receptors via protein kinase A (PKA) and G_qPCRs via protein kinase C (PKC). The activation of protein kinase A (PKA) after β -adrenergic receptor stimulation leads to the phosphorylation of the channels resulting in an increase of the PI(4,5)P₂ affinity. Mutations of KCNQ1 channels characterized by a low PI(4,5)P₂ affinity cause the long-QT syndrome. Phosphorylation of the mutated KCNQ1 channels by PKC leads to a strengthened KCNQ1 channel-PI(4,5)P₂ interaction and a weakened response to PI(4,5)P₂ changes. This compensatory effect is suggested to partially rescue the long-QT syndrome (Matavel et al., 2010).

It seems likely that many more channels are regulated by similar mechanisms that change the PI(4,5)P₂ affinity. However, to investigate this aspect of channel regulation a method for quantification of the PI(4,5)P₂ affinity in the living cell i.e. in the context of physiological regulation is required.

2.2.3 Spatially segregated PI signalling

A cellular strategy to increase the signalling specificity may be the sorting of proteins into subcellular compartments which contain enriched and spatially separated PI pools. Known examples for local PI changes include phagocytosis, where localized and transient remodelling of actin filaments is regulated by local accumulation of PI(4,5)P₂ in phagosomal cups (Botelho et al., 2000). In chemotaxis, PI(3,4,5)P₃ has been shown to be locally accumulated in the membrane at the cell's leading edge thereby promoting new actin polymerization driving the cells to migrate forward (Haugh et al., 2000, Wang et al., 2002).

A second, recently provided model suggests that PI(4,5)P₂ may be differentially distributed between lipid raft and non-lipid raft domains. A cell biological study suggested that PI(4,5)P₂ is concentrated in the inner leaflet of cholesterol-dependent lipid microdomains, the so called lipid rafts (Rozelle et al., 2000). It has been suggested that this accumulation amplifies the signalling for actin dynamics and the assembly of membrane associated protein coats, which mediate morphogenesis and membrane trafficking (Botelho et al., 2000, Rozelle et al., 2000, McLaughlin et al., 2002). Another group found in T cells that the enrichment of PI(4,5)P₂ in lipid rafts increased membrane ruffling and cell spreading (Johnson et al., 2008a). Accumulation of PI(4,5)P₂ in non-raft domains, however, inhibited ruffling as well as capping in stimulated T cells providing evidence for sequestration of PI(4,5)P₂-dependent functions between separate membrane fractions. A third study suggested that muscarinic receptors and KCNQ channels co-localize in lipid rafts, tightening the coupling between receptors and channels and enabling receptor-mediated suppression of the channel activity by PI(4,5)P₂ hydrolysis (Oldfield et al., 2009).

Functionally distinct PI(4,5)P₂ pools that are generated by different PIP5Ks have been identified in mast cells (Vasudevan et al., 2009). Thus, PIP5K-I γ has been shown to generate a pool that is hydrolysable by PLC γ which leads to the depletion of internal Ca²⁺ stores by I(1,4,5)P₃. PI(4,5)P₂ that was generated by PIP5K-I β , however, did not contribute to I(1,4,5)P₃-mediated Ca²⁺ release from the ER, but instead negatively regulated the so-called store-operated Ca²⁺ entry (Vasudevan et al., 2009).

However, theoretical considerations challenge these findings. PI(4,5)P₂ contains a polyunsaturated chain and is therefore unlikely to partition spontaneously into rafts by itself (Brown and London, 2000). Yet, protein-lipid interactions may

establish local PI concentration differences. Thus, it has been hypothesized that proteins may act as a “buffer”, binding and passively concentrating PI(4,5)P₂ (McLaughlin et al., 2002). A possible candidate is the myristoylated alanine-rich C kinase substrate (MARCKS) protein, which is usually concentrated in the ruffles of fibroblasts and the forming phagosomes of macrophages. Its concentration is comparable to that of PI(4,5)P₂, its polycationic effector domain binds PI(4,5)P₂ with high affinity. It has been suggested that PI(4,5)P₂ sequestration is achieved by the generation of a local positive electrical field potential by MARCKS proteins, thereby developing an electrical gradient to assemble and concentrate negatively charged PI(4,5)P₂ (McLaughlin et al., 2002). However, whether MARCKS is associated with lipid rafts and sequesters PI(4,5)P₂ under physiological conditions is controversial and requires further research.

2.2.4 Regulation of ion channels by PI(4,5)P₂

Ion channels such as Kir channels are regulated by PIs. Kir channels are ubiquitously expressed in both excitable and non excitable cells, where they play important roles in the control of cell excitability, K⁺ homeostasis, heart rate, vascular tone and insulin secretion by regulation of the membrane potential (Kubo et al., 1993, Doi et al., 1996, Fan and Makielski, 1997, Bradley et al., 1999). In their quaternary structure Kir channels form tetramers. Each subunit contains two transmembrane spanning helices (TM), TM1 and TM2, that are connected by the pore-forming loop (H5) and which contain the cytoplasmic amino (N)- and carboxy (C)-terminal domains (Figure 3). The Kir channel family consists of seven subfamilies (Kir1-7) with a total of 15 members (Table 1) (Logothetis et al., 2007a). The different subfamilies can be distinguished by their sequence homology, but also by functional properties like rectification properties and responses to cellular signals such as pH, phosphorylation and particularly, their affinity for PI(4,5)P₂ (Table 1).

Table 1: Kir channel properties and modulators

Subfamily members	Synonymes	Modulators	PI(4,5)P ₂ affinity	References
Kir1.1a-c	ROMK1-6	pH _i , K ⁺ _e , PKA, PKC, PI(4,5)P ₂	intermediate	1, 2, 3, 4, 5
Kir2.1-2.4	IRK1-4 BIR11 (2.3)	pH _i (2.3), PKC (2.3), PI(4,5)P ₂	high (2.1), intermediate (2.2, 2.3)	5, 6, 7, 8, 9, 10, 11
Kir3.1-3.4	GIRK1-3, K _{ATP}	G _α , G _{βγ} , Na ⁺ _i (3.2, 3.4), pH _i , PI(4,5)P ₂	low	5, 12, 13, 14, 15, 16, 17
Kir4.1-4.2	BIR10	pH _i , PI(4,5)P ₂	high	18, 19, 20, 21
Kir5.1	BIR9	pH _i , Na ⁺ _i (4.1/5.1), PI(4,5)P ₂	low	18, 19, 22, 23
Kir6.1-6.2	K _{ATP}	SURx, ATP _i , NDP _s _i , PKC, PI(4,5)P ₂	low	24, 25, 26, 27
Kir7.1	-	pH _i , PI(4,5)P ₂	low	28, 29, 30

References: 1 (Ho et al., 1993), 2 (Rapedius et al., 2007a), 3 (Lin et al., 2002), 4 (McNicholas et al., 1994), 5 (Tucker and Baukowitz, 2008), 6 (Kubo et al., 1993), 7 (Coulter et al., 1995), 8 (Zhu et al., 1999), 9 (Lopes et al., 2002), 10 (Lopatin et al., 1994), 11 (Carr and Surmeier, 2007) 12 (Stoffel et al., 1995), 13 (Ivanina et al., 2004) ,14 (Huang et al., 1998), 15 (Zhang et al., 1999), 16 (Mao et al., 2003), 17 (Pegan et al., 2005), 18 (Bond et al., 1994), 19 (Tanemoto et al., 2000), 20 (Du et al., 2004), 21 (Lam et al., 2006), 22 (Rosenhouse-Dantsker et al., 2008), 23 (Rapedius et al., 2007b), 24 (Schulze et al., 2003), 25 (Aguilar-Bryan et al., 1998), 26 (Tung and Kurachi, 1991), 27 (Shyng and Nichols, 1997), 28 (Hughes and Swaminathan, 2008), 29 (Rohacs et al., 2003), 30 (Doring et al., 1998).

ROMK: renal outer medullary potassium channel, IRK: inwardly rectifying potassium channel, BIR: basal inward rectifying potassium channel, GIRK: G protein activated potassium channel, G_α: G protein subunit alpha K_{ATP}: ATP-sensitive potassium channel, _i: intracellular, _e: extracellular, SUR: sulfunylurea receptor, ATP: adenosine triphosphate, NDP: nucleotide diphosphate

In the last decade extensive research has focused on the modulation of channel activity by direct interaction with membrane lipids like PIs. For all Kir channels, PI(4,5)P₂ is an indispensable cofactor as no activity can be observed in its absence (Hilgemann et al., 2001). Kir channels directly interact with the negatively charged phosphate groups of PI(4,5)P₂ via positively charged amino acid residues in the cytoplasmic amino (N)- and C-termini of the Kir channels which are essential for activation (Figure 3) (Fan and Makielski, 1997, Huang et al., 1998, Lopes et al., 2002, Schulze et al., 2003).

Kir channels are modulated by several factors such as intracellular Na⁺, pH, ATP or G_{βγ} (Figure 3). The regulation of Kir channels by the different modulators shows great dependence on the strength of channel-PI(4,5)P₂ interactions, and the influence is stronger when the channels exhibit low PI(4,5)P₂ affinity (Du et al., 2004). Representative Kir channel subfamily members that exhibit various PI(4,5)P₂ affinities and which are differently modulated are homomeric Kir2.1, 1.1, heteromeric 3.1/3.2 channels and K_{ATP} channels which are composed of Kir6.2 channel units and sulfonylurea receptor type 1 (SUR1) (Kir6.2/SUR1 channels) (Figure 3, protein sequences: paragraph 7). Kir2.1 channels exhibit a high PI(4,5)P₂ affinity and are barely modulated by other interactors than PI(4,5)P₂ (Huang et al., 1998, Tucker and Baukrowitz, 2008). Kir1.1 channels exhibit an intermediate PI(4,5)P₂ affinity (Huang et al., 1998). Their activity has been shown to be regulated at least by the extracellular K⁺ concentration, and PI(4,5)P₂. PI(4,5)P₂ degradation deactivates the channels and leads to an irreversible collapse of the Kir1.1 channel pore in the absence of extracellular K⁺ ions, a process called K⁺ inhibition (Doi et al., 1996, Schulte et al., 1999, Rapedius et al., 2007a). Kir3 channels are G protein activated potassium channels and exhibit a low PI(4,5)P₂ affinity (Huang et al., 1998, Tucker and Baukrowitz, 2008). Channel-PI(4,5)P₂ interaction has been shown to be strengthened by G_{βγ} (Huang et al., 1998). K_{ATP} channels were the first channels whose activity was shown to depend on PIs and they also exhibit a low PI(4,5)P₂ affinity (Schulze et al., 2003). Under resting conditions, K_{ATP} channels are inhibited by ATP. PI(4,5)P₂ sustains K_{ATP} channel activity by stabilizing the channels' open state and it decreases or even abolishes the channels inhibition by ATP (Shyng and Nichols, 1997, Baukrowitz et al., 1998).

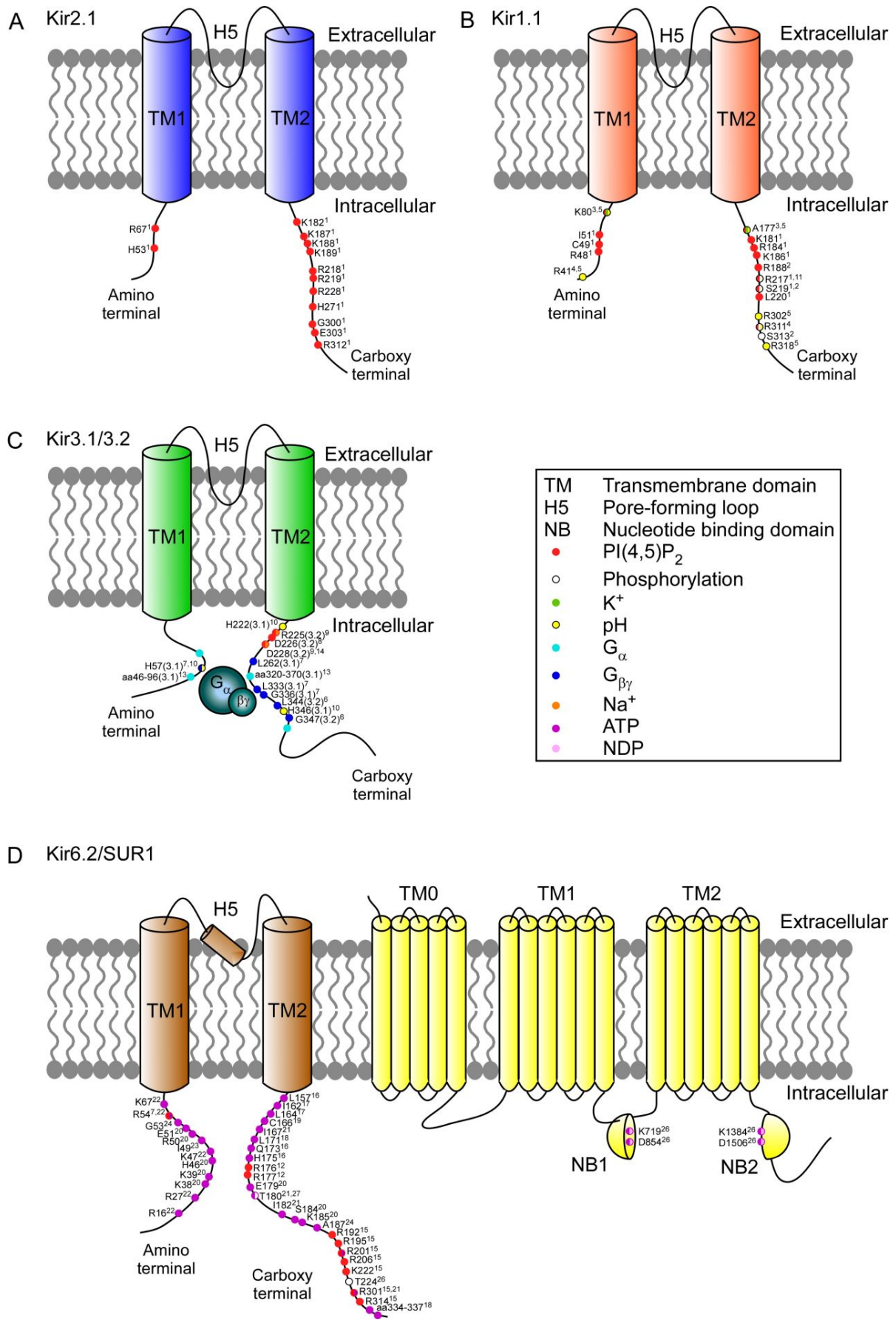


Figure 3: Interaction sites of Kir2.1, Kir1.1, Kir3.1/3.2 and Kir6.2/SUR1 channels.

A- D Structure of the Kir2.1, 1.1, 3.1/3.2 and Kir6.2/SUR1 channel subunits. Each Kir subunit contains a TM1 and a TM2 region, a H5 loop, and cytosolic N- and C-termini. Interaction sites with PI(4,5)P₂ (red), K⁺ (green), pH (yellow), G_α (light blue), G_{βγ} (blue), Na⁺ (orange), ATP (purple), nucleotide diphosphate (NDP) (pink) and phosphorylation sites (white) are indicated. References: ¹(Lopes et al., 2002), ²(Liou et al., 1999), ³(Rapedius et al., 2007b), ⁴(Schulte et al., 1999), ⁵(Rapedius et al., 2006), ⁶(Finley et al., 2004), ⁷(Hibino et al., 2010), ⁸(Ho and Murrell-Lagnado, 1999), ⁹(Rosenhouse-Dantsker et al., 2008), ¹⁰(Mao et al., 2003), ¹¹(Xu et al., 1996), ¹²(Fan and Makielski, 1997), ¹³(Ivanina et al., 2004), ¹⁴(Zhang et al., 1999), ¹⁵(Shyng et al., 2000), ¹⁶(Loussouarn et al., 2000), ¹⁷(Enkvetchakul and Nichols, 2003), ¹⁸(Drain et al., 1998), ¹⁹(Trapp et al., 1998), ²⁰(Tucker et al., 1998), ²¹(Antcliff et al., 2005), ²²(Cukras et al., 2002), ²³(Proks et al., 1999), ²⁴(Trapp et al., 2003), ²⁵(Yamada and Kurachi, 2004), ²⁶(Ueda et al., 1997), ²⁷(Light et al., 2000). Protein sequences are attached in paragraph 7. (Figure was modified after (Hibino et al., 2010)).

Physiologically, channel-PI(4,5)P₂ interactions are disrupted by the hydrolysis of PI(4,5)P₂ upon PLC activation by agonist binding to GPCRs and as a consequence the channels deactivate (Kobrinisky et al., 2000, Zhang et al., 2003). In pyramidal cells of the rodent layer V prelimbic/infralimbic cortex, e.g., PLC-triggered PI(4,5)P₂ hydrolysis after the stimulation of the muscarinic acetylcholine receptor type 1 (M1 receptor) reduced Kir2 channel currents resulting in a depolarization of the membrane and subsequent summation of excitatory synaptic potentials (Carr and Surmeier, 2007). In striatopallidal neurons, the resulting increase in the dendritic excitability and the resulting Ca²⁺ entry after Kir2 channel deactivation have been suggested to trigger the elimination of dendritic spines, a process called pruning (Shen et al., 2007). Nevertheless, it has been shown that the effect of receptor-induced PI(4,5)P₂ hydrolysis on Kir channels happens in a receptor-specific manner varying between 6 and 86% of channel inhibition (Cho et al., 2005). Therefore, it is controversial which Kir family and subfamily members are affected by PLC-mediated PI(4,5)P₂ hydrolysis (Jones, 1996, Kobrinisky et al., 2000, Selyanko et al., 2000, Lopatin and Nichols, 2001, Du et al., 2004).

2.3 Experimental approaches for examining the interaction of PI(4,5)P₂ with ion channels

2.3.1 Methods for the quantification of the PI(4,5)P₂ affinity of ion channels

The PI(4,5)P₂ affinity (as outlined in paragraph 2.2.1) is one of the most critical parameters regulating the activity of proteins in cells and organisms. In order to estimate the extend of the protein activity and the resulting influence on physiological processes at a given PI(4,5)P₂ concentration, it is indispensable to quantify the

distinct protein PI(4,5)P₂ affinities. Various methods have been used previously to estimate affinities of ion channels for PIs.

There are several approaches that have been used to evaluate the apparent PI(4,5)P₂ affinity of ion channels. First, the sensitivity of ion channels for PI(4,5)P₂ removal or enhancement can be measured. Application of the PI(4,5)P₂ sequestering substance neomycin, for example, leads to a gradual reduction of the free PI(4,5)P₂ concentration, thereby reducing channel PI(4,5)P₂ interactions that lead to channel deactivation. Vice versa, dose-dependent channel activation upon application of the water soluble PI(4,5)P₂ analogue (diC8-PI(4,5)P₂) can be measured quantitatively. For both substances, the dose-response relationships of ion channels were obtained by application to excised inside-out patches (Huang et al., 1998, Zhang et al., 1999, Xie et al., 2005, Rapedius et al., 2007a). Second, the speed of current augmentation or suppression can be measured in response to application of diC8-PI(4,5)P₂ or neomycin, respectively, to excised inside-out patches (Huang et al., 1998, Zhang et al., 1999, Xie et al., 2005, Rapedius et al., 2007a). And third, biochemical approaches such as lipid-protein overlays and pull-down assays can be used (Huang et al., 1998, Soom et al., 2001, Thomas et al., 2006).

Another powerful tool has been introduced recently. Chemically induced heterodimerization of protein domains is used to recruit PI-converting enzymes such as a PI(4,5)P₂ specific 5' phosphatase from yeast (Inp54p) or kinase to the membrane (Figure 4) (Suh et al., 2006, Varnai et al., 2006). Although in this approach no second messengers are produced and the concentration of PI(4,5)P₂ can be increased or decreased in the intact cellular environment there is no quantitative control over the level of PI(4,5)P₂ (Suh et al., 2006). Furthermore, the changes in PI(4,5)P₂ concentrations are irreversible.

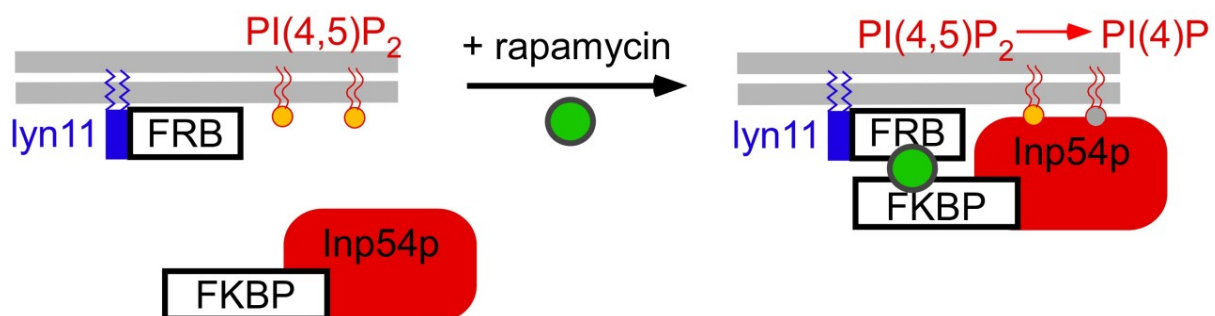


Figure 4: PI(4,5)P₂ depletion by Inp54p membrane translocation.

In the presence of rapamycin, the FRB protein (FRB: protein domain from mammalian target of rapamycin) complex dimerizes with the FK506 binding protein (FKBP) fused to Inp54p.

Membrane anchoring of FRB by fusion to the membrane targeting sequence of Lyn (FRB-Lyn11) results in rapamycin-dependent recruitment of Inp54p to the plasma membrane and PI(4,5)P₂ depletion.

Although the methods described above have been used to establish a rank order of PI(4,5)P₂ affinities for the Kir channel family and for a few additional channels from distinct ion channel families, substantial ambiguity concerning these affinities remains. This uncertainty results from a couple of drawbacks of all available methods. First, most techniques suffer from the inability to quantitatively control PI concentrations. Secondly, although diC8-PI(4,5)P₂ can be applied at defined concentrations, it may differ from endogenous PI(4,5)P₂ both in the binding properties and in its effects on channel activity. Finally, most methods (including application of diC8-PI(4,5)P₂) require the use of isolated membranes (excised patches), and therefore lack the physiological cellular environment. In summary, it is not clear, whether the relative sensitivities of channels and other effectors or sensors of PIs determined so far reflect their in-vivo properties. Moreover, the degree of PI(4,5)P₂-dependence of many other channels, and consequently the physiological relevance of any PI(4,5)P₂ modulation has remained elusive due to the lack of methods that allow for experimental control over cellular and membrane PI(4,5)P₂ levels. For this reason, novel techniques for controlling endogenous PI(4,5)P₂ concentrations in the intact cellular environment would be highly useful.

2.3.2 Genetically encoded sensors for measuring PI dynamics

Complementary to knowing the dependence of channels or other effectors on PI(4,5)P₂, understanding PI(4,5)P₂ signaling also requires detailed knowledge about the actual PI(4,5)P₂ concentration dynamics in time and space. These dynamics can be measured elegantly with genetically encoded probes.

Several proteins such as pleckstrin homology (PH) domains stereospecifically interact with distinct PIs (Lemmon, 2003). PI concentration changes that arise from activation of specific physiological processes (e.g. growth factor receptor or GPCR activation) lead either to a translocation of freely available domains towards a membrane region where the concentration is increased, or to a dissociation of bound domains from the membrane where the concentration is decreased into the cytoplasm. The lipid binding of the sensor domains can be utilized to monitor PI concentration changes by fusing them to fluorescent proteins (e.g. GFP) and

overexpression in heterologous expression systems, for example (Figure 5) (Xu et al., 2003). PI concentration increases or decreases resulting e.g. from receptor stimulation can then be measured with the help of fluorescence microscopy (Nelson et al., 2008, Quinn et al., 2008). Thus, the degree of membrane association of the PI probe represents the level of present PIs in a cellular region.

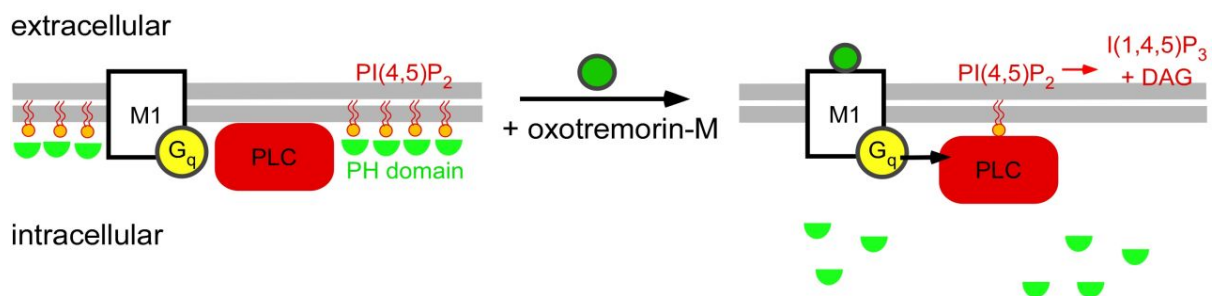


Figure 5: PLC-triggered PI(4,5)P₂ hydrolysis leads to the translocation of PI(4,5)P₂ sensor domains towards the cytoplasm.

Fluorescence labelled PH sensor proteins (green semicircles) interact with highly abundant PI(4,5)P₂ in the cell membrane (left). The fluorescence signal in the membrane is high, whereas the cytoplasmic signal is low. The hydrolysis of PI(4,5)P₂ by PLC leads to the a translocation of the sensor proteins towards the cytoplasm (right). Subsequently, the membrane signal decreases and the cytoplasmic signal increases.

Examples of proteins and PH domains that bind PIs are OSBP-PH domain for PI(4)P, TAPP1-PH domain for PI(3,4)P₂, PH domain of PLCδ1 (PLCδ1-PH domain), dynamin, class II PI3K for PI(4,5)P₂, and ARNO domain for PI(3,4,5)P₃ (Venkateswarlu et al., 1998, Kimber et al., 2002, Szentpetery et al., 2009).

As with ion channels, the PI affinity of the sensors domains may differ. Sensors with a low PI affinity can detect small concentration changes reliable, but they would be of limited usefulness in quantifying large concentration changes. A high PI affinity, however, may limit the use of a sensor domain when the increase or depletion of the PI is only moderate. Visualizing physiological dynamic PI concentration changes with a high sensitivity, therefore, requires fluorescently labelled binding probes which have a PI binding affinity that allows detecting changes in a broad physiological range.

To address PI(4,5)P₂ dynamics in particular, PLCδ1-PH has been used extensively (Varnai and Balla, 2006, Varnai et al., 2006, Szentpetery et al., 2009). However, PLCδ1-PH does not only bind to PI(4,5)P₂ but also to I(1,4,5)P₃ which is generated during breakdown of PI(4,5)P₂ by PLC. Therefore, the signal obtained with PLCδ1-PH upon activation of GPCRs may be an overestimation of receptor-induced

PI(4,5)P₂ hydrolysis, as cytosolic I(1,4,5)P₃ pulls the domain towards the cytoplasm. Consequently, it has often been unclear whether translocation of PLCδ1-PH reliably reports on changes of PI(4,5)P₂ and this led to considerable controversy and confusion in the field (Hirose et al., 1999, Szentpetery et al., 2009). Another, as yet less frequently used biosensor for PI(4,5)P₂ is the transcription factor tubby protein. Its C-terminally localized binding module (tubby-CT) mediates lipid binding and membrane localization (Santagata et al., 2001). Since tubby-CT lacks any I(1,4,5)P₃ binding (Nelson et al., 2008, Quinn et al., 2008, Szentpetery et al., 2009), it may be a more suitable PI(4,5)P₂ probe than PLCδ1-PH. However, relative affinities and thus usefulness of both sensors have been controversial. Tubby-CT appears to dissociate more slowly and less completely from the membrane than PLCδ1-PH upon activation of G_qPCRs, suggesting a higher affinity of tubby-CT (Quinn et al., 2008, Szentpetery et al., 2009). In contrast, when PI(4,5)P₂ depletion is induced by PI(4,5)P₂ phosphatases, tubby-CT readily dissociates from the plasma membrane, consistent with a low affinity for PI(4,5)P₂ (Quinn et al., 2008, Szentpetery et al., 2009).

In summary, a reliable and well-characterized sensor for PI(4,5)P₂ is pivotal for describing PI(4,5)P₂ signalling in general, and for understanding the regulation of ion channels by PI(4,5)P₂ in a physiological cellular context in particular. As noted above (paragraph 2.3.1), an approach for addressing the in-vivo PI(4,5)P₂ binding properties of both available PI(4,5)P₂ probes will require a method for the reliable experimental control over endogenous PI(4,5)P₂ concentrations. Again, these findings demonstrate that experimental control over cellular PI(4,5)P₂ is needed to settle these issues.

2.3.3 Ci-VSP as a potential novel tool to control cellular PI(4,5)P₂ levels

Recently, a PI 5' phosphatase, the *Ciona intestinalis* voltage sensor-containing phosphatase (Ci-VSP), was identified (Murata et al., 2005). The enzyme contains four channel-like TM domains which show significant sequence homology to the S1-4 segment of voltage-gated K⁺ channels (Figure 6). This positively charged voltage sensor domain is followed by a cytoplasmic phosphatase domain that is highly homologous to the PI 3' phosphatase PTEN. Experiments in *Xenopus laevis* oocytes indicated that enzymatic activity of the phosphatase domain is controlled by membrane voltage through the VSD. When expressed in heterologous expression systems, Ci-VSP displayed outward currents in response to depolarization and

inward currents in response to hyperpolarisation similar to ON and OFF gating currents of voltage-gated channels, respectively. The findings suggested that depolarization activates and repolarization deactivates the enzymatic activity (Murata et al., 2005, Murata and Okamura, 2007). The half-maximal voltage of charge movement was found to be strongly depolarized at +63 mV (Murata et al., 2005). Unlike PTEN that has 3' phosphatase activity, Ci-VSP acts as a 5' phosphatase. Recent studies (Halaszovich et al., 2008, Iwasaki et al., 2008) using total internal reflection fluorescence (TIRF) microscopy or biochemical approaches identified $PI(4,5)P_2$ and $PI(3,4,5)P_3$ as substrates and $PI(4)P$ as well as $PI(3,4)P_2$ as products of Ci-VSP (Figure 2, Figure 6).

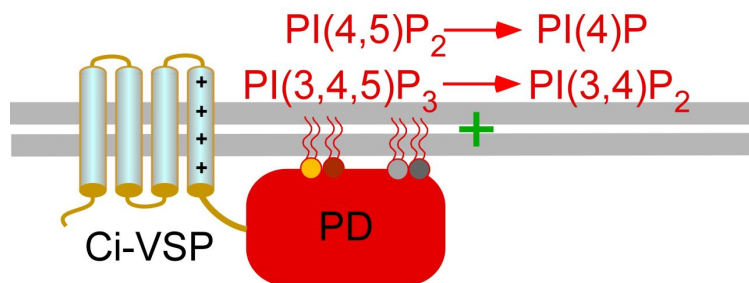


Figure 6: Ci-VSP is a voltage-dependent 5' phosphatase.

The voltage-sensor domain of Ci-VSP shows sequence homology the S1-4 segment of voltage-gated channels and is followed by a cytoplasmic domain which exhibits 5' phosphatase activity. Depolarization (+) induced activation of Ci-VSP leads to the depletion $PI(4,5)P_2$ and $PI(3,4,5)P_3$ and subsequent generation of $PI(4)P$ and $PI(3,4)P_2$.

The activation level of Ci-VSP can be controlled by variation of the cells membrane potential with the help of electrophysiological approaches. Clamping the cell membrane to varying holding potentials (V_{hold}) during whole-cell patch-clamp or two-electrode voltage clamp recordings allows for a graded alteration of $PI(4,5)P_2$ levels in the living cell. This effect was observed during combined whole-cell patch-clamp and TIRF microscopy studies in Chinese hamster ovary (CHO) cells where the fluorescence labeled $PI(4,5)P_2$ sensor domain PLC δ 1-PH and Ci-VSP were co-expressed. Depolarization of the membrane led to a decline of the membrane fluorescence indicating that the activation of Ci-VSP led to a $PI(4,5)P_2$ depletion upon depolarization (Figure 7). Repolarization of the membrane, however, led to a complete recovery of the membrane fluorescence, demonstrating the reversibility of Ci-VSP-induced $PI(4,5)P_2$ depletion. Membrane fluorescence progressively decreased with the level of depolarization, indicating that the strongest depolarization resulted in the strongest $PI(4,5)P_2$ depletion (Halaszovich et al., 2008). Furthermore,

the rapid decline of the membrane fluorescence upon the changing V_{hold} demonstrates the precise temporal control of both Ci-VSP and PI(4,5)P₂ levels.

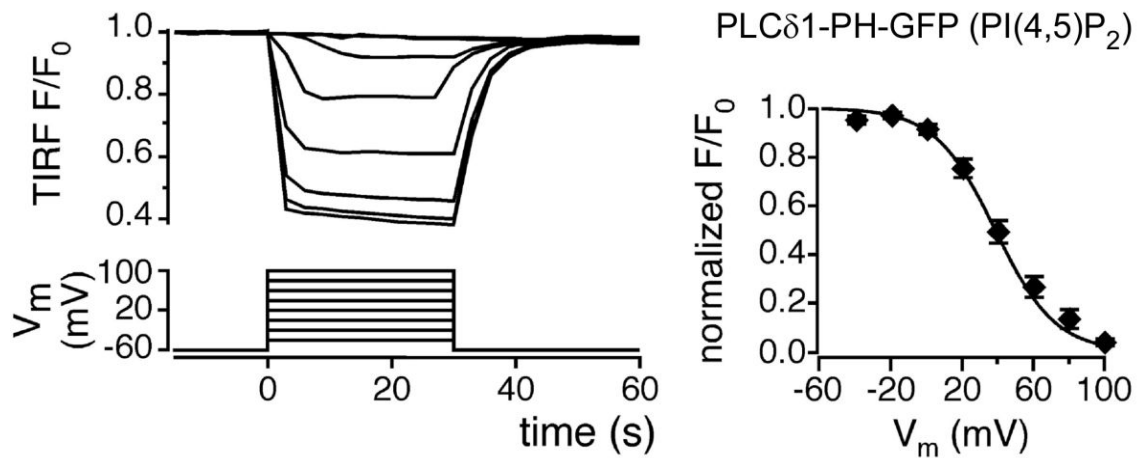


Figure 7: Reversible decline of membrane localized PLCδ1-PH-GFP fluorescence upon gradual Ci-VSP activation.

Membrane fluorescence of CHO cells co-expressing the PI(4,5)P₂ sensor PLCδ1-PH-GFP and Ci-VSP measured with TIRF microscopy. Simultaneous whole-cell patch-clamp recordings allowed membrane voltage control. Membrane depolarization led to an immediate and reversible decline of the membrane fluorescence (left). The strongest depolarization corresponds to the largest decline of the membrane fluorescence indicating graded PI(4,5)P₂ depletion (right) (modified from (Halaszovich et al., 2008)).

In conclusion, PI(4,5)P₂ depletion increases with the level of Ci-VSP activation by the strength of membrane depolarization. Ci-VSP may therefore be used as a tool to address the issue of in-vivo PI(4,5)P₂ affinities.

2.4 Aims of this study

The major goal of this work was to determine the feasibility of Ci-VSP as a general tool for the quantitative analysis of affinities of PI(4,5)P₂-binding proteins, by graded titration of endogenous PI(4,5)P₂ in intact cells. Ci-VSP was used to reevaluate the PI(4,5)P₂ affinity of a prototypical class of PI(4,5)P₂-dependent effectors, the Kir channels. Whole-cell patch-clamp recordings of CHO cells and two-electrode voltage-clamp recordings of *Xenopus laevis* oocytes co-expressing Kir channels and Ci-VSP were performed to gain voltage-control of the membrane and therefore to activate Ci-VSP gradually by varying the degree of depolarization.

Since four PIs are involved in the activity of Ci-VSP, the PI specificity of Kir channels was determined by application to inside-out giant patches excised from

oocytes in order to estimate the influence of the distinct PIs involved on the channel activity.

To this end, the sensitivity of Kir channels to Ci-VSP-mediated depletion of PI(4,5)P₂ was compared to previously established methods for changing PI concentrations. FKBP-Inp54p membrane translocation by the dimerization with FRP upon rapamycin application served as an independent approach to determine the reliability of Ci-VSP to analyze Kir channel-PI(4,5)P₂ interactions.

Next, the relationship between the PI(4,5)P₂ affinities of Kir channels derived from the Ci-VSP experiments and the channel behaviour during physiological, i.e. receptor-induced alteration of PI(4,5)P₂ concentrations was examined.

Finally, Ci-VSP was used to quantify the in-vivo PI(4,5)P₂ affinity (i.e. in the intact cell) of the two genetically encoded fluorescent PI(4,5)P₂ probes, PLCδ1-PH, domain and tubby-CT. In order to estimate the operational range of the sensors, combined patch-clamp and TIRF microscopy studies were performed to record the currents of low PI(4,5)P₂-affinity KCNQ2 channels and the membrane fluorescence during PI(4,5)P₂ depletion simultaneously.

The electrophysiological recordings on CHO cells and on *Xenopus laevis* oocytes were made in the laboratory of Prof. Dr. Bernd Fakler at the Department of Physiology II at the Albert-Ludwigs-University of Freiburg. TIRF microscopy and simultaneous patch-clamp studies were carried out in the laboratory of Prof. Dr. Dominik Oliver at the Department of Neurophysiology and Pathophysiology at the Philipps-University of Marburg.

3 Experimental procedures

3.1 Cell culture and transfection

CHO cells were cultured in Dulbecco's modified Eagle's medium (Gibco Invitrogen, Carlsbad, California/USA) supplemented with 10% fetal calf serum and 1% penicillin and streptomycin (Sigma-Aldrich, Munich, Germany) in an atmosphere of 95% air and 5% CO₂ at 37°C. For electrophysiological recordings cells were plated onto glass cover slips and transfected with jetPEI transfection reagent (Polyplus-transfection, Illkirch, France). Experiments were done 1 to 4 days after transfection. cDNA and expression vectors used are listed in Table 2.

Table 2: Vector constructs

Name	Accession	Amino acids	Vector
Kir2.1	NM_008425.4	full length	pEGFP-C1
Kir2.1R228Q	NM_008425.4 (+R228Q)	full length; aa exchange pos. 228	pEGFP-C1
Kir3.1/3.2	Y12259.1/L7848 0.1	full length, fusion	pcDNA3
GABA _B R1a	NM_031028.2	Δ aa 1-16 + aa 1-22 GluR5 at N-Terminus	pBF
GABA _B R2	CAA09592.1	Δ aa 1-41 + aa 1-22 GluR5 at N-Terminus	pBF
Kir1.1	L29403.1	full length	pBF-CMV
Kir1.1K80M	L29403.1 (+K80M)	full length; aa exchange pos. 80	pBF-CMV
Kir6.2	AF037313.1	full length	pBF
SUR1	L40624.1	full length	pGem-He
KCNQ2	Y15065.1	full length	pEGFP-C1
Ci-VSP	NP_001028998. 1	full length	pCFP-C1
M1 receptor	NM_000738.2	full length	pcD
PLCδ1-PH	P51178	1-170	pEGFP-N1
Tubby-CT	NP_068685.1	243-505	pEGFP-C1

EGFP: enhanced green fluorescent protein, aa: amino acid, pos.: position, GABA_B: gamma amino butyric acid receptor type B

Kir2.1 wild type (WT) and Kir2.1R228Q channel expression was identified through fused green fluorescent protein (GFP). Cells expressing Kir3.1/3.2 or Kir1.1 channels were identified by co-transfected GFP and electrophysiological recordings of characteristic inwardly rectified currents. Cells for electrophysiological recordings involving Ci-VSP were selected for membrane localization of red fluorescent protein (RFP)-Ci-VSP or channel deactivation characteristically observed upon depolarization. Successful functional co-expression of GABA_B receptors was confirmed by an increase of Kir3.1/3.2-mediated current upon application of GABA. Cells expressing the M1 receptor were identified by fluorescence of co-expressed GFP and function was tested by receptor-induced translocation of co-expressed PLC δ 1-PH-GFP. In experiments with PLC δ 1-PH and tubby-CT, expression was identified through fused GFP.

3.2 Electrophysiology on CHO cells

Patch-clamp experiments were performed in whole-cell configuration as described (Hamill et al., 1981) with an EPC-9 patch-clamp amplifier (HEKA, Lambrecht, Germany). Patchmaster software 2.32 (HEKA) was used for data acquisition. Experiments were performed at room temperature (22 – 24°C). Solutions used are given in Table 3.

Cells plated on glass cover slips were superfused with extracellular solution and observed through a BX50WI upright microscope (Olympus Deutschland GmbH, Hamburg, Germany). The filters EGFP HC Filterset (Bandpass) (AHC analysentechnik AG, Tübingen, Germany) and cyano fluorescent protein (CFP) HC Filterset (Bandpass) (AHC analysentechnik AG) were used for identification of transfected cells. Patch pipettes were pulled from quartz glass tubing (outer diameter, 1 mm; inner diameter, 0.7 mm) (Sutter Instrument, Novato/California, USA). When filled with intracellular solution, the resistance was 2 – 3 M Ω . The series resistance (2 – 10 M Ω) was not compensated. Pipettes were positioned with a Luigs & Neumann manipulator (Luigs & Neumann Feinmechanik und Elektrotechnik GmbH, Ratingen, Germany).

Table 3: Solutions for whole-cell recordings in CHO cells

Ingredients	Extracellular Solutions		Pipette Solution	Producer
	Kir2.1, Kir1.1, KCNQ	Kir3.1/3.2	all channels	
KCl	5.8 mM	20 mM	135 mM	Merck, Darmstadt, Germany
NaCl	144 mM	129.8 mM		Merck
MgCl ₂	0.9 mM	0.9 mM	2.5 mM	Merck
CaCl ₂	1.3 mM	1.3 mM	0.1 μ M (0.241 ml of 1 M stock solution)	Sigma-Aldrich ¹
NaH ₂ PO ₄	0.7 mM	0.7 mM		Merck
Glucose	5.6 mM	5.6 mM		Roth, Karlsruhe, Germany
HEPES	10 mM	10 mM	5 mM	Merck
EGTA			5 mM	Fluka, Steinheim, Germany
Na ₂ ATP			3 mM	Sigma-Aldrich
Na ₃ GTP			0.1 mM ²	Sigma-Aldrich
Spermine			10 μ M ³	Sigma-Aldrich
pH	7.4	7.4	7.3	
adjusted with	NaOH	NaOH	KOH	Roth (NaOH), Merck (KOH)

¹ producer in all solutions, except of OR-2 solution (see Table 4)

² Na₃GTP was not added during patch-clamp recordings with Ci-VSP

³ Spermine was omitted for patch-clamp recordings with KCNQ channels

InSolutionTM Rapamycin dissolved in dimethyl sulfoxide stock solution was purchased from Merck. Oxotremorin-M (Tocris, Ellisville/ Missouri, USA) was dissolved in extracellular solution. Final concentrations for rapamycin and oxotremorin-M diluted in extracellular solution were 5 μ M and 10 μ M, respectively. Kir (KCNQ) currents were filtered at 2.9 kHz and sampled at 50 kHz (20 kHz). Rapamycin and oxotremorin-M containing solutions were applied to CHO cells via a custom-made single-barrelled application device. Kir currents were evoked by test pulses to -100 mV applied every 2 or 3 s as indicated with V_{hold} of -60 mV. KCNQ

currents were evoked by test pulses to 0 mV applied every second or every 6 s as indicated with V_{hold} of -60 mV. Step protocols for Kir and KCNQ current recordings are shown in Figure 8.

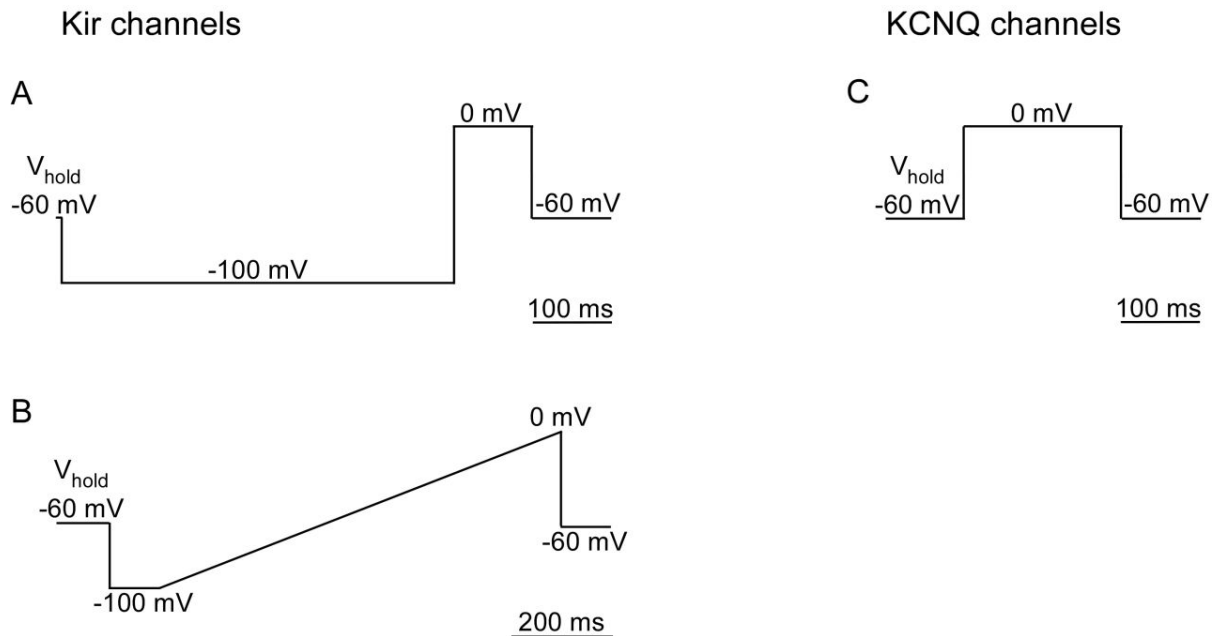


Figure 8: Step protocols for Kir and KCNQ current whole-cell recordings in CHO cells.

Protocols were used for recordings shown in Figure 11 and Figure 12 (A) Figure 15, Figure 26, and Figure 27A, B (B), and in Figure 14, Figure 27C, Figure 29, and Figure 30 (C).

3.3 *Xenopus laevis* oocyte preparation

Xenopus laevis oocytes were removed surgically from adult females, dissected manually, and stored in OR-2 solution (Table 4). About 50 nl of cRNAs containing solutions were injected. Oocytes were treated with 0.5 mg/ml collagenase type II (Sigma-Aldrich) and incubated in OR-2 solution at 18°C for 1 – 3 days before use. The follicle layer was removed with a pair surgical forceps immediately before two-electrode voltage clamp recordings. Additionally, the vitellin layer was removed for inside-out patch-clamp experiments.

Table 4: Solution for storage and incubation of oocytes

Ingredients	OR-2 solution	Producer
KCl	2.5 mM	
NaCl	82.5 mM	
Na ₂ HPO ₄	1 mM	Merck
PVP (M360.000)	0.5 g/l	Sigma
MgCl ₂	1 mM	
CaCl ₂	1 mM	Fluka
Penicillin	10,000 units/ml	Invitrogen, Darmstadt, Germany
Streptomycin	10,000 µg/ml	Invitrogen
HEPES	5 mM	
pH	7.3	
adjusted with	NaOH	

3.4 Electrophysiology on oocytes

3.4.1 Two-electrode voltage clamp recordings

Two-electrode voltage clamp recordings were performed with a Turbo tec-10 cx npi amplifier (npi electronic GmbH, Tamm, Germany). Patchmaster 2.32 software was used for data acquisition. Experiments were performed at room temperature (22 – 24°C). Solutions used are given in Table 5.

Table 5: Solutions for two-electrode voltage clamp recordings from oocytes

Ingredients	Extracellular Solutions		Electrode Solution
	Kir2.1	Kir3.1/3.2	all channels
KCl	3 mM	20 mM	3 M
NaCl	114.5 mM	97.5 mM	
MgCl ₂	0.9 mM	0.9 mM	
CaCl ₂	1.8 mM	1.8 mM	
HEPES	10 mM	10 mM	
pH	7.3	7.3	
adjusted with	NaOH	NaOH	

For some experiments with Kir3 channels, GABA (Merck) and tertiapin-Q (Tocris) were added to the bath solution at concentrations of 1 mM and 1 μ M, respectively. Electrodes were pulled from borosilicate glass tubing (outer diameter, 0.86 mm; inner diameter, 1.5 mm) (Science products, Hofheim, Germany). Pipette tips were broken with a microforge under microscopic observation to obtain a resistance between 0.2 and 1 M Ω . Kir currents were filtered at 1 kHz and sampled at 10 kHz. Currents were recorded in response to voltage ramps (-100 mV – 0 mV) applied every 3 s ($V_{\text{hold}} = -60$ mV) (Figure 9).

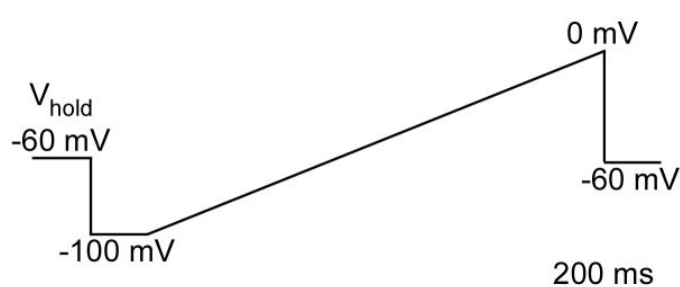


Figure 9: Ramp protocol for measuring Kir currents by two-electrode voltage clamp.

This protocol applies to data shown in Figure 13 and Figure 16.

3.4.2 Inside-out giant patch recordings

Inside-out patch-clamp recordings were performed with a protocol simplified from (Collins et al., 1992) by using an EPC-9 patch-clamp amplifier. Patchmaster 2.32 software was used for data acquisition, with low-pass filtering set to 2.9 kHz and a sampling rate of 10 kHz. Experiments were performed at room temperature (22 – 24°C). Solutions used are given in Table 6.

Table 6: Solutions for inside-out patch-clamp recordings in oocytes

Ingredients	Extracellular Solutions		Intracellular solutions	
	low K ⁺	high K ⁺	with Mg ²⁺	without Mg ²⁺
KCl	3 mM	120 mM	116 M	100 mM
NaCl	117 mM			
MgCl ₂			1.1 mM	
CaCl ₂	1 mM	1 mM		
HEPES	10 mM	10 mM	10 mM	10 mM
EGTA			2 mM	10 mM
pH	7.2	7.2	7.2	7.2
adjusted with	NaOH	KOH	KOH	KOH

Oocytes were put in the recording chamber and allowed to adhere to the glass bottom for ten minutes. They were observed through an inverse Zeiss Axiovert 25 microscope (Carl Zeiss AG, Jena, Germany). Electrodes were positioned with a Spindler & Hoyer manipulator (Spindler & Hoyer GmbH, Göttingen, Germany) electrically driven by a manipulator unit purchased from Bachofer (Bachofer Laboratoriumsgeräte, Reutlingen, Germany). Electrodes were pulled from thick-wall borosilicate glass tubing (outer diameter, 2 mm; inner diameter, 1 mm) (glass: Hilgenberg, Malsfeld, Germany; preparation of tubings: Zinsstag GmbH, Stuttgart, Germany). Electrode tips were fire polished and briefly immersed in paraffin oil (Sigma-Aldrich), before back-filling with extracellular solution. Open pipette resistance was 0.2 – 0.5 M Ω . Oocytes were superfused with intracellular solution. Giant patches were excised after gigaseal formation and quick withdrawal of the pipette, thus ripping the membrane patch off the cell. Subsequently, the intracellular side of the membrane patch attached to the pipette faced the intracellular solution. Ramp protocols for Kir current inside-out patch-clamp recordings in oocytes are shown in Figure 10.

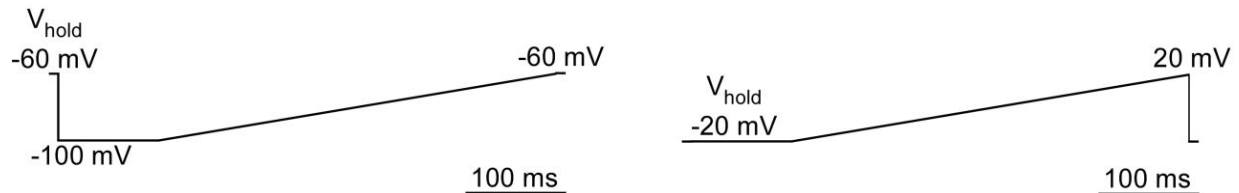


Figure 10: Ramp protocol for measuring Kir currents in inside-out giant patches.

This protocol applies to data shown in Figure 18 – Figure 25 (left) and Figure 22B (right).

Stock solutions of PIs (PI(4,5)P₂ and PI(3,4,5)P₃ (Avanti Polar Lipids, Alabaster/Alabama, USA); PI(3,4)P₂ and PI(4)P (Merck)) (10 mM) were prepared with intracellular solution without Mg²⁺ by sonication for 15 min twice. The working concentration of each PI solution applied to the cytoplasmic face of giant patches was 10 μ M prepared from frozen stock solutions each day by sonication for ten minutes twice in Mg²⁺-free intracellular solution. Solutions were applied via a custom-made multi-barrelled application system.

3.5 Fluorescence microscopy

TIRF microscopy recordings were performed with a BX51WI upright microscope (Olympus, Hamburg, Germany) equipped with a EGFP filter (EGFP HC Filterset Bandpass filter), a HQ TIRF-condenser (NA 1.45; Olympus) and a 488 nm laser (20 mW; Picarro, Sunnyvale, California/USA). A LUMPlanFI/IR 40x/0.8 NA water-immersion objective (Olympus) was used for fluorescence imaging and a TILL-Imago QE cooled CCD camera (TILL photonics, Gräfelfing, Germany) was used for image acquisition. Wide-field fluorescence illumination was obtained with a monochromator (Polychrome IV; TILL photonics) which was coupled to the BX51WI through fiber optics. GFP (RFP) fluorescence was excited at a wave length of 488 nm (569 nm). TILLvision software (TILL-photonics) was used to control the laser shutter for TIRF illumination, the monochromatic light source and image acquisition. The sample interval for image acquisition was 1 s for Ci-VSP experiments and 6 s for M1 receptor experiments.

3.6 Data analysis and statistics

Data were analyzed using Patchmaster software and IgorPro (Wavemetrics, Lake, Oswego, Oregon/USA). Steady state deactivation curves obtained during Ci-VSP experiments (Figure 12 – Figure 16) were calculated after one minute of depolarization and fitted with the Boltzmann function $I = I_{min} + (I_{max} - I_{min}) / (1 + \exp((V - V_{1/2})/s))$, where I denotes the current amplitude, V is membrane voltage, $V_{1/2}$ is the voltage of half-maximal current inhibition and s is the steepness of the curve. Data were normalized to the average of the baseline currents obtained before depolarization. The time constants (τ) in all experiments (Figure 12 – Figure 16, Figure 28) were obtained from monoexponential fits. All data are given as \pm standard error of the mean (SEM). Statistics were calculated with IBM SPSS 17.0 (IBM Corporation, Somers/New York, USA) for MS Excel. Gaussian distribution was verified for all data by the use of the Kolmogorow-Smirnow-test. Because all data were normally distributed, differences were tested with student's t-test. Stars represent significant differences between $p < 0.05$ and 0.001 (indicated in the text).

4 Results

4.1 Quantification of the PI(4,5)P₂ affinities of K⁺ channels using Ci-VSP

4.1.1 Effects of Ci-VSP activity on Kir2.1WT channels

Kir2.1WT channels were chosen as an initial paradigm for testing the responsiveness of PI(4,5)P₂ effector proteins to PI(4,5)P₂ depletion by Ci-VSP. CHO cells that represent a simple recombinant system were co-transfected with Kir2.1WT channels and Ci-VSP. Whole-cell patch-clamp recordings, allowing for the precise control of membrane voltage, were performed on transfected CHO cells. Stable baseline currents mediated by Kir2.1WT were obtained at a V_{hold} of -60 mV (Figure 11A, B) where Ci-VSP is known to be inactive (Murata et al., 2005, Halaszovich et al., 2008). Activation of Ci-VSP by depolarization to +60 mV (Figure 11A, B) induced a nearly complete decline of Kir2.1WT currents to residual amplitudes of $7.6 \pm 4\%$ (Figure 11C). Currents recovered upon repolarization to -60 mV (Figure 11A, B). In the absence of Ci-VSP, depolarization failed to affect the current amplitudes (current amplitude: $88 \pm 3.4\%$, $p < 0.001$) (Figure 11B, C). These findings indicate that channel closure results from activation of Ci-VSP, consistent with depletion of PI(4,5)P₂ (Halaszovich et al., 2008). Consequently, recovery of the currents most likely resulted from replenishment of PI(4,5)P₂ via cellular resynthesis as suggested previously (Halaszovich et al., 2008).

Having established sensitivity of Kir2.1WT to Ci-VSP-induced PI(4,5)P₂ depletion, next, gradual activation of Ci-VSP was used to test for a quantitative relation between enzymatically controlled PI(4,5)P₂ levels and channel activity (Halaszovich et al., 2008). Depolarizing voltage steps to various V_{hold} were used to gradually activate Ci-VSP (Figure 12A, B). Subsequent PI(4,5)P₂ depletion led to a V_{hold} -dependent current decline. The largest current decline corresponded to the strongest depolarization. Plotting the mean normalized steady state currents against the corresponding V_{hold} yielded sigmoid steady state deactivation curves. Fitting the data with a Boltzmann function yielded a $V_{1/2}$ of 34.1 ± 1.7 mV (Figure 12D). Values of $V_{1/2}$ were reproducible across many individual cells, thus providing a quantitative description of the channel's affinity for PI(4,5)P₂.

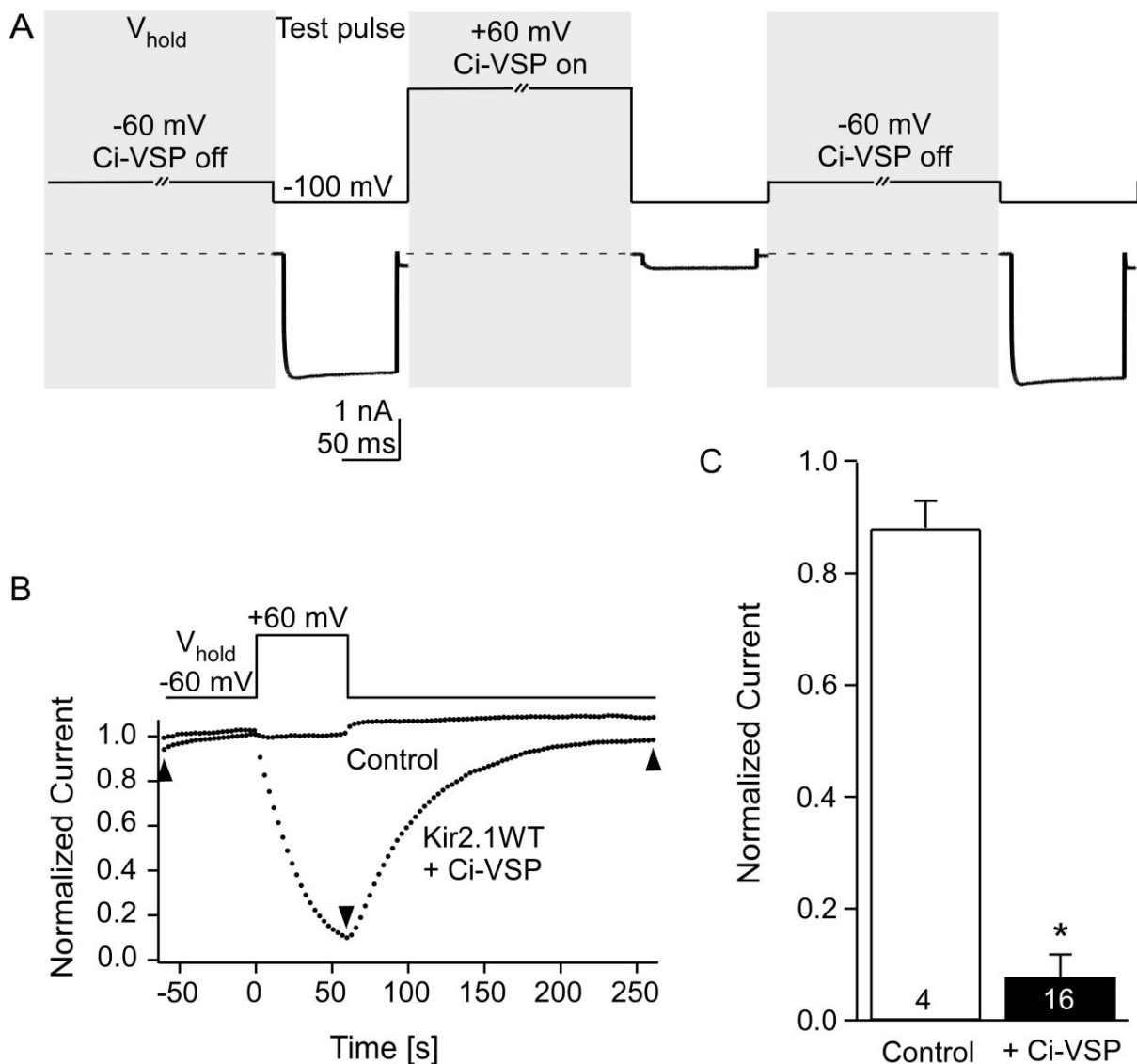


Figure 11: Deactivation of Kir2.1WT channels upon Ci-VSP activation.

A Representative whole-cell currents from a CHO cell co-expressing Kir2.1WT and Ci-VSP. Starting from a V_{hold} (upper trace, interrupted bars) of -60 mV, baseline Kir2.1WT currents (lower trace) were evoked by test pulses to -100 mV (upper trace, continuous bars) applied every 3 s. Ci-VSP was activated by depolarization (V_{hold} of +60 mV) and subsequently inward currents declined. Currents recovered to the initial level upon repolarization (V_{hold} of -60 mV).

B Normalized currents of a CHO cell co-expressing Kir2.1WT and Ci-VSP. Currents declined when Ci-VSP was activated by depolarization to +60 mV (Kir2.1WT + Ci-VSP). Current decline upon depolarization was not observed when Ci-VSP was not co-expressed (Control). Current amplitudes were measured 10 ms before the end of each test pulse. Arrowheads indicate time points of current traces shown in A.

C Summary data of experiments as in (B) show significant channel inhibition by activation of Ci-VSP. Numbers of independent experiments as indicated.

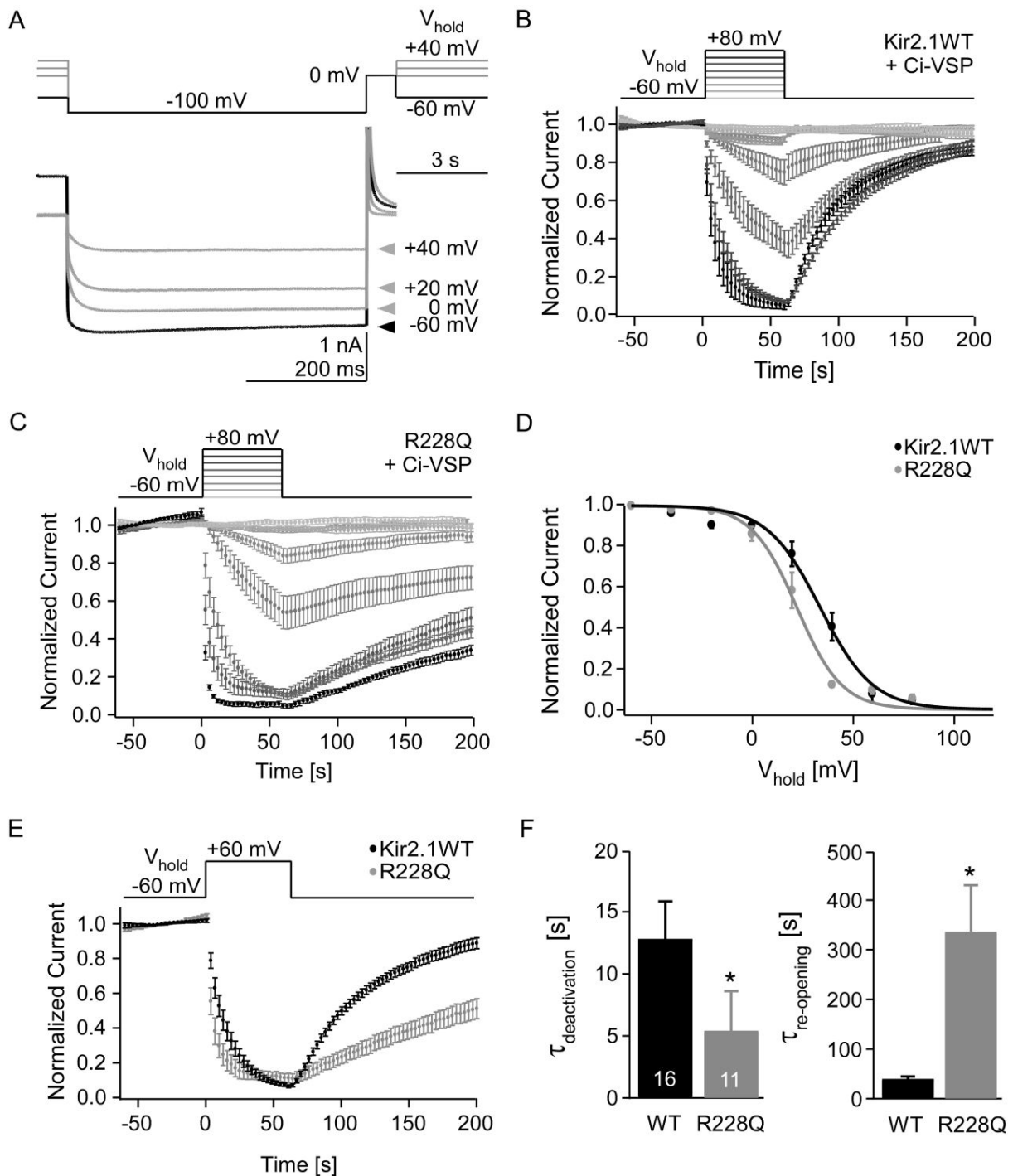


Figure 12: Kir2.1 channel deactivation upon activation of Ci-VSP measured in CHO cells.

A Representative whole-cell currents of a CHO cell co-expressing Kir2.1WT channels and Ci-VSP. Starting from a V_{hold} of -60 mV (upper panel, black) test pulses to -100 mV were applied every 3 s. The cell was depolarized to different V_{hold} (0 mV, +20 mV, and +40 mV) to gradually activate the Ci-VSP (upper panel, grey). Kir2.1WT currents declined upon Ci-VSP activation depending on the degree of depolarization (lower panel, grey).

B, C Mean normalized Kir2.1WT (B, $n = 10 - 16$ cells) or Kir2.1R228Q currents (C, $n = 6 - 11$ cells). Ci-VSP was gradually activated by increasing depolarization between -60 mV and +80 mV in 20 mV steps for 1 min. Current amplitudes were averaged over the last 10 ms of each test pulse.

D Steady state deactivation curves of Kir2.1WT (black) and Kir2.1R228Q (grey) after gradual Ci-VSP activation for 1 min obtained from experiments in B and C. Steady state

deactivation curve of Kir2.1R228Q channels was shifted towards hyperpolarisation compared to that of Kir2.1WT channels. Continuous curves are Boltzmann fits to the averaged data.

E Mean normalized Kir2.1WT (n = 16, black) and Kir2.1R228Q currents (n = 11, grey) before, during and after depolarization to +60 mV.

F Summary data of experiments as in (E) show significant differences for $\tau_{\text{deactivation}}$ and $\tau_{\text{re-opening}}$ between WT and mutant channels. Numbers of independent experiments as indicated.

4.1.2 Quantification of the PI(4,5)P₂ affinities of Kir2.1WT and Kir2.1R228Q channels

The responsiveness of the channels to gradual activation of Ci-VSP characterized as $V_{1/2}$ should directly reflect the channel's PI(4,5)P₂ affinity. In order to test this hypothesis, similar channels exhibiting a different PI(4,5)P₂ affinity were examined. Kir2.1WT was previously characterized as a high affinity channel (Huang et al., 1998). Many point mutations, usually removing a positive charge at a putative PI interaction site, have been reported to reduce the PI(4,5)P₂ affinity and subsequently lead to severe diseases such as Anderson's syndrome (Zhang et al., 1999). The positively charged arginine at position 228 in Kir2.1 channels e.g. is a well-known amino acid interacting with PI(4,5)P₂. Its replacement with a glutamine affects the PI(4,5)P₂ interaction and therefore reduces binding affinity (Zhang et al., 1999, Lopes et al., 2002). Therefore, the sensitivity of Kir2.1R228Q to gradual Ci-VSP activation was examined, again using whole-cell patch-clamp recordings (Figure 12C). Kir2.1R228Q channels, in principle, behaved similar to WT channels upon Ci-VSP-induced PI(4,5)P₂ depletion. However, characteristic differences were observed: channel deactivation was significantly faster for Kir2.1R228Q mutant channels compared to Kir2.1WT channels ($\tau_{\text{deactivation, Kir2.1R228Q}} = 5.4 \text{ s} \pm 0.7 \text{ s}$ vs $\tau_{\text{deactivation, Kir2.1WT}} = 12.8 \text{ s} \pm 3 \text{ s}$, $p < 0.05$) when Ci-VSP was activated (Figure 12E, F left). Vice versa, current recovery was significantly slower for the mutant ($\tau_{\text{re-opening, Kir2.1R228Q}} = 428.1 \text{ s} \pm 98.5 \text{ s}$ vs $\tau_{\text{re-opening, Kir2.1WT}} = 40.6 \text{ s} \pm 5.1 \text{ s}$, $p < 0.01$) (Figure 12E, F right). Interestingly, the fit of the steady state deactivation with a Boltzmann function was shifted towards hyperpolarizing potentials in comparison to WT channels and yielded a $V_{1/2, \text{Kir2.1R228Q}}$ of $21.6 \pm 1.5 \text{ mV}$ (Figure 12D). These results indicate that a smaller degree of depolarization and therefore less Ci-VSP activation and less PI(4,5)P₂ depletion was necessary to deactivate Kir2.1R228Q channels to the same degree as WT channels.

This conclusion is equivalent to a reduced PI(4,5)P₂ affinity of the mutant channel, matching the expectation from the previously published affinities for Kir2.1WT and mutant Kir2.1R228Q. Gradual Ci-VSP activation therefore allows the quantification of the relative (apparent) PI(4,5)P₂ affinities of ion channels. Specifically, V_{1/2} appears to yield a quantitative measure for this binding affinity.

Additionally, equivalent experiments were performed in *Xenopus laevis* oocytes using the two-electrode voltage clamp technique (Figure 13). Steady state deactivation curves of Kir2.1WT channels and Kir2.1R228Q channels during Ci-VSP activation gave similar results in comparison to those obtained for mammalian CHO cells (V_{1/2,Kir2.1WT} = 40.7 ± 1.4 mV vs V_{1/2,Kir2.1R228Q} = 25.9 ± 1.8 mV) (Figure 13 A – D). Channel inhibition upon activation of Ci-VSP upon depolarisation to +60 mV was significantly faster for Kir2.1R228Q compared to Kir2.1WT (τ_{deactivation,Kir2.1R228Q} = 3.7 s ± 0.7 s vs τ_{deactivation,Kir2.1WT} = 10.8 s ± 2.3 s, p < 0.001) and recovery was significantly slower (τ_{re-opening,Kir2.1R228Q} = 91.4 s ± 18.9 s vs τ_{re-opening,Kir2.1WT} = 10.1 s ± 1.1 s, p < 0.001) (Figure 13E, F).

In summary, the sensitivity of Kir2.1 channels to activation of Ci-VSP was quantitatively very similar despite the use of two highly distinct model systems (mammalian cells (CHO) and *Xenopus laevis* oocytes), indicating that Ci-VSP is well suited to determine the PI(4,5)P₂ affinity of ion channels as effector proteins across a large diversity of cellular systems.

Having established Ci-VSP as a tool to quantify the high PI(4,5)P₂ affinity of Kir2.1WT and the reduced affinity of mutant channels, I next applied this tool to other K⁺ channels, the KCNQ channels, and to selected members within the Kir channel family, that have been proposed to largely differ in their interaction with PIs.

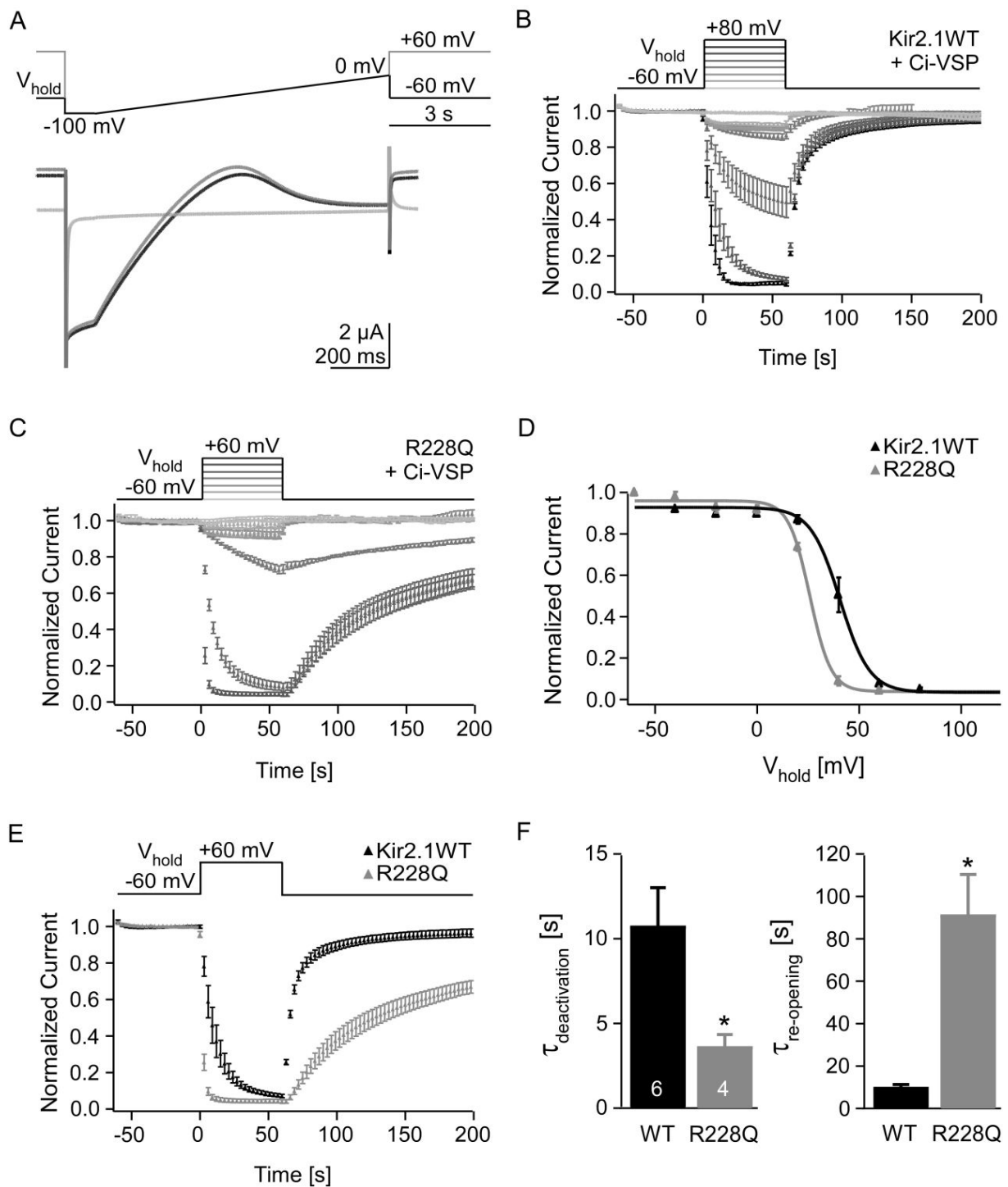


Figure 13: Kir2.1 channel deactivation upon activation of Ci-VSP measured in *Xenopus laevis* oocytes.

A Representative currents of an oocyte co-expressing Kir2.1WT and Ci-VSP before (black), during (light grey), and after (dark grey) Ci-VSP activation. Ramp protocol was applied every 3 s.

B, C Mean normalized Kir2.1WT (B, $n = 6 - 10$ oocytes) or Kir2.1R228Q currents (C, $n = 2 - 8$ oocytes) after gradual Ci-VSP activation as described in Figure 12.

D Steady state deactivation curves of Kir2.1WT (black) and Kir2.1R228Q channels (grey) after gradual Ci-VSP activation for 1 min obtained from experiments as in B and C. Continuous curves are Boltzmann fits to the averaged data.

E Mean normalized Kir2.1WT ($n = 6$, black) or Kir2.1R228Q currents ($n = 4$, grey) before, during, and after depolarization to +60 mV.

F Summary data of experiments as in (E) show significant differences for $\tau_{\text{deactivation}}$ and $\tau_{\text{re-opening}}$ between WT and mutant channels. Numbers of independent experiments as indicated.

4.1.3 Quantification of KCNQ channel-PI(4,5)P₂ affinity

The possibility of quantifying the PI(4,5)P₂ affinity with Ci-VSP is not restricted to the Kir channel family. The PI(4,5)P₂ affinities of another class of K⁺ channels, the KCNQ channels, were successfully quantified using Ci-VSP (Figure 14). CHO cells were co-transfected either with homomeric KCNQ2 or KCNQ3 channels or with heteromeric KCNQ2/3 channels and whole-cell patch-clamp recordings were performed. Steady state deactivation curves were obtained after gradual Ci-VSP-induced PI(4,5)P₂ depletion induced by depolarization from -60 to +80 mV (KCNQ3) or to +100 mV (KCNQ2, KCNQ2/3) in 20 mV steps. Fitting the curves with a Boltzmann function yielded a $V_{1/2}$ that was most depolarized for KCNQ3 channels ($V_{1/2} = 23.3 \pm 2.7$ mV, $n = 12$), most hyperpolarized for KCNQ2 channels ($V_{1/2} = -22.7 \pm 1.1$ mV, $n = 11$), and intermediate for KCNQ2/3 channels ($V_{1/2} = -2.6 \pm 1.2$ mV, $n = 10$). These data indicate high, low, and intermediate PI(4,5)P₂ affinities, respectively. This rank order nicely corresponds to the affinities previously established through measuring dose-response curves by application of diC8-PI(4,5)P₂ to these channels in inside-out patches (Li et al., 2005).

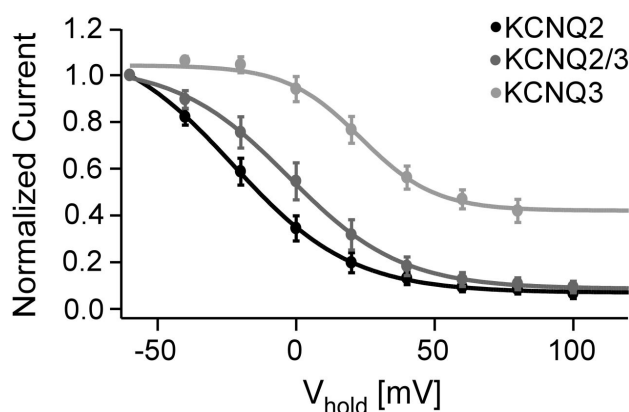


Figure 14: KCNQ channel deactivation upon activation of Ci-VSP in CHO cells.

Steady state deactivation curves of KCNQ2 (black), KCNQ2/3 (dark grey) and KCNQ3 (light grey) after gradual Ci-VSP activation for 1 min. Continuous curves are Boltzmann fits to the averaged data.

4.1.4 Quantification of Kir1.1WT channel-PI(4,5)P₂ affinity

Next, Ci-VSP was used to quantify the PI(4,5)P₂ affinity a second member of the Kir channel family, Kir1.1, that was reported to exhibit an intermediate PI(4,5)P₂ affinity,

lower than that of Kir2.1WT channels (Huang et al., 1998). To confirm this, CHO cells were co-transfected with Ci-VSP and Kir1.1WT channels. Similar to the results obtained with Kir2.1, activation of Ci-VSP by depolarization to +60 mV led to a reversible decline in current (Figure 15A). Current decline was never observed when Ci-VSP was not co-expressed (n = 2). Gradual Ci-VSP activation by depolarization between -60 and +100 mV in 20 mV steps led to a V_{hold} dependent current decline. Fitting the data obtained with a Boltzmann function yielded a $V_{1/2, \text{Kir1.1WT}}$ of 12.4 ± 2.9 mV (Figure 15C).

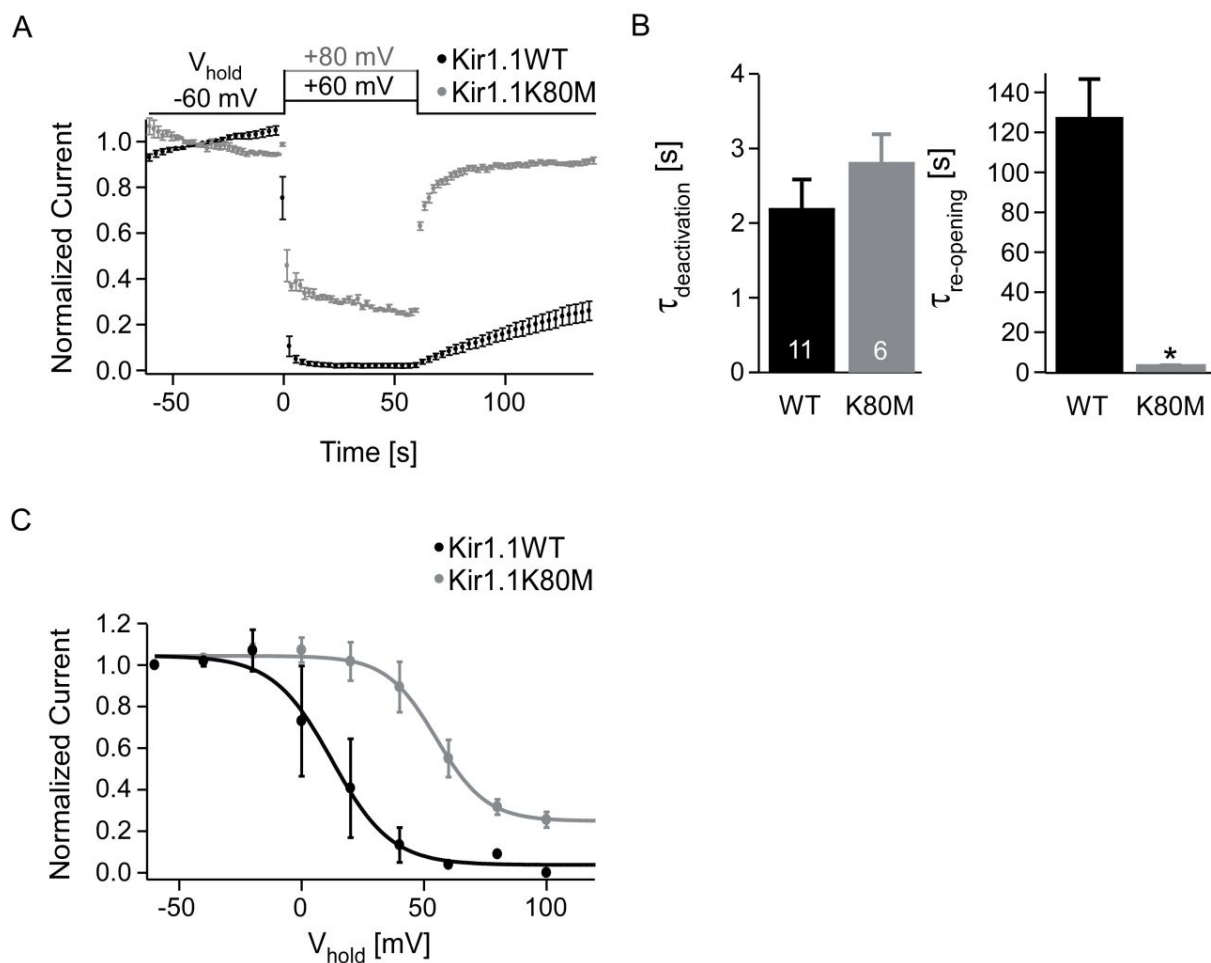


Figure 15: Kir1.1 channel deactivation upon activation of Ci-VSP measured in CHO cells.

A Mean normalized currents of CHO cells co-expressing Ci-VSP and Kir1.1WT (n = 11 cells, black) or Kir1.1K80M channels (n = 4, grey) before, during, and after Ci-VSP activation by depolarization to +60 mV (Kir1.1WT) or +80 mV (Kir1.1K80M). Ramp protocols were applied every 3 (Kir1.1WT) or 2 s (Kir1.1K80M). Current amplitudes were averaged over the last 10 ms of each test pulse.

B Summary data of experiments as in (A) show significant differences for $\tau_{\text{re-opening}}$ and show no difference for $\tau_{\text{deactivation}}$ between Kir1.1 channels and mutant channels. Numbers of independent experiments as indicated.

C Steady state deactivation of Kir1.1WT (n = 2 – 11 cells, black) and Kir1.1K80M (n = 7 – 9 cells, grey), after gradual Ci-VSP activation for 1 min. Continuous curves are Boltzmann fits to the averaged data.

4.1.5 Quantification of Kir1.1K80M channel-PI(4,5)P₂ affinities

Kir1.1WT channel activity strongly depends on the extracellular K⁺ concentration. Channel deactivation induced e.g. by PI(4,5)P₂ depletion results in the collapse of the channel pore at the selectivity filter (also named K⁺ inhibition) in zero or low concentrations of extracellular K⁺, leading to a prolonged rate of channel re-activation (Schulte et al., 2001, Dahlmann et al., 2004, Rapedius et al., 2007a). Because the recordings here were performed under physiological low extracellular K⁺ conditions, it is likely that downstream effects of Kir1.1WT channels may be monitored during Ci-VSP activity, e.g. an artificially prolonged channel re-opening time upon PI(4,5)P₂ resynthesis by the pore collapse. Furthermore, it can not be ruled out that due to the K⁺ inhibition the steady state deactivation curve was shifted towards hyperpolarized values, apparently indicating a lower channel-PI(4,5)P₂ affinity than expected.

Amino acid K80 is the sensor for changes of extracellular K⁺ concentrations and a mutation at this position decouples the channels from K⁺-sensitivity, thereby increasing the activation rate after channel deactivation (Rapedius et al., 2007a). Therefore, K80M was subjected to PI(4,5)P₂ depletion by Ci-VSP with the expectation that the mutant's behaviour more accurately reflects the interaction of the channel with PI(4,5)P₂. Previous work (Rapedius et al., 2007a) where PI(4,5)P₂ sequestration by neomycin was used to quantify the channel's PI(4,5)P₂ affinities, found, that the affinities of WT and K80 mutant channels were similar. In order to establish Kir1.1K80M as a representative channel with intermediate PI(4,5)P₂ affinity being K⁺ insensitive, whole-cell recordings of CHO cells co-expressing Kir1.1K80M channels and Ci-VSP were performed. As found for the WT channel, activation of Ci-VSP by depolarization to +80 mV led to a reversible decline of Kir1.1K80M currents (Figure 15A). Analysis of the channel kinetics upon Ci-VSP activation showed that the K80M mutation significantly speeded up the re-opening kinetics in comparison to WT channels ($\tau_{\text{re-opening, Kir1.1K80M}} = 4 \pm 0.5 \text{ s}$ vs $\tau_{\text{re-opening, Kir1.1WT}} = 127 \pm 20.5 \text{ s}$, $p < 0.001$) (Figure 15A, B right). Channel deactivation, however, was similar for WT and mutant channels ($\tau_{\text{deactivation, Kir1.1WT}} = 2.2 \pm 0.4 \text{ s}$ and $\tau_{\text{deactivation, Kir1.1K80M}} = 2.8 \pm 0.2 \text{ s}$) (Figure 15A, B left). These findings agree with the results of previous

studies (Rapedius et al., 2007a), where deactivated Kir1.1WT channels re-opened significantly slower than K80 mutant channels. The underlying mechanism describing this observation was suggested to be the helix bundle crossing between K80 in TM1 and A177 in TM2 of Kir1.1 channels (Rapedius et al., 2007a). This correlation between the formation of TM1-TM2 hydrogen (H) bonding and the channel re-opening rate indicates that the activation energy for channel opening is determined by the ability of H bonding in the closed state. The finding that the rate of channel re-opening, but not deactivation, was affected, led to the consideration that a rupture of this H bond occurs upon channel opening (Rapedius et al., 2007a). The observations obtained after Ci-VSP activation demonstrate that the channel activity changes upon activation of Ci-VSP not simply reflect the unbinding of PI(4,5)P₂ to the channel, but rather a multi-step transition including conformational changes downstream of binding or unbinding of the lipid. The sensitivity to Ci-VSP thus yields an 'apparent' affinity, rather than a description of the true binding properties.

The steady state channel deactivation curve of Kir1.1K80M channels obtained with gradual Ci-VSP activation by depolarization between -60 mV and +100 mV was shifted towards depolarized values in comparison to that of Kir1.1WT channels. Fitting the data with a Boltzmann function yielded a $V_{1/2, K80M}$ of 55 ± 1.6 mV (Figure 15C). However, the $V_{1/2}$ of Kir1.1K80M was unexpectedly more depolarized than that of Kir1.1WT, indicating an increase of the apparent PI(4,5)P₂ affinity due to the K80 mutation. These results allow the conclusion that contrary to previous studies (Rapedius et al., 2007a), the apparent PI(4,5)P₂ affinity of Kir1.1K80M channels is higher than that of Kir1.1WT channels. Nevertheless, the apparent affinity of Kir1.1WT channels was, consistent with previous estimates, lower than that of Kir2.1WT channels (Huang et al., 1998).

4.1.6 Quantification of Kir3.1/3.2 channel-PI(4,5)P₂ affinity

Subsequently, the PI(4,5)P₂ affinity of Kir3.1/3.2 channels as a third member of the Kir channel family was examined with Ci-VSP. These experiments were performed in *Xenopus laevis* oocytes, because the obtained expression levels were higher than in CHO cells and possible effects were expected to be markedly visible. Kir3.1/3.2 heterotetrameric channels were expressed together with Ci-VSP in oocytes, and two-electrode voltage clamp recordings were performed. Depolarization induced Ci-VSP

activation led to a reversible decline in Kir3.1/3.2 currents (Figure 16C). Current decline was never observed when Ci-VSP was not co-expressed ($n = 3$). Gradual activation of Ci-VSP by increasing depolarization from -60 mV to +60 mV in 20 mV steps resulted in a current decline that increased with the degree of depolarization. Fitting the steady state deactivation of Kir3.1/3.2 currents after 1 min of Ci-VSP activation with a Boltzmann function yielded a $V_{1/2, Kir3.1/3.2}$ of -1.1 ± 3.3 mV (Figure 16B), more negative compared to Kir2.1 and Kir1.1 channels, indicating a lower PI(4,5)P₂ affinity.

Strikingly, however, Kir3.1/3.2 currents were only incompletely inhibited by maximal activation of Ci-VSP, i.e. inhibition was less complete than observed with Kir2.1. To exclude the possibility that remaining Kir3.1/3.2 currents during saturating Ci-VSP activation represent leak currents, two-electrode voltage clamp recordings from oocytes expressing Kir3.1/3.2 channels and Ci-VSP were performed and residual currents were blocked by bath application of tertiapin-Q (Figure 16E). A depolarizing pulse of +60 mV was applied to activate Ci-VSP and to deactivate Kir3.1/3.2 channels. 30 s after starting the depolarizing pulse Kir3.1/3.2 current partially declined to 50% of the initial current amplitude and reached a plateau. Subsequent application of tertiapin-Q, a Kir3.1/3.2 channel blocker (Jin and Lu, 1998), additionally and reversibly decreased currents of Kir3.1/3.2 channels. The results show that 50% of Kir3.1/3.2 channels remain open during Ci-VSP activation.

4.1.7 Quantification of the dynamically altered PI(4,5)P₂ affinities of modulated Kir3.1/3.2 channels using Ci-VSP

Next, the dynamic regulation of the PI(4,5)P₂ affinity of Kir3.1/3.2 channels by G_{βγ} was identified with Ci-VSP. Consistent with previous data (Huang et al., 1998, Tucker and Baukowitz, 2008), the present results showed that the PI(4,5)P₂ affinity of Kir3.1/3.2 channels is lower than that of Kir2.1 and Kir1.1 channels. Kir3 channels are known to be activated by the G protein subunit G_{βγ}, e.g. after GABA_B receptors activation (Pfaffinger et al., 1985, Dascal, 1997) and previous research showed that the activation is mediated by an increased channel-PI(4,5)P₂ interaction (Huang et al., 1998). To examine whether this affinity change can be detected as an altered sensitivity to Ci-VSP, Kir3.1/3.2 channels were expressed together with GABA_B receptors in Ci-VSP containing oocytes and two electrode voltage-clamp recordings were performed. First, Kir3.1/3.2 currents were measured before and after GABA_B

receptor activation. The currents increased significantly upon the application of 1 mM GABA (Figure 16A, $p < 0.001$), suggesting an increase in the channel-PI(4,5)P₂ affinity which is consistent with previous research (Huang et al., 1998). Next, the Ci-VSP was activated by depolarization to +60 mV leading to a reversible Kir3.1/3.2 current decline of channels simply co-expressed together with GABA_B receptors and of channels whose PI(4,5)P₂ interaction was strengthened by GABA_B receptor activation. Co-expression of Kir3.1/3.2 channels and GABA_B receptors led to a shift of the steady state deactivation curve obtained with gradual Ci-VSP activation by depolarization between -60 mV and +60 mV in 20 mV steps and the resulting $V_{1/2}$ in the direction of depolarization ($V_{1/2, \text{Kir3.1/3.2+GABAB}} = 5.1 \pm 1.4$ mV) (Figure 16B). This effect was further enhanced when more active $G_{\beta\gamma}$ was generated by the application of the receptor agonist GABA ($V_{1/2, \text{Kir3.1/3.2+GABAB+GABA}} = 7.4 \pm 1.5$ mV) (Figure 16B). Comparison of the kinetics showed that channel deactivation after Ci-VSP activation was equal under all three experimental conditions described ($\tau_{\text{deactivation, Kir3.1/3.2}} = 3.6 \pm 0.4$ s, $\tau_{\text{deactivation, Kir3.1/3.2+GABAB}} = 2.6 \pm 0.4$ s and $\tau_{\text{deactivation, Kir3.1/3.2+GABAB+GABA}} = 3.9 \pm 0.2$ s) (Figure 16D, left). However, channel re-opening was significantly faster when GABA_B receptors were co-expressed ($\tau_{\text{re-opening, Kir3.1/3.2+GABAB}} = 15.1 \pm 2.6$ s, $p < 0.05$) and when the co-expressed receptors were additionally activated by bath application of 1 mM GABA ($\tau_{\text{re-opening, Kir3.1/3.2+GABAB+GABA}} = 11.3 \pm 0.9$ s, $p < 0.01$) in comparison to Kir3.1/3.2 channels without co-expressed receptors ($\tau_{\text{re-opening, Kir3.1/3.2}} = 26 \pm 3.5$ s) (Figure 16D, right). These results indicate that an increase in the PI(4,5)P₂ affinities of Kir3.1/3.2 channels in the presence of $G_{\beta\gamma}$ can be monitored by gradual activation of Ci-VSP.

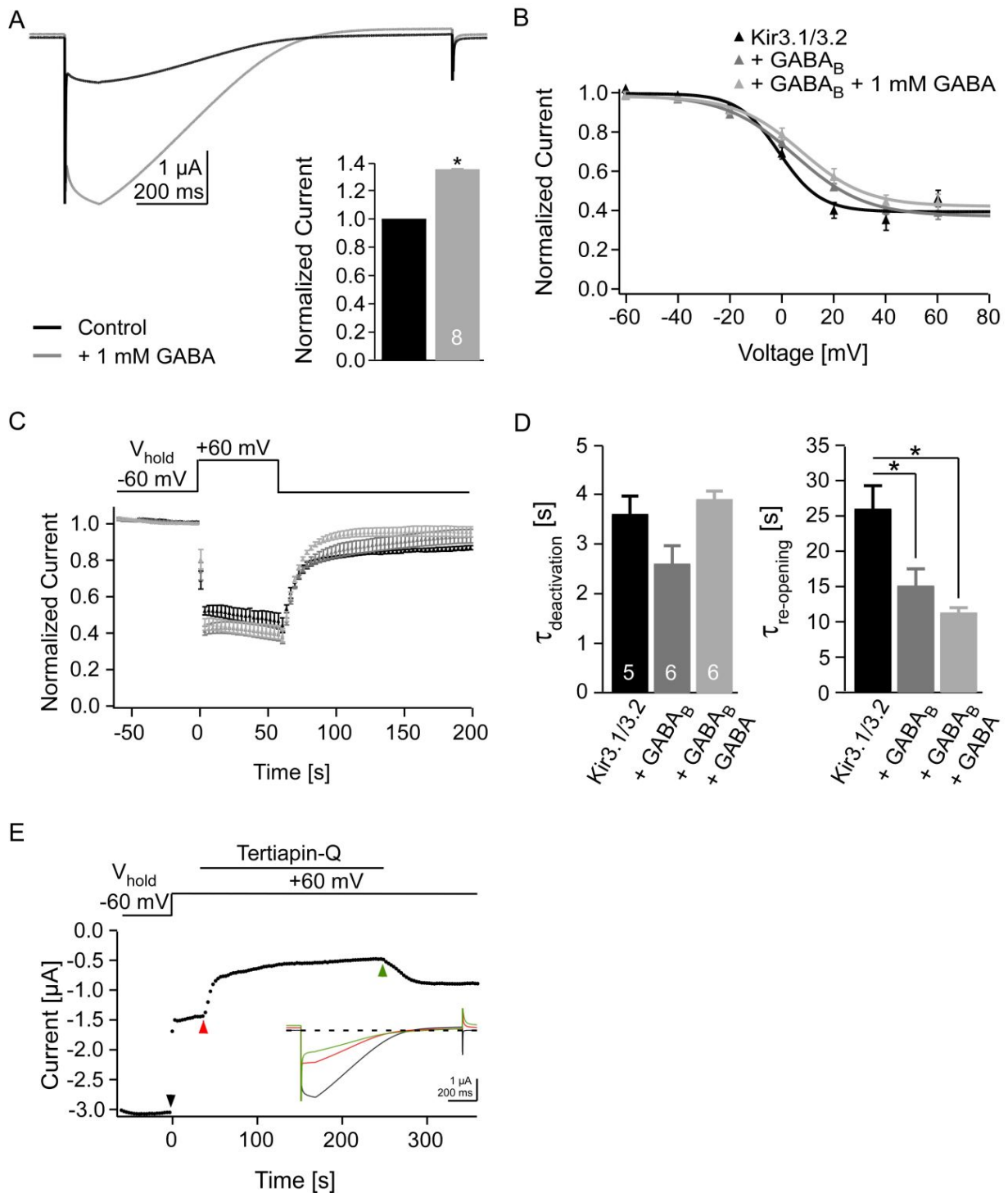


Figure 16: Kir3.1/3.2 channel deactivation and stabilizing effects of G_{BV} upon activation of Ci-VSP measured in *Xenopus laevis* oocytes.

A Control Kir3.1/3.2 current amplitudes increased significantly when co-expressed GABA_B receptors were activated by bath application of 1 mM GABA. Numbers of independent experiments as indicated.

B Steady state deactivation curves of Ci-VSP containing oocytes expressing Kir3.1/3.2 channels (n = 3 – 6; black), channels and GABA_B receptors (n = 4 – 6; dark grey), and channels co-expressing GABA_B receptors which were activated by bath application of 1 mM GABA (n = 4 – 6; light grey). Ci-VSP was gradually activated by depolarization between -60 mV and +60 mV in 20 mV steps. Mean responses were obtained after depolarization for 1 min. Continuous curves are Boltzmann fits to the averaged data.

C Mean normalized currents of oocytes expressing the same constructs as described in (B) before, during, and after depolarization to +60 mV. Current amplitudes were averaged over the last 10 ms of each test pulse.

D Summary data of experiments as in (C) show significant differences of $\tau_{\text{re-opening}}$ and no difference for $\tau_{\text{deactivation}}$ between Kir3.1/3.2 channels modulated or not modulated by $G_{\beta\gamma}$. Numbers of independent experiments as indicated.

E Residual Kir3.1/3.2 currents after Ci-VSP activation were reversibly blocked by bath application of tertiapin-Q (1 μ M). Current amplitudes were averaged over the last 10 ms of each test pulse. Inset: Single current traces evoked by voltage ramps applied at the time points indicated by arrowheads. Dashed line marks zero current.

4.2 Comparison of the Kir channel sensitivities to Ci-VSP-induced PI(4,5)P₂ depletion

In summary, these data show that Ci-VSP can be used as a tool to manipulate PI(4,5)P₂ levels in cells and oocytes reversibly, and to study the dependence and regulation of ion channels by PI(4,5)P₂. Channel deactivation and re-opening kinetics after Ci-VSP-induced PI(4,5)P₂ depletion as well as the experimental determination of $V_{1/2}$ by gradual Ci-VSP activation allowed the quantification of the apparent PI(4,5)P₂ affinities of the heterogenic Kir channel family. Furthermore, affinity changes upon mutations and dynamic cellular regulation by channel modulators were successfully detected with Ci-VSP. Thus, in agreement with previous work (Huang et al., 1998, Rohacs et al., 1999, Rohacs et al., 2003), these data suggest that Kir2.1WT channels exhibit the highest, Kir1.1WT channels intermediate and Kir3.1/3.2 channels the lowest apparent PI(4,5)P₂ affinity of the Kir channels investigated.

In general these findings were consistent with the results of previous studies (Huang et al., 1998, Zhang et al., 1999). However, comparing the behaviour of Kir channels upon Ci-VSP-induced PI(4,5)P₂ depletion, namely the amount of current decrease, kinetic behaviour including channel deactivation and re-opening, and $V_{1/2}$ value for current inhibition, showed apparent discrepancies and therefore raised a major question:

As a result of Ci-VSP activation by depolarization to +60 mV steady state currents of high-affinity Kir2.1WT and intermediate-affinity Kir1.1WT channels declined to $7.6 \pm 4\%$ or $3.9 \pm 1.2\%$ ($p < 0.001$), respectively, whereas the low PI(4,5)P₂-affinity Kir3.1/3.2 channels show $46 \pm 9.5\%$ ($p < 0.001$) of current resistant to Ci-VSP activity (Figure 17A, B). Why did the steady state currents of Kir3.1/3.2 channels not decline to the same level as those of high-affinity Kir2.1WT or intermediate-affinity Kir1.1WT channels, although complete channel deactivation was

expected from the low PI(4,5)P₂ affinity of Kir3.1/3.2 channels? These considerations led to the idea that other PIs maybe involved in determining channel activity of one or more of the channel types examined here.

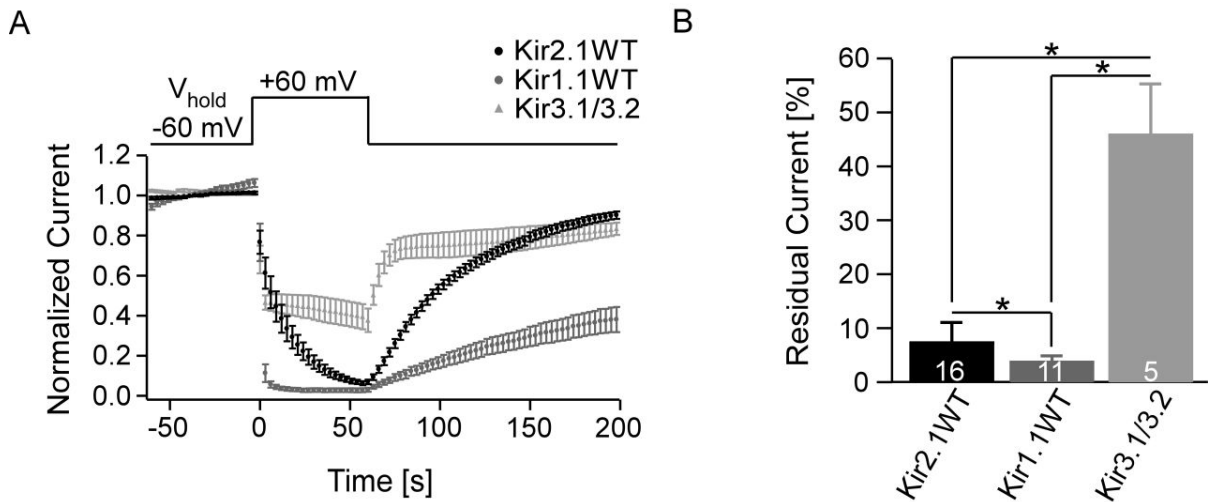


Figure 17: Comparison of current decline and dose-response properties of Kir channels with different PI(4,5)P₂ affinities after Ci-VSP activation.

A Mean normalized Kir2.1WT (black), Kir1.1WT (dark grey) and Kir3.1/3.2 channels (light grey) currents before, during and after depolarization to +60 mV. Note residual Kir3.1/3.2 currents during Ci-VSP activation. Current amplitudes were averaged over the last 10 ms of each test pulse.

B Summary of data from (A) shows significant differences of residual currents between all three channel family members. Numbers of independent experiments as indicated.

It has been shown that the activation of Ci-VSP leads to the conversion of the substrates PI(4,5)P₂ and PI(3,4,5)P₃, to PI(4)P and PI(3,4)P₂, respectively, thereby reducing the cellular substrate concentrations and simultaneously increasing the concentrations of the products (Halaszovich et al., 2008, Iwasaki et al., 2008). Therefore, it appeared possible that the degree of channel deactivation observed upon activation of Ci-VSP not exclusively results from depletion of PI(4,5)P₂, but may also depend on concentration changes of the other three PIs affected by Ci-VSP activity. In particular, the production of PI(4)P or PI(3,4)P₂ may limit channel deactivation despite depletion of PI(4,5)P₂, if the channels are not perfectly selective for PI(4,5)P₂ but can be activated by these other PIs as well.

4.2.1 Effects of substrates and products of Ci-VSP on Kir channel family members

An influence of other PIs on the channel activity, e.g. the level of current decline during Ci-VSP activation, would restrict the usefulness of the results obtained with Ci-VSP and therefore should be investigated. In order to identify the PI specificity of the channels investigated with Ci-VSP with an independent approach, inside-out giant patches from oocytes expressing Kir channels were performed. This recording technique offers the opportunity to apply those PIs affected by the enzymatic activity of Ci-VSP one by one to the intracellular side of the membrane (Rohacs et al., 2003). In principle, binding of PIs may either activate or inhibit channels. In the most simple case, if the substrates of Ci-VSP, PI(4,5)P₂ and PI(3,4,5)P₃ were promoting channel opening, their depletion could account for the inhibition observed for all channels upon activation of Ci-VSP. Vice versa, if these PIs were acting as inhibitors of channel activity, their depletion may even facilitate channel activation. Similarly, if the products of Ci-VSP, PI(4)P and PI(3,4)P₂ promote channel activity they would oppose channel inhibition due to depletion of PI(4,5)P₂ and could be responsible for residual Kir3.1/3.2 currents. Inhibiting activity of these PIs, however, may induce channel deactivation which could contribute the strong channel inhibition observed for Kir2.1WT and Kir1.1WT channels.

In the following experiments inside-out patches were excised from oocytes and the PIs involved were applied either to open channels or to deactivated channels, in order to examine inhibiting or activating effects, respectively. Channel deactivation ('current rundown') was induced by the removal of PI levels by endogenous lipid phosphatases or phospholipases, which occurs rapidly in excised patches in the presence of free Mg²⁺ (Rohacs et al., 1999).

4.2.2 Effects of PIs on Kir2.1WT channels

Given the high PI(4,5)P₂ affinity of Kir2.1WT as determined previously (Huang et al., 1998), the highly efficient inhibition of these channels by Ci-VSP was unexpected. It therefore seemed possible that the lipid products of Ci-VSP might promote channel closure and thereby contributed to the observed full current inhibition. To test for putative inhibiting effects of PIs during Ci-VSP activation, substrates or products of Ci-VSP were applied to open channels (Figure 18). Application of PI(4,5)P₂ and

PI(4)P to open channels led to a slight increase of the current amplitudes. PI(3,4,5)P₃ and PI(3,4)P₂ application, however, did not affect current amplitudes, indicating that none of these PIs inhibited open Kir2.1WT channels.

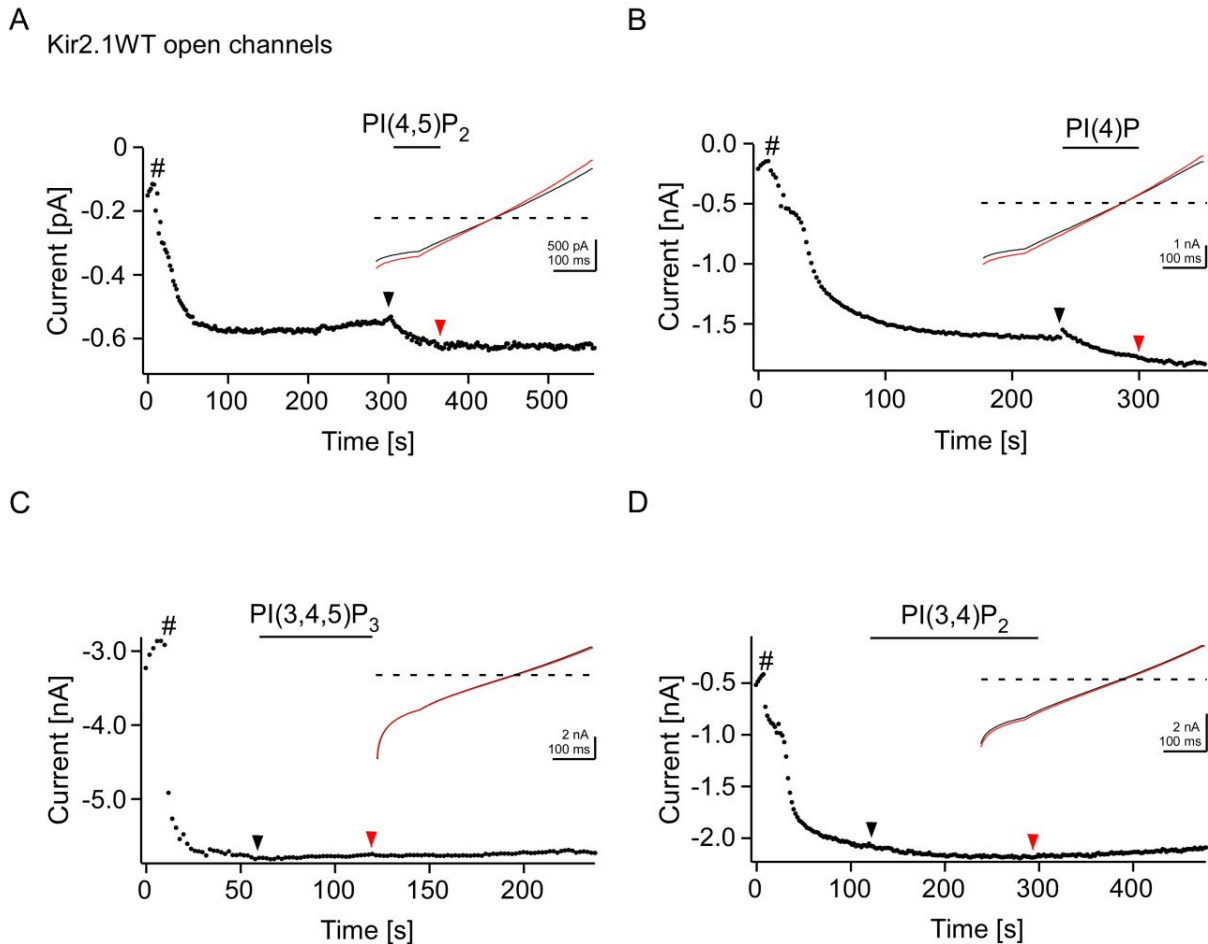


Figure 18: Open Kir2.1WT channels are not inhibited by any of the PI investigated.

A – D Representative inside-out giant patch recordings excised from oocytes expressing Kir2.1WT channels. Time of patch excision is marked by #. PIs were applied to open channels for 1 min (PI(4,5)P₂ (n = 3), PI(4)P (n = 4)), 2 min (PI(3,4,5)P₃ (n = 4) or 4 min (PI(3,4)P₂ (n = 7)) when the current increase after patch excision reached a steady state level. Current amplitudes were averaged over the last 10 ms of each test pulse. Black bars indicate time points when PIs were applied. Insets: Single current traces evoked by voltage ramps applied at the time points indicated by arrowheads. Dashed lines mark zero current.

Possible activating effects and their contribution to channel deactivation (substrates) or activation (products) of PI(4,5)P₂, PI(4)P, PI(3,4,5)P₃ and PI(3,4)P₂ were investigated by application to deactivated channels. For that purpose, full rundown of Kir2.1WT currents was induced by the application of intracellular solution containing 1.1 mM Mg²⁺ prior to application of PIs (Figure 19). Application of PI(4,5)P₂ re-activated Kir2.1WT currents after Mg²⁺-induced rundown (Figure 19A) as reported

previously (Zhang et al., 1999). In contrast, none of the other PI investigated rescued the current, indicating that neither PI(4)P, PI(3,4,5)P₃ nor PI(3,4)P₂ is able to activate Kir2.1WT channels (Figure 19B – D). These results clearly establish an absolute specificity of Kir2.1WT channels for PI(4,5)P₂.

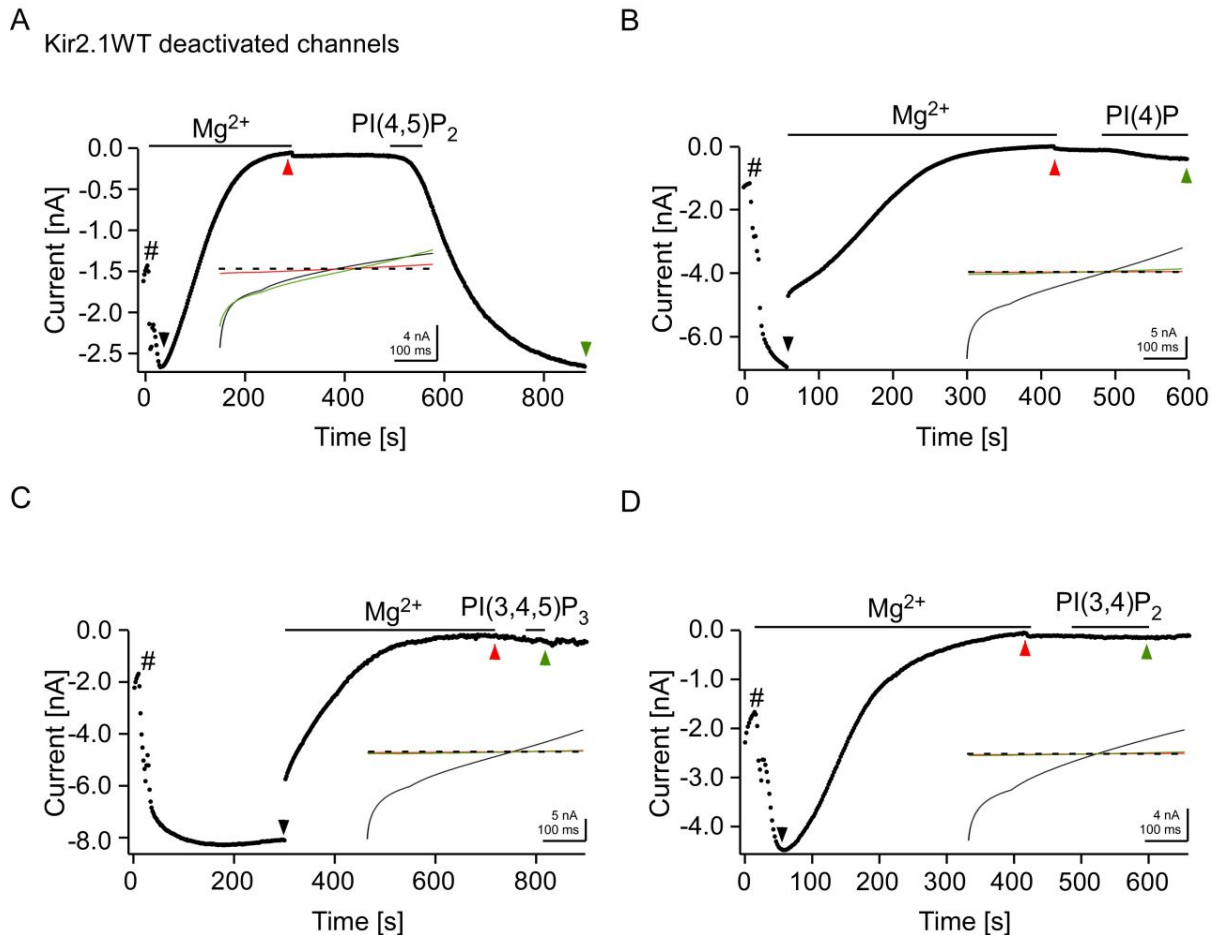


Figure 19: Deactivated Kir2.1WT channels after Mg²⁺ application are activated by PI(4,5)P₂.

A – D Representative recordings of Kir2.1WT currents in inside-out patches excised from oocytes. Time of patch excision is marked by #. Currents were allowed to run down in Mg²⁺-containing intracellular solution and recovered upon the application of PI(4,5)P₂ (n = 5) (A). PIs were applied for 1 min (PI(4,5)P₂, PI(3,4,5)P₃ (n = 3) or 2 min (PI(4)P (n = 3), PI(3,4)P₂ (n = 2)). Black bars indicate time points when Mg²⁺ containing intracellular solution (1.1 mM) or PIs (10 μM each) were applied. Current amplitudes and insets: see Figure 18.

4.2.3 Effects of PIs on Kir6.2/SUR1 channels

Kir3 channels are difficult to measure in inside-out giant patches because channel activity depends on multiple interactions with regulatory factors, which results in rapid and irreversible current rundown in excised patches (Huang et al., 1998). Therefore, giant patch recordings were performed with Kir6.2/SUR1 as a substitute model

channel, because the reported PI(4,5)P₂ affinity and PI specificity is similar to that of Kir3.1/3.2 channels (Shyng and Nichols, 1998, Ho and Murrell-Lagnado, 1999, Rohacs et al., 1999, Rohacs et al., 2003, Tucker and Baukrowitz, 2008).

In order to investigate possible inhibitory effects and their contribution to channel deactivation on Kir6.2/SUR1, PI(4,5)P₂, PI(4)P, PI(3,4,5)P₃, or PI(3,4)P were applied to open channels (Figure 20). In the cell-attached configuration no currents were observed, because the channels are blocked by the endogenous source of ATP in oocytes. After patch excision (#), currents rapidly increased as a result of ATP wash-out (Baukrowitz et al., 1998). Application of the PIs investigated did not affect current amplitudes, indicating that none inhibited open Kir6.2/SUR1 channels.

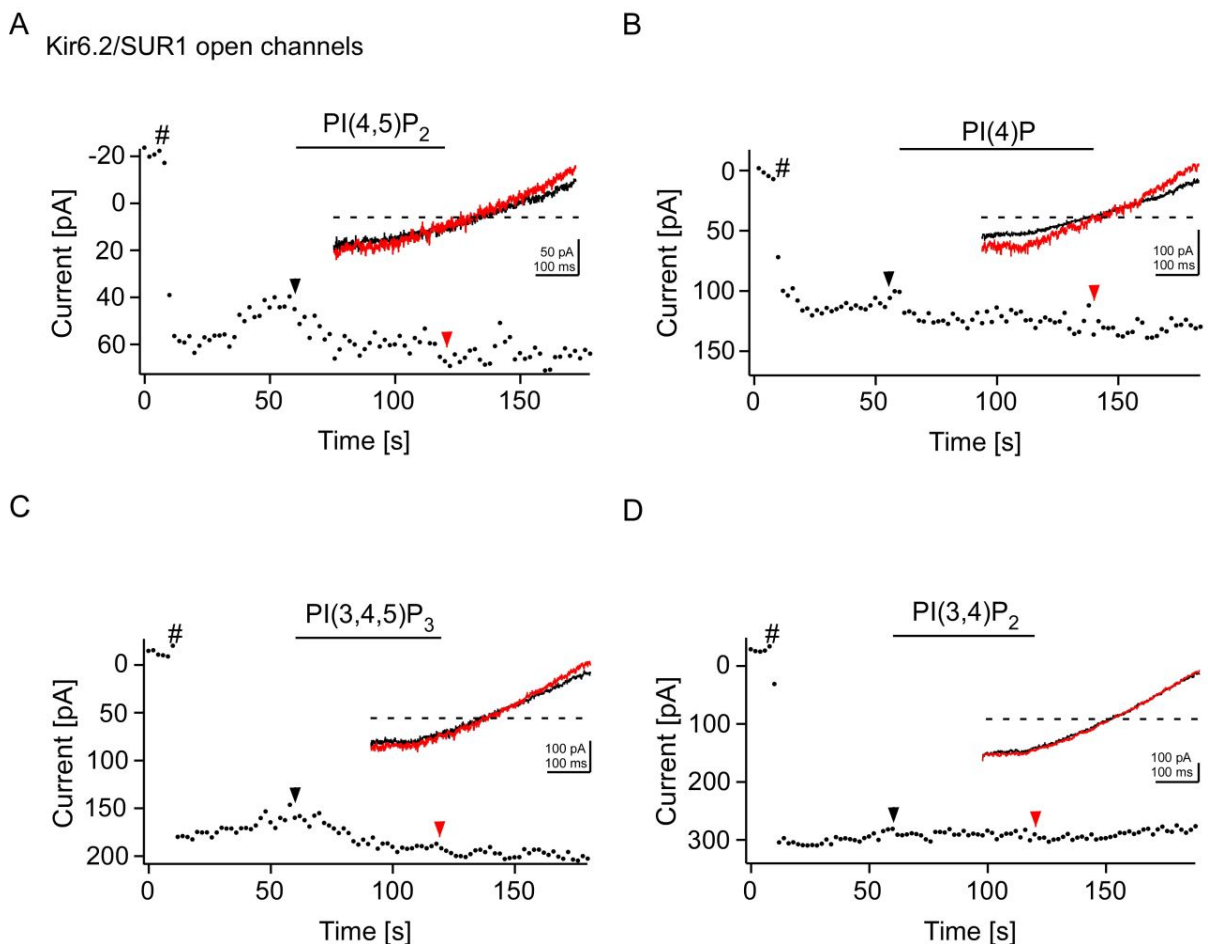


Figure 20: Effects of PI(4,5)P₂, PI(4)P, PI(3,4,5)P₃ and PI(3,4)P₂ on open Kir6.2/SUR1 channels.

A – D Representative recordings of Kir6.2/SUR1 in inside-out patches excised from oocytes. Currents rapidly increased after patch excision. Time of patch excision is marked by #. PIs were applied for 1 min (PI(4,5)P₂ (n = 4) (A), PI(4)P (n = 3) (B), PI(3,4,5)P₃ (n = 5) (C), PI(3,4)P₂ (n = 5) (D)). Black bars indicate time points when PIs (10 μM each) were applied. The inward current amplitudes observed at -100 mV were smaller than the outward currents at -60 mV. For a better illustration of the effects, current amplitudes were averaged over the last 10 ms of the ramp protocol at -60 mV and plotted upside-down. Insets: Single current

traces evoked by voltage ramps applied at the time points indicated by arrowheads. Dashed lines mark zero current.

The application of 1.1 mM Mg^{2+} -containing intracellular solution to open Kir6.2/SUR1 channels led to channel closure (Figure 21). Possible activating effects of PI(4,5)P₂, PI(4)P, PI(3,4,5)P₃, and PI(3,4)P₂ were investigated by their application to closed channels. Application of any PI investigated recovered Kir6.2/SUR1 currents, indicating that all these PIs activated closed Kir6.2/SUR1 channels, demonstrating high nonspecificity of the channels for PIs. According to that observation it is likely, that the activating effect of the Ci-VSP products PI(4)P and PI(3,4)P₂ may contribute to the maintenance of residual currents as observed e.g. for Kir3 channels.

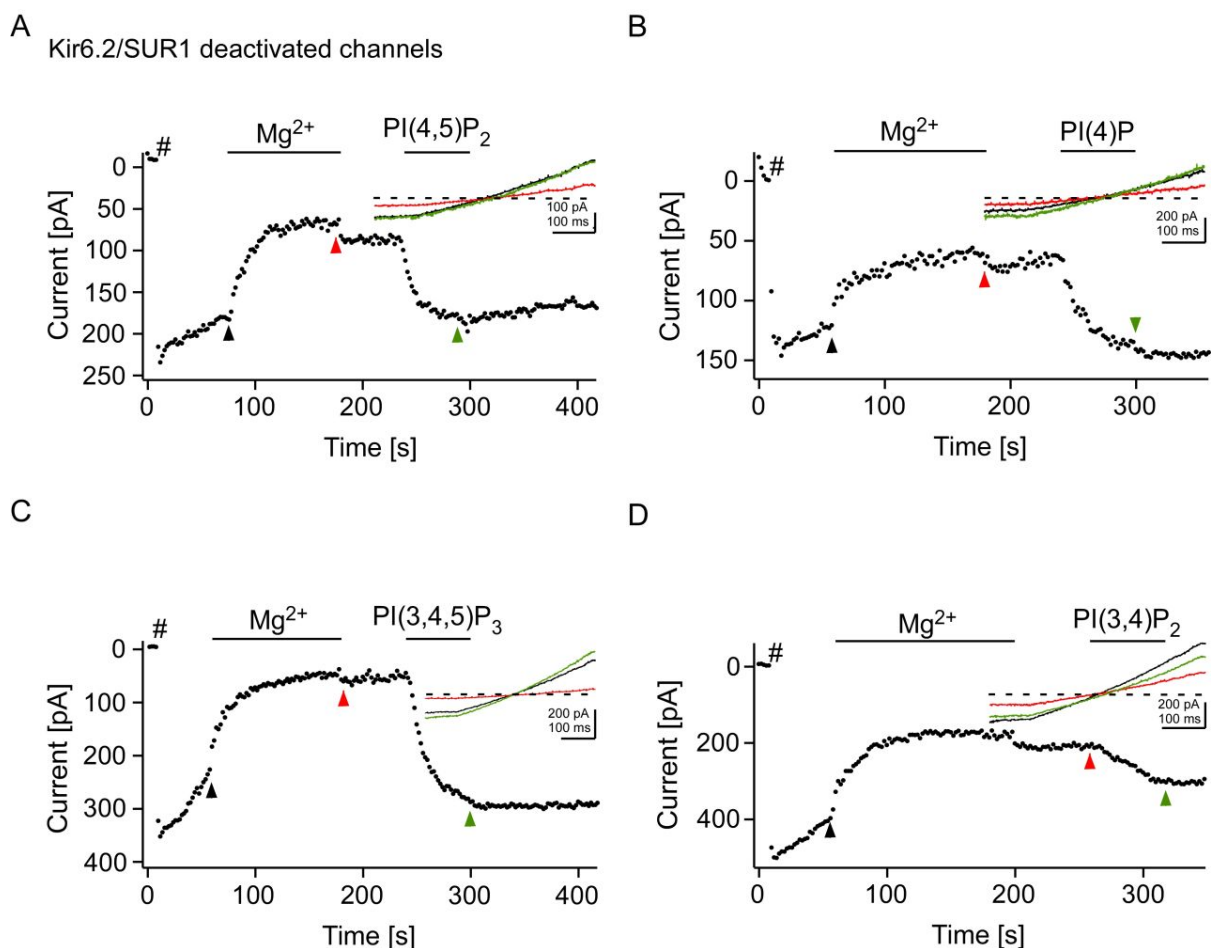


Figure 21: Deactivated Kir6.2/SUR1 channels after Mg^{2+} application are activated by all PIs investigated.

A – D Representative recordings of Kir6.2/SUR1 in inside-out patches excised from oocytes. Currents rapidly increased upon patch excision. Time of patch excision is marked by #. Currents were allowed to run down in Mg^{2+} -containing intracellular solution and recovered upon the application of any PI investigated. PIs were applied for 1 min (PI(4,5)P₂ (n = 4) (A), PI(4)P (n = 7) (B), PI(3,4,5)P₃ (n = 5) (C), PI(3,4)P₂ (n = 5) (D)). Black bars indicate time points when Mg^{2+} -containing intracellular solution (1.1 mM) or PIs (10 μ M each)

were applied. Current amplitudes and insets were analyzed and plotted as described in Figure 20.

4.2.4 Effects of PIs on Kir1.1WT channels

Third, inside-out patches from oocytes expressing Kir1.1WT channels, which display an intermediate apparent PI(4,5)P₂ affinity, were excised. Kir1.1WT channels are gated by extracellular K⁺ ions in a way that a decreasing extracellular K⁺ ion concentration promotes an irreversible inactivation after channel deactivation by PI(4,5)P₂ depletion (see paragraph 4.1.5) (Doi et al., 1996, Rapedius et al., 2007a). This phenomenon depends on K80 in Kir1.1WT channels that forms an H bond to A177, thereby preventing channel re-opening after deactivation in inside-out giant patches. As a consequence, deactivated channels did not re-open upon PI(4,5)P₂ application when recorded under physiological low extracellular K⁺ conditions (Rapedius et al., 2007a) (Figure 22A). However, PI(4,5)P₂ application restored the activity of Kir1.1WT channels when the recordings were performed with high extracellular K⁺ concentrations (Rapedius et al., 2007a) (Figure 22B).

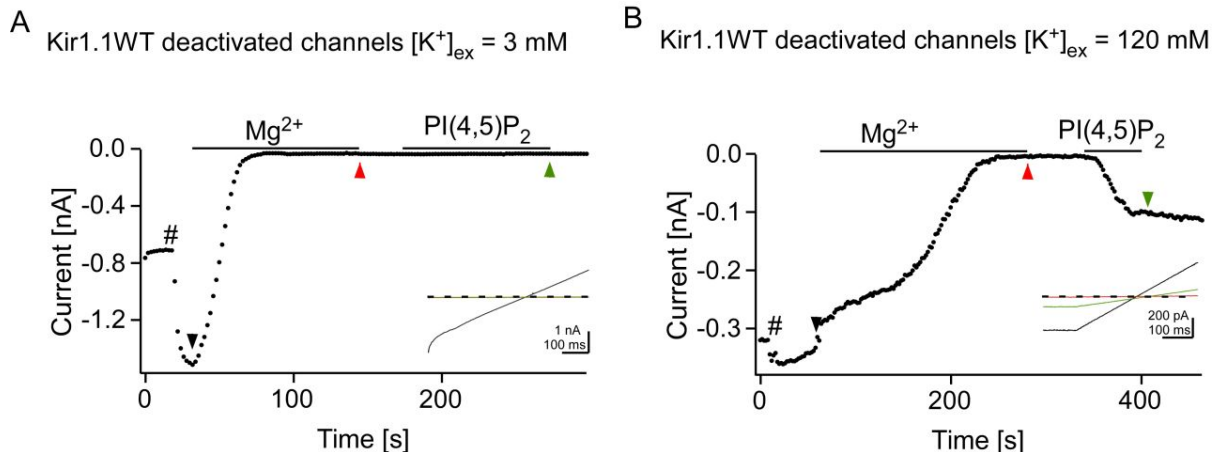


Figure 22: Kir1.1WT channel re-opening depends on the extracellular K⁺ concentration.

A, B Representative inside-out patch-clamp recordings from oocytes expressing Kir1.1WT channels. Time of patch excision is marked by #. Currents were allowed to run down in Mg²⁺-containing intracellular solution. Under low extracellular K⁺ concentration, PI(4,5)P₂ application to closed channels for 80 s did not affect the current amplitude (n = 5) (A). Partial current recovery was observed after PI(4,5)P₂ application for 1 min when extracellular solution contained high K⁺ concentration (n = 3) (B). Current amplitudes and insets: see Figure 18.

Since the recordings here were performed under physiological conditions with a low extracellular K⁺ concentration of 3 mM where K⁺ inhibition is expected to occur, only

possible inhibiting effects of PI(4,5)P₂, PI(4)P, PI(3,4,5)P₃ and PI(3,4)P₂ and their contribution to the level of Kir1.1WT channel deactivation were investigated. Possible activating effects of these PIs were studied on mutant Kir1.1K80M channels that are insensitive to the extracellular K⁺ concentration.

Possible inhibitory effects of the PIs involved in Ci-VSP activity were investigated by their application to open Kir1.1WT channels (Figure 23). After patch excision (#), currents slowly ran down. Application of PI(4,5)P₂ did not affect the current amplitudes (Figure 23A). However, application of PI(4)P, PI(3,4,5)P₃ and PI(3,4)P₂ (Figure 23B – D) to open Kir1.1WT channels accelerated current rundown, indicating inhibitory activity. It is likely that channel inhibition by both products increased the deactivation level during Ci-VSP activation.

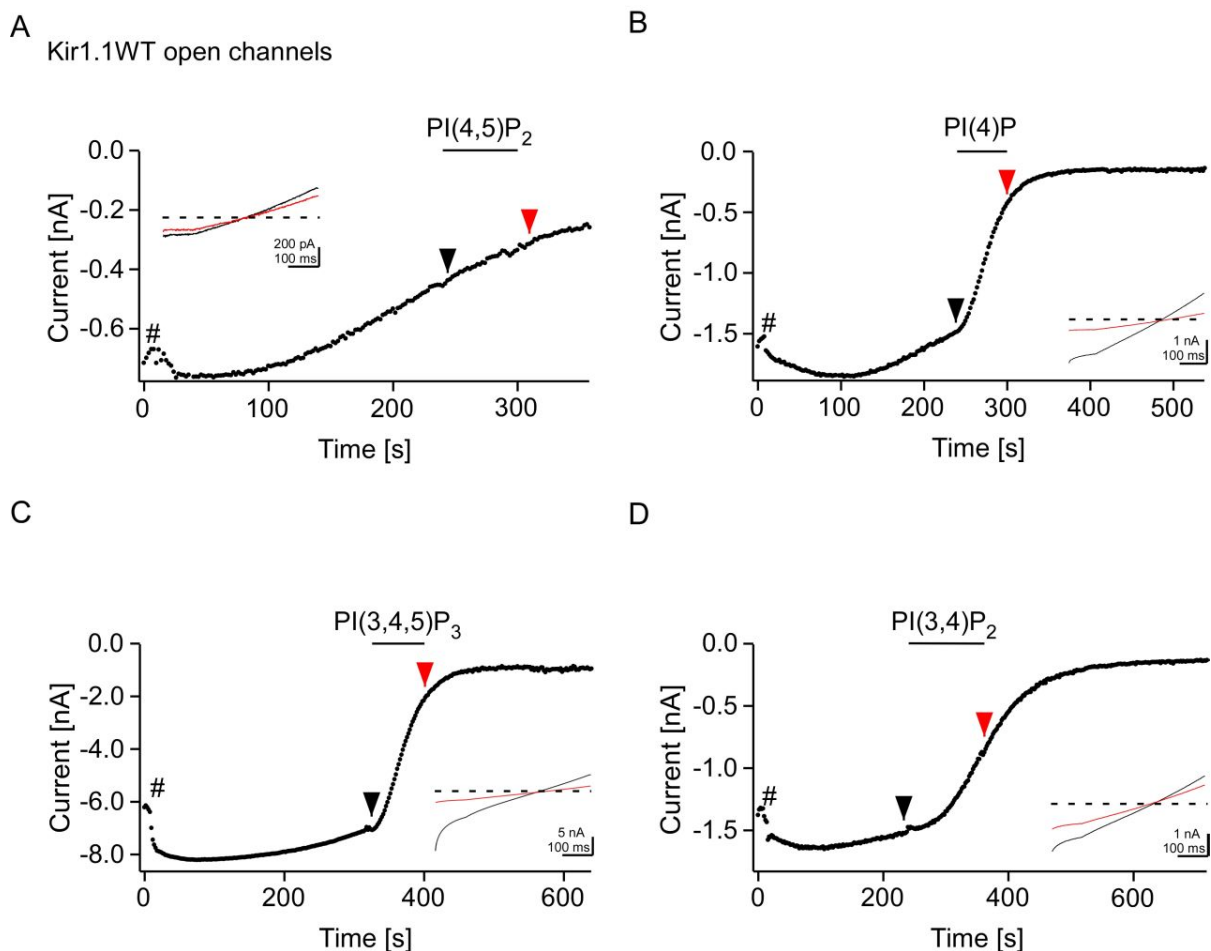


Figure 23: Open Kir1.1WT channels are inhibited by PI(4)P, PI(3,4,5)P₃ and PI(3,4)P₂.

A – D Representative recordings of Kir1.1WT in inside-out patches excised from oocytes. Time of patch excision is marked by #. PIs were applied for 1 min (PI(4,5)P₂ (n = 3) (A), PI(4)P (n = 8) (B), PI(3,4,5)P₃ (n = 5) (C)) or 2 min (PI(3,4)P₂ (n = 9) (D)) when the current rundown after patch excision reached a linear progression. Black bars indicate time points when PIs (10 μM each) were applied. Current amplitudes and insets: see Figure 18.

4.2.5 Effects of PIs on Kir1.1K80M channels

Possible inhibitory effects of PIs on Kir1.1K80M channels and their contribution to channel deactivation were investigated by application of PI(4,5)P₂, PI(4)P, PI(3,4,5)P₃ and PI(3,4)P₂ to open channels (Figure 24). Application of the PIs investigated did not affect current amplitudes, indicating that none of these PIs inhibited open Kir1.1K80M channels.

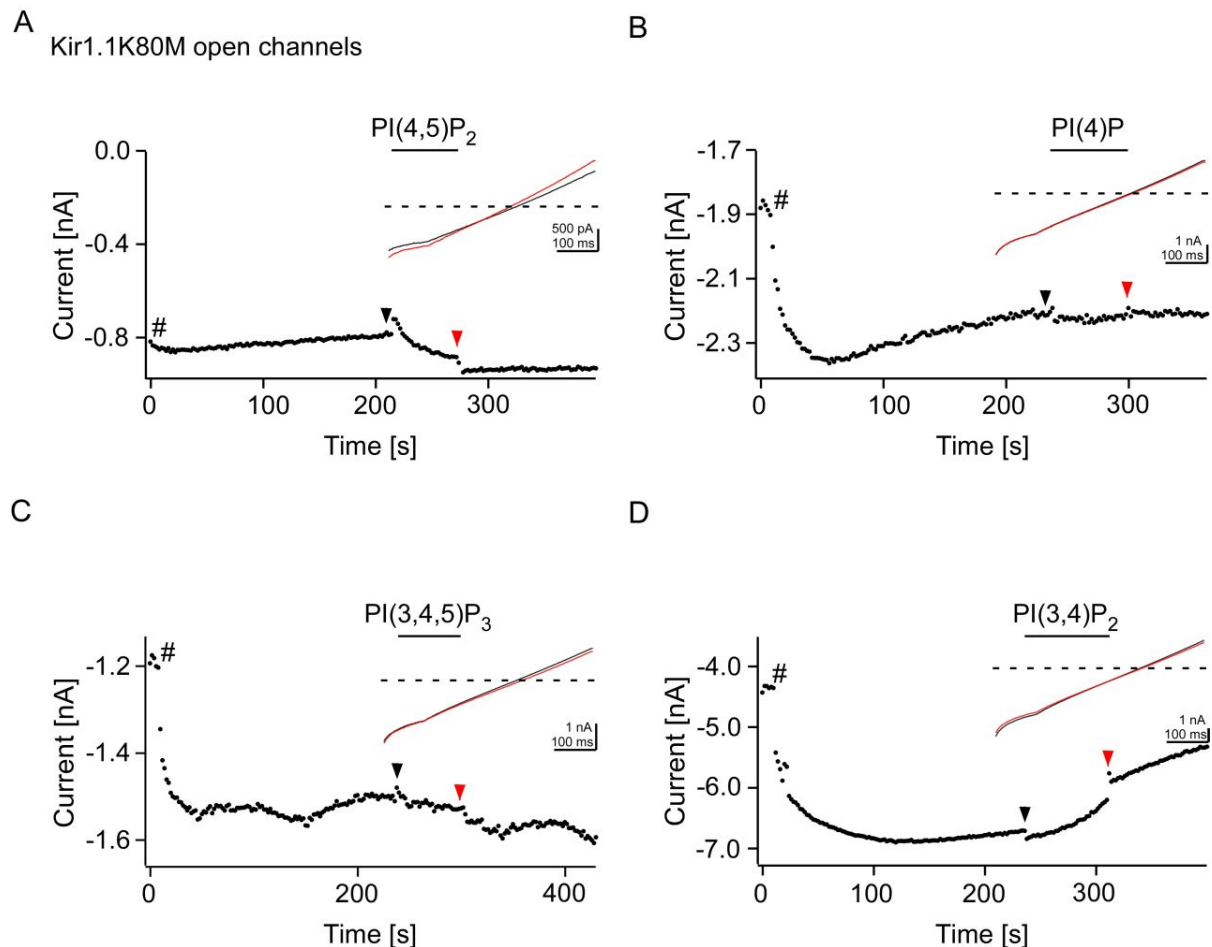


Figure 24: Open Kir1.1K80M channels are not inhibited by any PI investigated.

A – D Representative recordings of Kir1.1K80M currents in inside-out patches excised from oocytes. Time of patch excision is marked by #. PIs were applied for 1 min (PI(4,5)P₂ (n = 4) (A), PI(4)P (n = 5) (B), PI(3,4,5)P₃ (n = 5) (C), PI(3,4)P₂ (n = 4) (D)). Black bars indicate time points when PIs (10 μM each) were applied. Current amplitudes and insets: see Figure 18.

Possible activating effects of PI(4,5)P₂, PI(4)P, PI(3,4,5)P₃ and PI(3,4)P₂ on Kir1.1K80M channels were investigated by their application to closed channels. Channel closure was achieved by the application of 1.1 mM Mg²⁺-containing intracellular solution to open channels (Figure 25). Complete Kir1.1K80M current recovery was observed when PI(4,5)P₂ was applied (Figure 25A). Partial recovery

was observed after application of PI(4)P and PI(3,4)P₂ that was completed by a subsequent application of PI(4,5)P₂, indicating that these PIs activated closed Kir1.1K80M channels (Figure 25B, D). Application of PI(3,4,5)P₃ did not affect current amplitudes (Figure 25C).

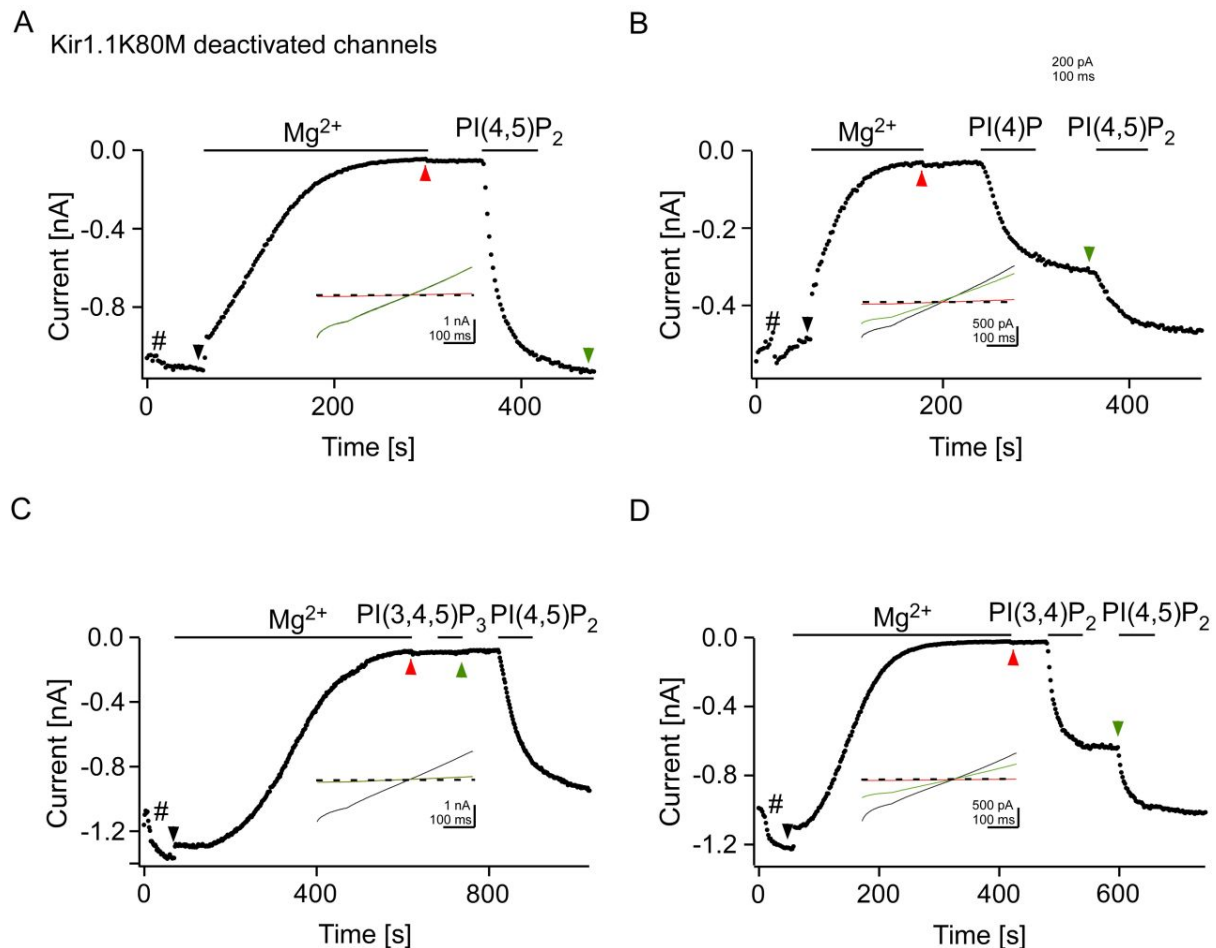


Figure 25: Deactivated Kir1.1K80M channels after Mg²⁺ application are activated by PI(4,5)P₂, PI(4)P and PI(3,4)P₂.

A – D Representative recordings of Kir1.1K80M currents in inside-out patches excised from oocytes. Time of patch excision is marked by #. Currents were allowed to run down in Mg²⁺-containing intracellular solution. PIs were applied for 1 min (PI(4,5)P₂ (n = 6) (A), PI(4)P (n = 4) (B), PI(3,4,5)P₃ (n = 8) (C), PI(3,4)P₂ (n = 8) (D)). Subsequent PI(4,5)P₂ application lasted 1 min after PI(4)P and PI(3,4)P₂ application and 80 s after PI(3,4,5)P₃ application. Black bars indicate time points when Mg²⁺-containing intracellular solution (1.1 mM) or PIs (10 μM each) were applied. Current amplitudes and insets: see Figure 18.

4.2.6 Summary of the PI effects on Kir channels

The individual effects of the PIs investigated on the different Kir channel family members are summarized in Table 7.

Table 7: Overview of PI effects on open and deactivated Kir channel family members

		PI(4,5)P ₂	PI(4)P	PI(3,4,5)P ₃	PI(3,4)P ₂
Kir2.1WT	open	yellow	yellow	yellow	yellow
	closed (Mg ²⁺ rundown)	green	yellow	yellow	yellow
Kir6.2/SUR1	open	yellow	yellow	yellow	yellow
	closed (Mg ²⁺ rundown)	green	green	green	green
Kir1.1WT	open	yellow	red	red	red
Kir1.1K80M	open	yellow	yellow	yellow	yellow
	closed (Mg ²⁺ rundown)	green	green	yellow	green

■ activating effect
 ■ inhibiting effect
 ■ no effect

In summary these results show that the Kir channels investigated exhibit, additionally to their different PI(4,5)P₂ affinities, variable PI specificities. Kir2.1WT channels exhibited the highest PI(4,5)P₂ specificity and Kir6.2/SUR1 channels were rather nonspecifically activated by PI(4,5)P₂, PI(4)P, PI(3,4,5)P₃, and PI(3,4)P₂. Since previous work showed that Kir3 and Kir6 channels behave very similar in their interaction with PIs (Shyng and Nichols, 1998, Ho and Murrell-Lagnado, 1999, Rohacs et al., 1999, Rohacs et al., 2003, Tucker and Baukowitz, 2008), it is very likely that the residual Kir3 currents during Ci-VSP activation in whole-cell experiments were maintained by the activating activity of the Ci-VSP products PI(4)P and PI(3,4)P₂.

Furthermore, Kir1.1WT channels were inhibited by PI(4)P, PI(3,4,5)P₃ and PI(3,4)P₂ when recorded under physiological low extracellular K⁺ conditions. K⁺ insensitive Kir1.1K80M channels, on the other hand, were activated by PI(4,5)P₂, PI(4)P and PI(3,4)P₂. Thus, K80 might determine the ability of Kir1.1WT channels to

close in response to increasing membrane concentrations of PI(4)P, PI(3,4)P₂ and PI(3,4,5)P₃. Further studies would be required to clarify these observations.

4.3 Verification of the usefulness of Ci-VSP with an independent approach

4.3.1 PI(4,5)P₂ depletion by inducible Inp54p membrane translocation

In order to examine the usefulness of the Ci-VSP methodology an alternative method for the depletion of PI(4,5)P₂ in living cells was used. Although not allowing for a quantitative control of PI(4,5)P₂, a heterodimerization approach was used, where the PI(4,5)P₂ specific 5' phosphatase Inp54p was translocated to the membrane (see paragraph 2.3.1 and Figure 4) (Suh et al., 2006, Varnai et al., 2006). PI(4,5)P₂ depletion by Inp54p membrane translocation induced by rapamycin application led to a current decline of all channels investigated (Figure 26A – C). As a control, when the heterodimerization proteins were not co-expressed, rapamycin did not affect on Kir current amplitudes (e.g. Kir2.1WT currents: 104.3 ± 4.3%) (Figure 26A, D). After Inp54p-induced PI(4,5)P₂ depletion, Kir2.1WT residual currents (42.7 ± 4.7%) were significantly larger than residual Kir2.1R228Q currents (22.6 ± 4%, $p < 0.01$) (Figure 26D). Conversely, Kir1.1WT residual currents (14.6 ± 3.1%) were significantly smaller than residual Kir1.1K80M currents (68.4 ± 4.1%, $p < 0.001$). Kir3.1/3.2 currents declined partially to 52.9 ± 4.4%, indicating a degree of channel inhibition that was similar to Kir2.1WT but significantly less complete than found with Kir1.1WT channels ($p < 0.001$).

In principle, similar channel-PI(4,5)P₂ affinities maybe deduced from similar levels of Kir2.1WT and Kir3.1/3.2 residual currents, after Inp54p-induced PI(4,5)P₂ depletion. However, gradual Ci-VSP activation allowed the discrimination of the affinities, indicating high affinity for Kir2.1WT channels and low affinity for Kir3.1/3.2 channels, as reported previously (Huang et al., 1998, Zhang et al., 1999).

The Kir3.1/3.2 residual currents observed after Inp54p-induced PI(4,5)P₂ depletion were similar to those remaining after Ci-VSP activity. It was suggested in paragraph 4.2.6 that due to the property of the Ci-VSP products PI(4)P and PI(3,4)P₂ to activate Kir3.1/3.2 channels (Ho and Murrell-Lagnado, 1999, Rohacs et al., 1999), residual currents were maintained because of the interaction of the channels with

those lipids. (Varnai et al., 2006) suggested that the enzymatic activity of Inp54p leads to the depletion of PI(4,5)P₂ and the generation of PI(4)P. Therefore it is likely that the residual currents of Kir3.1/3.2 channels remaining after Inp54p-induced PI(4,5)P₂ depletion are, similar to those observed after Ci-VSP activation, mediated by the activating properties of PI(4)P. Residual currents were also observed for Kir1.1K80M channels after Inp54p-induced PI(4,5)P₂ depletion. This observation is consistent with the results described in paragraph 4.2.5 where the application of PI(4)P to deactivated Kir1.1K80M channels in giant patches partially restored the currents. Therefore it is likely that the residual Kir1.1K80M currents are also maintained due to the property of PI(4)P to activate the channels.

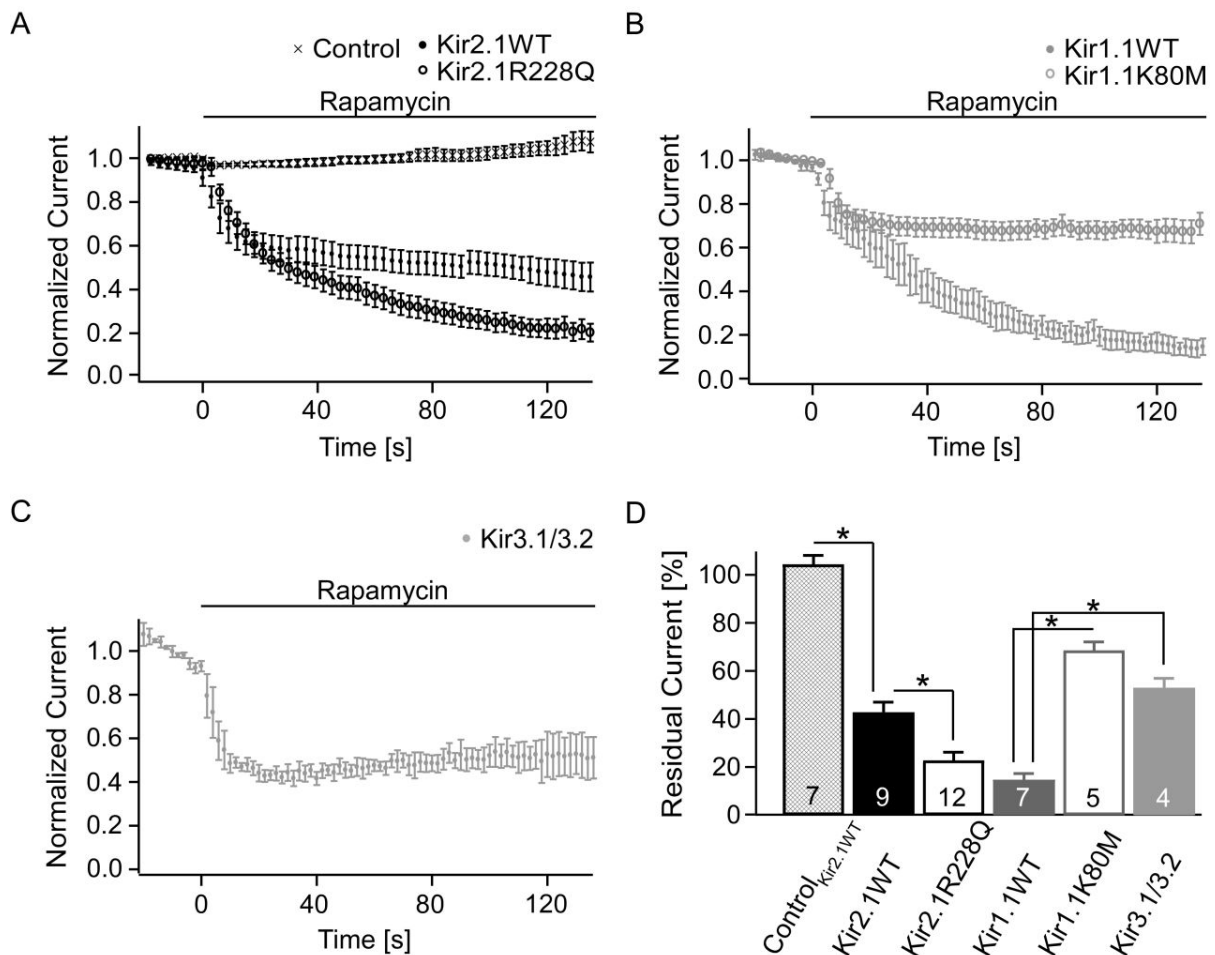


Figure 26: Deactivation of Kir channels upon Inp54p-induced PI(4,5)P₂ depletion.

A – C Normalized mean currents of whole-cell recordings from CHO cells expressing Kir2.1WT, Kir2.1R228Q (A), Kir1.1WT, Kir1.1K80M (B) or Kir3.1/3.2 (C) channels together with Lyn11-FRB and FKBP-Inp54p protein. The application rapamycin (5 μ M), led to membrane translocation of Inp54p, subsequent PI(4,5)P₂ depletion and channel deactivation. Current decline during rapamycin application was never observed when heterodimerization

proteins were not co-expressed (A, Control). Current amplitudes were averaged over the last 10 ms of each test pulse.

D Summary data of experiments as in (A – C). Numbers of independent experiments as indicated.

4.3.2 Modulation of Kir channels by physiologically occurring dynamic PI(4,5)P₂ changes

In order to examine how the PI(4,5)P₂ affinities derived from Ci-VSP experiments relate to channel behaviour during physiological, i.e. receptor-induced alteration of PI(4,5)P₂ concentrations, PLC-triggered PI(4,5)P₂ hydrolysis was induced by the stimulation of heterologously expressed M1 receptors upon oxotremorin-M application. Neither co-expressed Kir2.1WT and mutant Kir2.1R228Q channels (Figure 27A) nor Kir1.1WT and mutant Kir1.1K80M channels (Figure 27B) were affected by M1 receptor-induced activation of PLC. In contrast, voltage-gated KCNQ2/3 channels, were strongly and reliably inhibited by activation of co-expressed M1 receptors (Figure 27C), as shown previously (Suh and Hille, 2002, Zhang et al., 2003). Since it is established that homomeric as well as heteromeric KCNQ channels are inhibited by hydrolysis of PI(4,5)P₂ (Shapiro et al., 2000, Zhang et al., 2003) the suppression of KCNQ currents confirms the efficient reduction of the PI(4,5)P₂ concentrations by activation of M1 receptors, despite the lack of changes in Kir current amplitudes under the same experimental conditions. In summary, the impact of Ci-VSP activity on Kir channels seems to be higher than that of PLC-triggered PI(4,5)P₂ hydrolysis. This finding was unexpected, since first, the same degree of KCNQ channel inhibition by PLC and Ci-VSP indicated similar degrees of PI(4,5)P₂ depletion, and second, the $V_{1/2}$ values obtained with gradual Ci-VSP activation suggested that KCNQ3 and Kir2.1R228Q channels have similar PI(4,5)P₂ affinities.

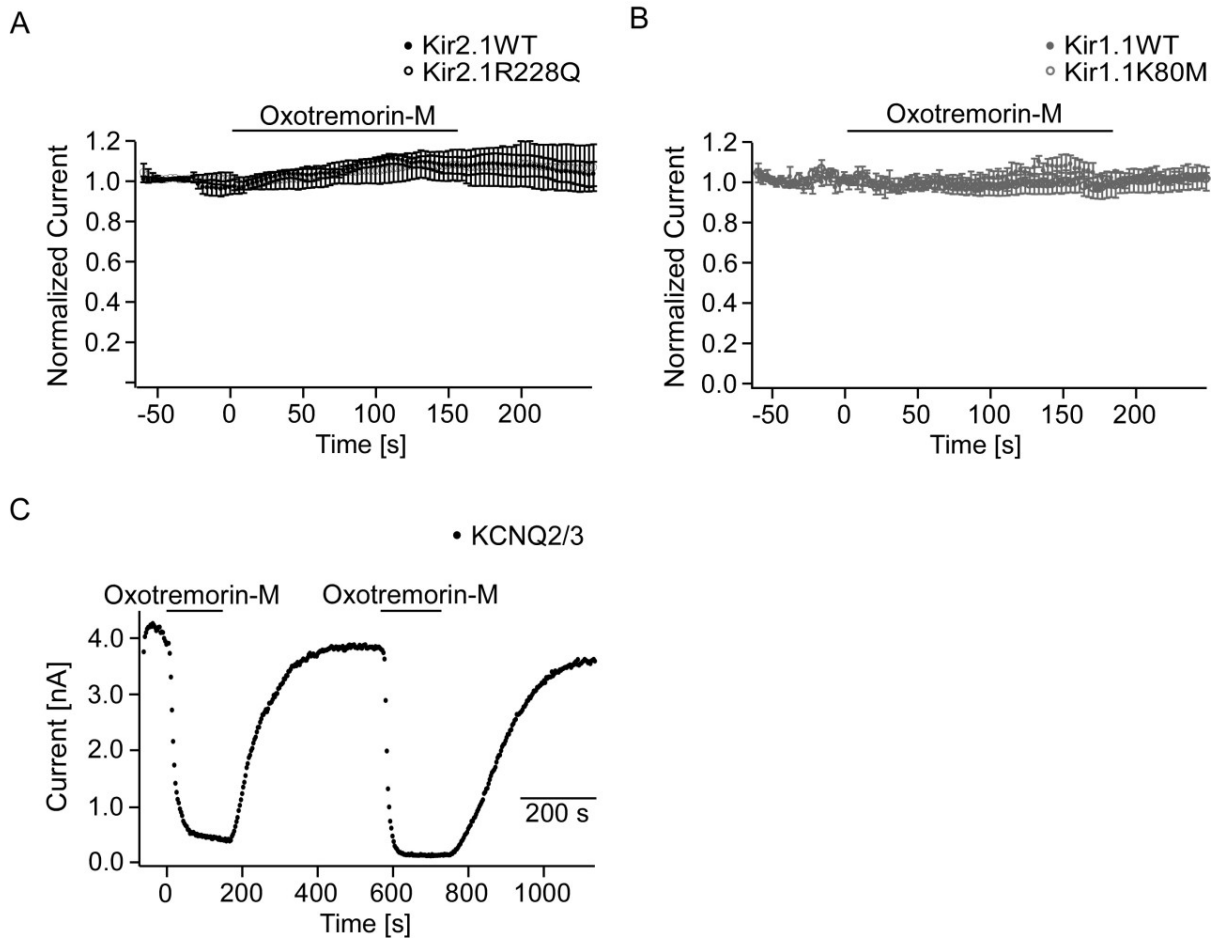


Figure 27: PLC induced PI(4,5)P₂ hydrolysis is ineffective on Kir2.1 and Kir1.1 channels.

A, B Whole cell recordings from CHO cells expressing Kir2.1WT (n = 5), Kir2.1R228Q (n = 7) (A), Kir1.1WT (n = 4) or Kir1.1K80M channels (n = 6) (B) and M1 receptors. Kir2.1 and Kir1.1 currents did not decline upon M1 receptor stimulation by oxotremorin-M and subsequent PLC-triggered PI(4,5)P₂ hydrolysis. Current amplitudes were averaged over the last 10 ms of each test pulse.

C Whole-cell current amplitudes of a CHO cell co-expressing KCNQ2/3 heteromeric channels and M1 receptors. PLC-mediated PI(4,5)P₂ hydrolysis by M1 receptor stimulation upon oxotremorin-M application led to reversible and repeatable current decline.

4.4 Characterization of two fluorescent PI(4,5)P₂ sensors

4.4.1 Quantification of the PI(4,5)P₂ affinities of fluorescent sensors using Ci-VSP

Understanding PI(4,5)P₂ signalling requires the knowledge about temporal and spatial concentration changes of PI(4,5)P₂. These dynamical changes can be measured with fluorescence labelled sensors that bind specifically to PI(4,5)P₂. Two such specific PI(4,5)P₂ sensors, PLCδ1-PH domain and tubby-CT, have been described previously (Stauffer et al., 1998, Santagata et al., 2001). However, their

usefulness is controversial and remains to be investigated (see paragraph 2.3.2). In this part of the study it was investigated whether reversible binding and unbinding of these two sensors to PI(4,5)P₂ occurs in the range of physiological concentration changes. Therefore it was relevant to quantify their PI(4,5)P₂ affinities. PLCδ1-PH domain was suggested to have a low PI(4,5)P₂ affinity, because its membrane dissociation was fast in response to PLC-triggered PI(4,5)P₂ hydrolysis (Hirose et al., 1999, Szentpetery et al., 2009). However, PLCδ1-PH domain also binds to the hydrolysis product I(1,4,5)P₃. It is likely that the cytosolic I(1,4,5)P₃ pulls the domain towards the cytoplasm which possibly leads to an overestimation of the underlying PI(4,5)P₂ depletion. Tubby-CT translocation upon PLC activation was described to be slow and incomplete, leading to the suggestion that tubby-CT has a higher PI(4,5)P₂ binding affinity than PLCδ1-PH (Quinn et al., 2008, Szentpetery et al., 2009). In contrast, PI(4,5)P₂ depletion by phosphatases showed that tubby-CT readily dissociates from the plasma membrane, consistent with a low affinity for PI(4,5)P₂ (Quinn et al., 2008, Szentpetery et al., 2009).

Here, Ci-VSP was used to clarify the PI(4,5)P₂ affinities of PLCδ1-PH domain and tubby-CT. CHO cells were co-transfected with fluorescent-labelled PLCδ1-PH domain or tubby-CT and Ci-VSP. Membrane binding of both domains was characterized by TIRF microscopy. TIRF microscopy selectively collects fluorescence from the plasma membrane, such that the fluorescence signal is directly proportional to the number of GFP-labelled PI(4,5)P₂ binding domains associated to the plasma membrane. TIRF microscopy and whole-cell patch-clamp recordings were performed to measure the membrane fluorescence and to control the membrane potential, respectively. Membrane fluorescence was high when the membrane was hyperpolarized to -60 mV, where Ci-VSP is inactive, indicating a high PI(4,5)P₂ concentration at rest (Figure 28A left, B). Depolarization to +100 mV to activate Ci-VSP resulted in a decline in membrane fluorescence, indicating dissociation of both sensors from the membrane (Figure 28A middle, B). Upon repolarization to -60 mV membrane fluorescence recovered fully, indicating re-binding of the sensors due to PI(4,5)P₂ resynthesis by endogenous kinases (Figure 28A right, B). These observations suggest that both sensors bind to PI(4,5)P₂. However, comparison of dissociation and re-binding kinetics of the fluorescent probes showed that dissociation of tubby-CT was significantly faster ($\tau_{\text{dissociation,tubby-CT}} = 1.5 \pm 0.05$ s vs $\tau_{\text{dissociation,PLC}\delta 1\text{-PH}} = 2.5 \pm 0.9$ s, $p < 0.001$) and re-binding was significantly slower than

that of PLC δ 1-PH ($\tau_{\text{re-binding,tubby-CT}} = 15.5 \pm 3.7$ s vs $\tau_{\text{re-binding,PLC}\delta$ 1-PH} = 6.8 ± 3.3 s, $p < 0,001$) (Figure 28B, C). These kinetic differences suggested that the PI(4,5)P₂ binding affinity of tubby-CT was lower compared to that of PLC δ 1-PH domain.

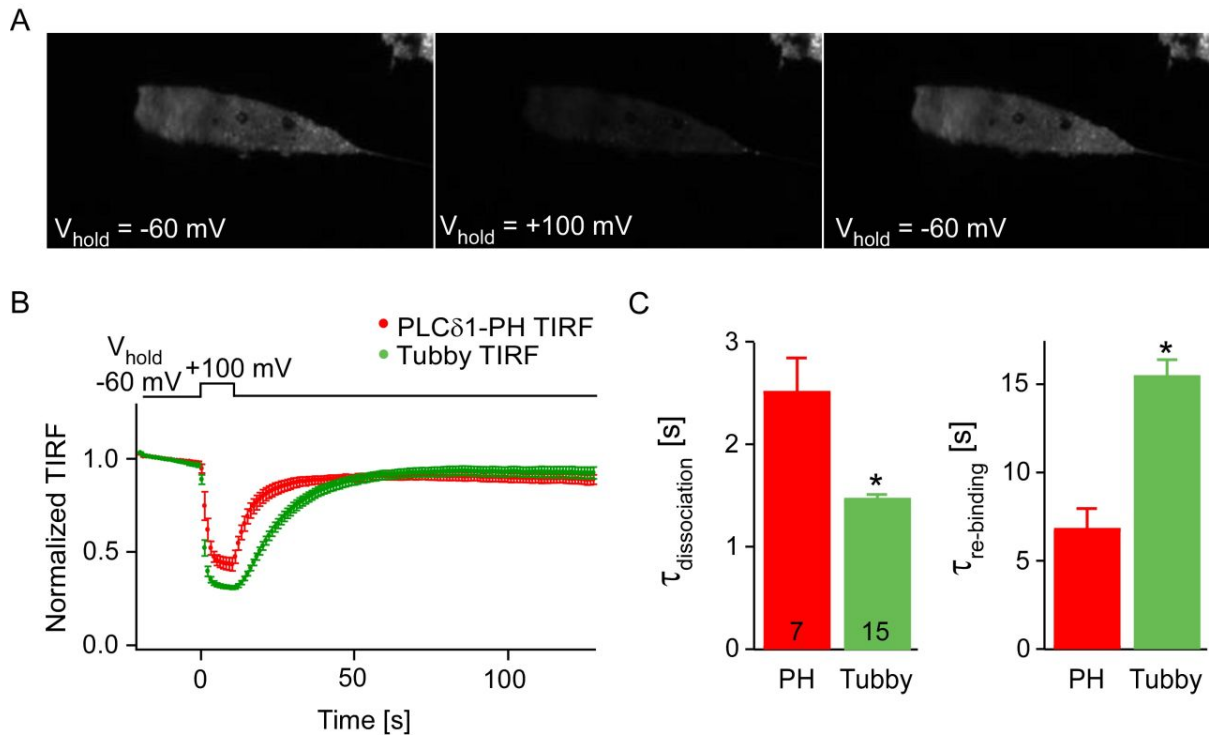


Figure 28: Translocation of PLC δ 1-PH domain and tubby-CT upon Ci-VSP activation.

A TIRF microscopy images of a CHO cell co-expressing tubby-CT and Ci-VSP before (left), during (middle), and after (right) depolarization.

B Tubby-CT TIRF signal decreased faster upon Ci-VSP-induced PI(4,5)P₂ depletion and recovered more slowly when PI(4,5)P₂ was resynthesized than fluorescent signal of PLC δ 1-PH domain.

C Summary data of experiments as in (B) show significant differences for $\tau_{\text{dissociation}}$ and $\tau_{\text{re-binding}}$ between PLC δ 1-PH domain and tubby-CT. Numbers of independent experiments as indicated.

4.4.2 Estimation of the dynamic range and the PI(4,5)P₂ affinity of fluorescence sensors

Various physiological signals such as GPCR or phosphatase activation induce changes in the cellular PI(4,5)P₂ concentration. These changes were to be monitored by the PI(4,5)P₂ sensors PLC δ 1-PH domain and tubby-CT. However, it remained to be investigated which part of the changing PI(4,5)P₂ concentration range determined by physiological stimuli was detected by the sensors. Therefore, it was first necessary to establish the physiological PI(4,5)P₂ concentration range, and then this

was compared to the range covered by the sensors. In order to determine the physiological PI(4,5)P₂ concentration range, e.g. the activity of ion channels that are known to be physiologically regulated by PI(4,5)P₂ concentration changes can be used. Suitable candidates are M current generating KCNQ2 channels, because they deactivate in response to physiological PI(4,5)P₂ concentration dynamics, such as depletion PI(4,5)P₂ during GPCR-triggered activation of PLC (Shapiro et al., 2000). An optimal PI(4,5)P₂ sensor is required to display a robust signal across the whole range of various PI(4,5)P₂ concentrations that affect the PI(4,5)P₂-sensitive channel. In other words, the 'dynamic operation range' of the sensor should match the response range of the physiological PI(4,5)P₂ effector protein.

Therefore, the activity of KCNQ2 channels and the sensor fluorescence (PLCδ1-PH domain or tubby-CT) were simultaneously recorded in CHO cells co-expressing Ci-VSP using whole-cell patch-clamp and TIRF, respectively. KCNQ2 currents and membrane fluorescence reversibly declined upon activation of Ci-VSP and subsequent PI(4,5)P₂ depletion by depolarization to +100 mV (Figure 29A, B). In order to analyse a range of continuously changing PI(4,5)P₂ concentration as broad as possible, normalized currents (indicating the physiologically relevant PI(4,5)P₂ concentration range) were plotted against normalized fluorescence during the recovery phase after Ci-VSP activation (10 s – 110 s) (Figure 29C). These plots showed that the current-TIRF relationship obtained with PLCδ1-PH was steeper than that of tubby-CT. In fact, for PLCδ1-PH, the slope increased, finally running parallel to the y-axis (Figure 29C), as fluorescence recovery was complete while the current still increased (Figure 29A). This indicated that the PLCδ1-PH TIRF signal was already saturated (full PI(4,5)P₂ binding of the domain) while current increase reported an on-going physiologically relevant increase of the cellular PI(4,5)P₂. The current-TIRF relationship of tubby-CT, however, was almost linear over the total range described by KCNQ2 channel activity. This shows that the tubby-CT TIRF signal did not saturate during the PI(4,5)P₂ concentration range that was sensed by the KCNQ2 channels. These findings indicate that a broader part of the physiological PI(4,5)P₂ concentration range as defined by the KCNQ2 activity was covered by tubby-CT than by PLCδ1-PH domain. Moreover, the linear relation between KCNQ2 current and membrane binding of tubby-CT directly shows that both proteins have similar PI(4,5)P₂ affinities. As the absolute affinity of the KCNQ2 has been estimated

previously using independent methods (Li et al., 2005), it is possible to arrive at an estimate for the molar PI(4,5)P₂ affinity of the sensor domains (see paragraph 5.1.3).

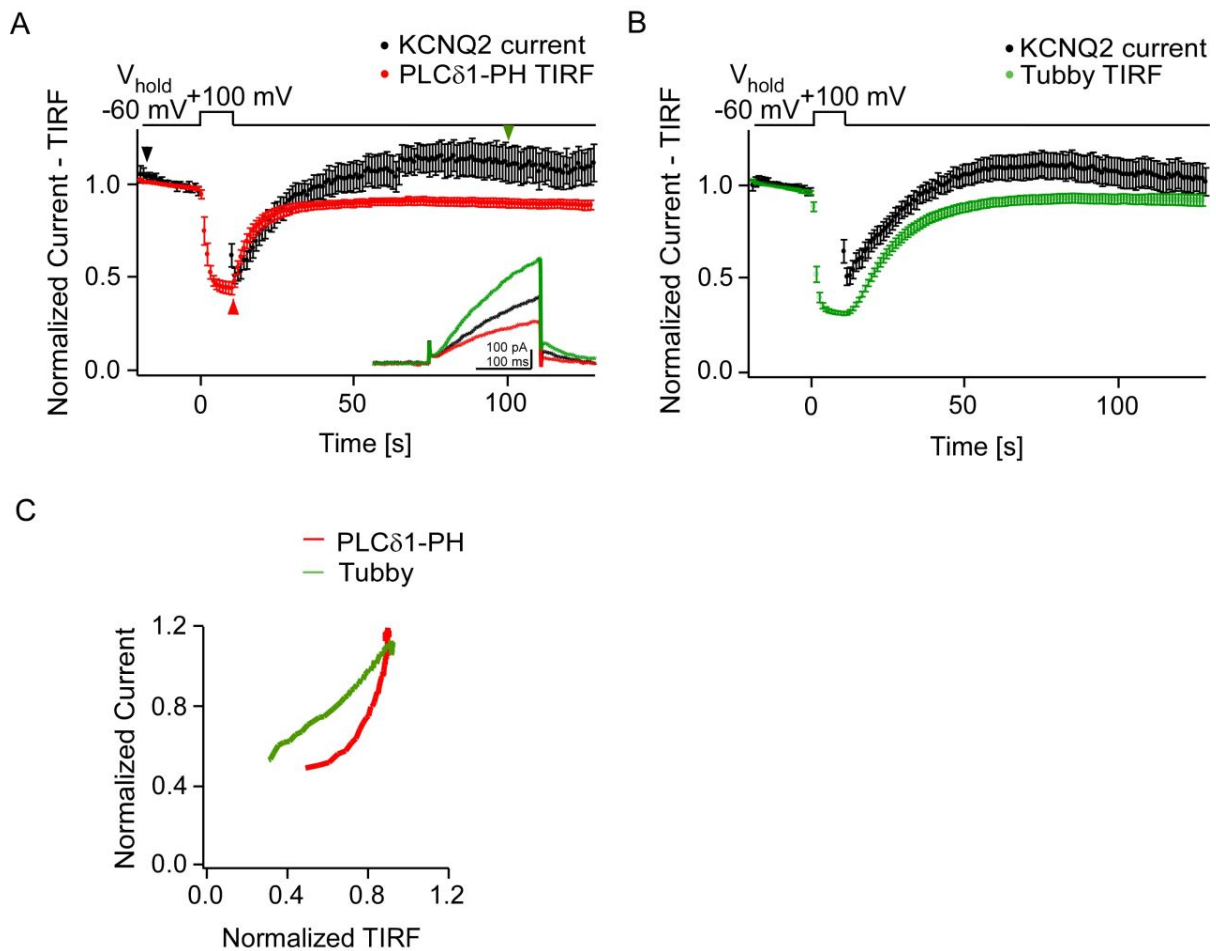


Figure 29: Simultaneous KCNQ2 channel deactivation and PLCδ1-PH or tubby-CT translocation upon Ci-VSP activation.

A, B Mean normalized KCNQ2 currents and TIRF signals ($n_{\text{PLC}\delta 1\text{-PH}} = 7$, $n_{\text{tubby-CT}} = 6$) of CHO cells decreased reversibly upon Ci-VSP-induced PI(4,5)P₂ depletion by depolarization to +100 mV for 10 s. Current amplitudes were averaged over the last 10 ms of each test pulse. Inset: Single current traces evoked by test pulses applied at the time points indicated by arrowheads.

C Averaged normalized KCNQ2 current amplitudes plotted against corresponding TIRF fluorescent signal during recovery (10 – 110 s) for PLCδ1-PH and tubby-CT.

4.4.3 Biosensor fluorescence signals during PLC-mediated cellular PI(4,5)P₂ dynamics

After characterizing the differential characteristics of the PI(4,5)P₂ sensors PLCδ1-PH domain and tubby-CT during PI(4,5)P₂ changes imposed by Ci-VSP, finally, their suitability to detect changed PI(4,5)P₂ levels upon PLC activation was investigated. Therefore, CHO cells were co-transfected with KCNQ2 channels, fluorescent

domains and M1 receptors. Simultaneous TIRF microscopy and whole-cell patch-clamp recordings were performed to compare the behaviour of PLC δ 1-PH and tubby-CT during PLC-triggered PI(4,5)P₂ hydrolysis. At the beginning of the recordings KCNQ2 mediated M currents increased continuously for 1 – 5 min (Figure 30). PLC-triggered PI(4,5)P₂ hydrolysis was started when currents reached a steady state level. M1 receptors were stimulated by the application of oxotremorin-M for 2 min. Upon activation of the receptor, KCNQ currents declined and PLC δ 1-PH probe dissociated reversibly from the membrane. Tubby-CT, however, did not respond to the activation of the M1 receptors (Figure 30). This observation was unexpected, since tubby-CT was suggested to have a lower PI(4,5)P₂ affinity than PLC δ 1-PH domain.

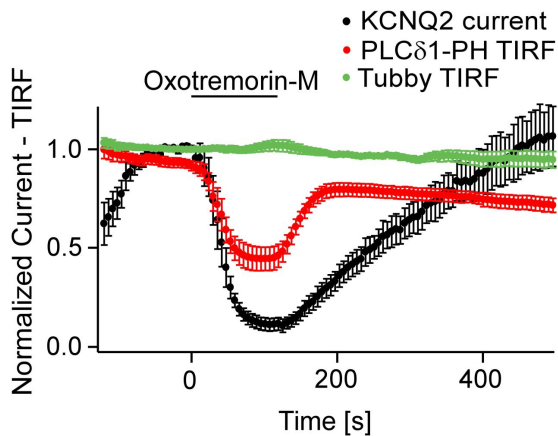


Figure 30: Translocation of PLC δ 1-PH domain upon PLC-triggered PI(4,5)P₂ depletion.

Mean normalized KCNQ2 currents and PLC δ 1-PH (n = 6), but not tubby-CT (n = 5) TIRF signal declined reversibly upon PLC-triggered PI(4,5)P₂ hydrolysis. Current amplitudes were averaged over the last 10 ms of each test pulse.

5 Discussion

5.1 Efficiency of Ci-VSP in quantification of the PI(4,5)P₂ affinities of ion channels

So far, the effect of VSP activity on ion channels has been examined a couple of times, either to demonstrate catalytic activity of the phosphatase (Murata et al., 2005, Murata and Okamura, 2007, Hossain et al., 2008) or, vice versa, to obtain evidence for a PI(4,5)P₂ dependence of the channel (Halaszovich et al., 2008, Iwasaki et al., 2008). Thus, Kir2.1WT and Kir3 channels (Murata et al., 2005, Murata and Okamura, 2007), KCNQ2/3 channels (Murata and Okamura, 2007, Hossain et al., 2008, Falkenburger et al., 2010), and on Cav channels (Suh et al., 2010) were found to deactivate upon activation of Ci-VSP by depolarization. However, the possibility for quantitative use of VSPs has not been explored so far. Here, gradual Ci-VSP activation was used for the first time in order to examine and to compare the apparent PI(4,5)P₂ affinities of K⁺ channels and PI(4,5)P₂ sensors.

5.1.1 Parameters that describe the apparent PI(4,5)P₂ affinity of Kir channels-reversibility, gradual activation, and velocity

Three parameters that characterize the channel's behaviour in response to Ci-VSP activity may be used to derive quantitative information on the PI(4,5)P₂-channel interaction: steady state channel deactivation, deactivation and re-opening kinetics, and the presence of residual currents during Ci-VSP activity.

Steady state channel deactivation (and the obtained $V_{1/2}$ value) is the most informative parameter for estimating the apparent PI(4,5)P₂ affinity of a certain ion channel. Thus, the most positive $V_{1/2}$ value of Kir2.1WT channels indicated a high apparent PI(4,5)P₂ affinity, which is consistent with previous studies (Huang et al., 1998). By contrast, the hyperpolarized $V_{1/2}$ value of Kir3.1/3.2 channels showed a low one, and the $V_{1/2}$ value of Kir1.1WT channels located between that of Kir2.1WT and Kir3.1/3.2 an intermediate one. Additionally, previously described alterations of the channel-PI(4,5)P₂ interaction by mutation (Kir2.1R228Q) (Lopes et al., 2002) or strengthening of the Kir3.1/3.2 channel-PI(4,5)P₂ interaction caused by accumulation of G_{βγ} (Huang et al., 1998) were reliably detected through the shift of the steady state

channel deactivation curves towards hyperpolarized or depolarized values, respectively.

The steady state deactivation curve of Kir1.1K80M channels was strongly depolarized in comparison to WT channels, indicating a high PI(4,5)P₂ affinity for the mutant channels. This observation deviates from results obtained elsewhere (Rapedius et al., 2007a), suggesting that the PI(4,5)P₂ affinities of Kir1.1WT and Kir1.1K80 mutant channels are equal. This conclusion was based on the finding that similar dose-response curves for Kir1.1WT and Kir1.1K80 mutant channels were obtained by the use of channel inhibition by neomycin application and channel activation by diC8-PI(4,5)P₂ application to inside-out giant patches, respectively (see also paragraph 2.3.1).

There are at least two possibilities that may explain this discrepancy. First, Kir1.1K80M channels may have a higher PI(4,5)P₂ affinity than Kir1.1WT and Kir2.1WT channels when recorded under physiologically low extracellular K⁺ conditions. Second, Kir1.1WT may be inhibited by the products of Ci-VSP, PI(4)P and/or PI(3,4)P₂. In combination with the K⁺-dependent inactivation occurring at physiological K⁺ levels, may account for a higher sensitivity to Ci-VSP activation in comparison to Kir1.1K80M channels, as indicated by the more hyperpolarized V_{1/2} value. Kir2.1WT channels that were expected to have the highest PI(4,5)P₂ affinity of the channels investigated, however, were not inhibited by PI(4)P and PI(3,4)P₂. Therefore, the lower V_{1/2} value of Kir2.1WT channels in comparison to that of Kir1.1K80M channels is not expected to be shifted towards hyperpolarized values. This observation supports the hypothesis that Kir1.1K80M channels when recorded under low extracellular K⁺ conditions have a higher PI(4,5)P₂ affinity than WT channels. However, further research is required to clarify this discrepancy.

Channel deactivation and re-opening kinetics can be used to compare the affinities between WT and mutant channels (Kir2.1WT and Kir2.1R228Q) or to investigate affinities during dynamic regulation (Kir3.1/3.2 in the presence or absence of G_{βγ}). The rate of deactivation was equal or slower and re-opening was faster for channels exhibiting high PI(4,5)P₂ affinity in comparison to channels exhibiting low affinity. However, it is not useful to compare the kinetics between Kir1.1WT and Kir1.1K80M channels in order to investigate their PI(4,5)P₂ affinities. Deactivated WT channels enter a non-activatable state (even when PI(4,5)P₂ is restored) under low

extracellular K^+ conditions when there is helix bundle crossing between TM1 and TM2 (see paragraph 4.1.4). This finding indicates that it is not $PI(4,5)P_2$ binding to the channels which is rate limiting for channel re-opening, but rather the subsequent conformational change, as reported previously (Rapedius et al., 2007a). For the same reason channel kinetics are not useful for estimating the affinities between Kir channel family members, thereby limiting the versatility of Ci-VSP. The re-opening kinetics of Kir2.1WT channels after Ci-VSP activation, for example, was slower than that of Kir3.1/3.2 channels, although Kir2.1WT channels exhibit a higher $PI(4,5)P_2$ affinity than Kir3.1/3.2, as consistently demonstrated by the $V_{1/2}$ in response to Ci-VSP activity (this study) and previous work using independent methods (Huang et al., 1998). Rather than delivering an information on $PI(4,5)P_2$ binding, fast recovery indicates that the conformational change (channel opening) following $PI(4,5)P_2$ binding is faster for Kir3.1/3.2 than for Kir2.1WT channels.

In a simplistic approach, the occurrence of residual currents during maximal Ci-VSP activity may be taken as measure for the channel's $PI(4,5)P_2$ affinity. In this scenario, large fractional residual currents might imply a high affinity, because $PI(4,5)P_2$ depletion by Ci-VSP seems to be insufficient to completely deactivate the channels. Surprisingly, residual currents were observed for Kir3.1/3.2, that clearly exhibit a low $PI(4,5)P_2$ affinity (this study and e.g. (Huang et al., 1998)), and no residual currents were observed for high-affinity Kir2.1WT channels. However, this apparent contradiction can be understood by taking into account the complexity of the enzymatic activity of Ci-VSP acting on the endogenous membrane PIs, if the affected channels are not entirely selective for $PI(4,5)P_2$. As previously shown (Halaszovich et al., 2008, Iwasaki et al., 2008), Ci-VSP converts its substrates $PI(4,5)P_2$ and $PI(3,4,5)P_3$, to $PI(4)P$ and $PI(3,4)P_2$, respectively, thereby reducing the cellular substrate concentrations but simultaneously increasing the concentrations of the products in a stoichiometric manner. PI nonspecificity of ion channels may modify the response to $PI(4,5)P_2$ depletion during Ci-VSP activity, leading e.g. to residual currents being observed for Kir3.1/3.2 channels, if the products ($PI(4)P$ and $PI(3,4)P_2$) can sustain channel activity. In order to fully understand the effects of Ci-VSP, it was necessary to determine the PI specificity of the channels. To this end, measurements of the ion channel activity in inside-out giant patches during selective application of various PIs were performed.

These experiments in a simplified cell-free system showed that Kir6.2/SUR1 channels, previously suggested to exhibit PI(4,5)P₂ affinity and PI specificity similar to that of Kir3.1/3.2 channels (Shyng and Nichols, 1998, Ho and Murrell-Lagnado, 1999, Rohacs et al., 1999, Rohacs et al., 2003, Tucker and Baukrowitz, 2008), were nonspecifically activated by all four PIs implicated in Ci-VSP activity. Therefore, the residual Kir3.1/3.2 currents observed during full activity of Ci-VSP are readily explained by binding of PI(4)P and PI(3,4)P₂ that are produced stoichiometrically with the depletion of PI(4,5)P₂ and PI(3,4,5)P₃. High PI(4,5)P₂ specificity of Kir2.1WT channels, on the other hand, nicely explains the lack of residual Kir2.1WT currents during Ci-VSP activity.

Recently, VSP activation was used to investigate the effect of PI(4,5)P₂ depletion on Cav channels and the results were compared to that obtained after PLC-triggered PI(4,5)P₂ hydrolysis (Suh et al., 2010). During VSP activity residual Cav currents occurred and they were larger than that observed during PLC-triggered PI(4,5)P₂ hydrolysis. This study also suggested that the VSP product PI(4)P might support channel activity leading to the maintenance of residual currents. The larger current decline during PLC activation was suggested to be mediated by downstream products of PLC such as arachidonic acid or PKC (Suh et al., 2010). This shows that the interpretation of such results is difficult when the PI specificity of the channels is unknown.

In conclusion, the analysis of residual currents during Ci-VSP activity is of very limited informative value with respect to channel-PI(4,5)P₂ affinities, unless detailed information on the PI selectivity of the channel is available. In fact, residual currents rather appear to be confounding factors that complicate the characterization of the PI(4,5)P₂ affinity of ion channels with unknown PI specificity.

5.1.2 Usefulness of Ci-VSP in comparison to alternative approaches for controlling PI(4,5)P₂ levels

Inp54p membrane translocation served as an independent approach to determine the reliability of Ci-VSP for analyzing Kir channel-PI(4,5)P₂ interactions. All Kir channels investigated were deactivated by Inp54p-mediated PI(4,5)P₂ depletion in a way comparable to the results obtained with Ci-VSP. Interestingly, deactivation of Kir2.1WT, Kir1.1K80M and Kir3.1/3.2 channels was incomplete during Inp54p-mediated PI(4,5)P₂ depletion, indicated by residual currents. The residual currents of

Kir3.1/3.2 channels after Ci-VSP activation seem to be, as already discussed, maintained by the activating influence of the Ci-VSP products PI(4)P and/or PI(3,4)P₂. Most likely, the product resulting from Inp54p-induced PI(4,5)P₂ depletion is PI(4)P, as suggested in (Varnai et al., 2006). Similarly, the activating influence of PI(4)P during Inp54p-induced PI(4,5)P₂ depletion can be considered to be responsible for the residual Kir3.1/3.2 and Kir1.1K80M currents, because partial Kir1.1K80M current recovery was observed after PI(4)P application to excised giant patches (see Figure 25).

Kir2.1WT channels did not display residual currents during Ci-VSP activity but residual currents remained when PI(4,5)P₂ was depleted with Inp54p. As discussed in 5.1.1, Kir2.1WT channels were found to exhibit a high PI(4,5)P₂ specificity. This finding is supported by a recent study using an independent approach where exclusive PI(4,5)P₂ specificity of Kir2.1WT channels has been identified by liposomal ⁸⁶Rb⁺ flux assays and patch-clamp recordings of giant liposomes containing Kir2.1WT channels (D'Avanzo et al., 2010). These findings rule out that the complete channel deactivation achieved during Ci-VSP activity is induced by the inhibiting effect of another PI involved. The present results indicate that the rate or the strength of Ci-VSP-induced PI(4,5)P₂ depletion is higher than that of Inp54p. PI(4,5)P₂ resynthesis by endogenous kinases may partially counter-balance the Inp54p activity, producing enough PI(4,5)P₂ molecules to keep the high-affinity Kir2.1WT channels partially open.

In summary, the results obtained using Ci-VSP as a tool to manipulate PI(4,5)P₂ levels were comparable to previously accepted methods such as Inp54p membrane translocation. Ci-VSP, however, has distinct advantages, because its use allows a more precise temporal control of cellular PI(4,5)P₂ concentration changes as indicated by the fast channel deactivation after Ci-VSP activation and the slower deactivation after Inp54p membrane translocation. A similar observation was described previously (Suh et al., 2010) for Cav channel deactivation in response to PI(4,5)P₂ depletion mediated by triggered Inp54p- versus VSP activation. Furthermore, Ci-VSP activity and the resulting depletion of PI(4,5)P₂ is rapidly reversible, which is in sharp contrast to the rapamycin-induced Inp54p translocation, where persisting channel deactivation after removal of rapamycin indicates irreversible PI(4,5)P₂ depletion. Finally, Ci-VSP enables the graded titration of endogenous PI(4,5)P₂ thereby allowing to measure a PI(4,5)P₂ dose-dependence

with endogenous (native) cellular PI(4,5)P₂ for effectors such as ion channels (the 'steady state channel deactivation curve' of ion channels). This property allows for an in-vivo estimation of their apparent channel-PI(4,5)P₂ affinity as discussed above. Nevertheless, Ci-VSP does not specifically deplete PI(4,5)P₂ but also uses PI(3,4,5)P₃ as a substrate which leads to the generation of PI(4)P and PI(3,4)P₂, four PIs that may influence the target proteins investigated. This can complicate the interpretation of data obtained with Ci-VSP, as outlined above. Therefore, e.g. the separate application of PIs to excised inside-out giant patches seems to be a possibility to determine the specificity of target proteins such as ion channels and transporters. However, current rundown and the irreversibility of PI accumulation in the patch membrane limit the suitability of inside-out patches.

5.1.3 Quantification of the PI(4,5)P₂ affinities of K⁺ channels

The apparent PI(4,5)P₂ affinities of the Kir channels investigated detected with Ci-VSP activation were Kir1.1K80M ($V_{1/2} = 55$ mV) > Kir2.1WT ($V_{1/2} = 34$ mV) > Kir2.1R228Q ($V_{1/2} = 22$ mV) > Kir1.1WT ($V_{1/2} = 12$ mV) > Kir3.1/3.2 ($V_{1/2} = -1$ mV). The affinities for KCNQ channels were KCNQ3 ($V_{1/2} = 23$ mV) > KCNQ2/3 ($V_{1/2} = -3$ mV) > KCNQ2 ($V_{1/2} = -23$ mV). Thus it appears that Kir1.1K80M channels have the highest and KCNQ2 channels have the lowest apparent PI(4,5)P₂ affinity of the channels investigated. Furthermore, the affinities of KCNQ3 channels or KCNQ2/3 channels were in the same order like that of Kir2.1R228Q channels or Kir3.1/3.2 channels, respectively.

Rank order of affinities of Kir channels established by Ci-VSP was consistent with previous studies (Huang et al., 1998), thus confirming the results obtained by alternative approaches. Furthermore, the results go along with findings that Kir channels containing a leucine at the position homologous to Kir2.3I213, exhibit high (e.g. Kir2.1 and Kir1.1), whereas isoleucine-containing Kir channels (e.g. Kir3 and Kir2.3) show weak apparent PI(4,5)P₂ affinity (Du et al., 2004).

In previous studies (Zhang et al., 2003, Du et al., 2004, Li et al., 2005, Rapedius et al., 2007a, Hernandez et al., 2008) dose-response relationships of K⁺ channels obtained with application of diC8-PI(4,5)P₂ to excised inside-out patches were used to estimate apparent PI(4,5)P₂ affinities. Consistent with the results obtained with Ci-VSP, they found that the concentration for half-maximal channel

activation (EC_{50}) was high for KCNQ4 and KCNQ2 channels, intermediate for KCNQ2/3 channels and low for Kir1.1WT, KCNQ3, Kir2.1WT, Kir1.1K80 mutant channels, indicating low, intermediate, and high $PI(4,5)P_2$ affinity, respectively (Figure 31). The EC_{50} values reported markedly vary for individual channels (e.g. KCNQ4 and KCNQ2/3 channels). Furthermore, similar EC_{50} values for different channels (e.g. 6 μM for KCNQ3 channels (Hernandez et al., 2008) and 5 μM for Kir2.1WT channels (Du et al., 2004)) indicated similar $PI(4,5)P_2$ affinities. Ci-VSP, however, suggested that the affinities of these channels are different (high $PI(4,5)P_2$ affinity for Kir2.1WT ($V_{1/2} = 34$ mV) and a lower $PI(4,5)P_2$ affinity for KCNQ3 ($V_{1/2} = 23$ mV)), indicating high precision of Ci-VSP to discriminate the channel- $PI(4,5)P_2$ affinities in comparison to diC8- $PI(4,5)P_2$ application (Figure 31).

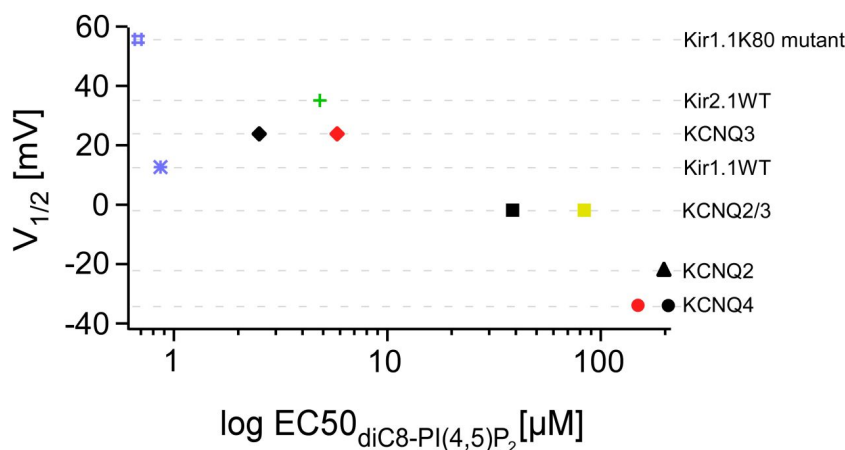


Figure 31: Correlation of the K^+ channel- $PI(4,5)P_2$ affinities measured with diC8- $PI(4,5)P_2$ and Ci-VSP.

Ci-VSP allows a precise discrimination of the $PI(4,5)P_2$ affinities of the channels illustrated. Estimating the affinities by measuring the diC8- $PI(4,5)P_2$ dose-response properties and resulting EC_{50} values is more variable. Symbols represent $V_{1/2}$ values obtained by Ci-VSP activation plotted against the EC_{50} values taken from various previous studies Blue: (Rapedius et al., 2007a), green: (Du et al., 2004), black: (Li et al., 2005), red: (Hernandez et al., 2008), yellow: (Zhang et al., 2003).

5.2 Does sensitivity to Ci-VSP predict the regulation of channels by physiological $PI(4,5)P_2$ dynamics?

The second aim of this study was to examine the relationship between the $PI(4,5)P_2$ affinities of Kir channels derived from the Ci-VSP experiments and the channel behaviour during physiological, i.e. receptor-induced alteration of $PI(4,5)P_2$ concentrations. In this study, neither channels exhibiting high $PI(4,5)P_2$ affinity

(Kir2.1WT, Kir1.1K80M) nor channels with lower affinity (Kir2.1R228Q, Kir1.1WT), as confirmed by Ci-VSP effects, were deactivated by PLC-triggered PI(4,5)P₂ hydrolysis. Previous studies also reported that Kir2.1WT and Kir1.1WT channels were not inhibited by muscarinic stimulation (Chuang et al., 1997, Kobrinsky et al., 2000, Zhang et al., 2003). The finding that Kir2.1R312Q channels with reduced PI(4,5)P₂ affinity in comparison to WT channels were shown to be inhibited by GPCR activation (Du et al., 2004) led to the suggestion that only channels with intermediate or low PI(4,5)P₂ affinities respond to muscarinic PI(4,5)P₂ hydrolysis. Similarly, intermediate-affinity KCNQ2/3 channels were deactivated by PLC induced PI(4,5)P₂ hydrolysis and Kir3.1/3.2 channels that have a comparable PI(4,5)P₂ affinity, indicated by similar V_{1/2} values obtained by gradual Ci-VSP activation, were reported to be deactivated by the activation of M1 receptors (Zhang et al., 2003). However, (Jones, 1996) found that M1 receptor stimulation with carbachol led to Kir2.1WT channel inhibition. Replicating Jones' experiments by using carbachol to stimulate M1 receptors, however, never affected Kir2.1 (n = 5) or Kir1.1 channels (n = 5), corroborating the suggestion that channels with high PI(4,5)P₂ affinities are not affected by PLC-triggered PI(4,5)P₂ hydrolysis.

Surprisingly, Kir2.1R228Q channels that have reduced PI(4,5)P₂ affinity in comparison to Kir2.1WT channels as confirmed by gradual Ci-VSP activation were not deactivated by GPCR activation whereas KCNQ3 channels with an affinity similar to that of Kir2.1R228Q channels are robustly inhibited by muscarinic stimulation (e.g. (Shapiro et al., 2000)). This finding suggested that the PI(4,5)P₂ affinity is not the only factor determining sensitivity to GPCR stimulation.

Thus, the observation that the sensitivity of the channels to Ci-VSP and thus their apparent PI(4,5)P₂ affinity does not predict the sensitivity to GPCR stimulation led to the question: Given that the depletion of PI(4,5)P₂ by phosphatases is effective enough to deactivate high-affinity Kir2.1 and Kir1.1 channels, why is PLC-triggered PI(4,5)P₂ hydrolysis insufficient to do the same but rather appears to discriminate between different K⁺ channel families?

A possible explanation could be the hydrolysis of variable quantities of PI(4,5)P₂ molecules by phosphatases versus PLC. Models predict that the turnover rate of PLC-triggered PI(4,5)P₂ hydrolysis is 35-fold slower than VSP induced depletion (Falkenburger et al., 2010) under experimental conditions similar to the ones used here. However, a recent study using fluorescence resonance energy

transfer to monitor PI(4,5)P₂ concentration changes showed that PI(4,5)P₂ depletion with VSP was comparable to that seen with M1 receptors (Suh et al., 2010). The same study also reported that the current decline of PI(4,5)P₂-regulated Cav channels was stronger upon PLC-triggered PI(4,5)P₂ hydrolysis than during VSP activation. Finally, the deactivation of KCNQ3 channels upon PLC-mediated PI(4,5)P₂ hydrolysis (Shapiro et al., 2000) shows that the quantity of hydrolysed PI(4,5)P₂ is sufficient to deactivate high-affinity channels.

Second, I(1,4,5)P₃ triggered Ca²⁺ responses has been found to enhance the resynthesis of PI(4,5)P₂ during PLC activation (Carney et al., 1985, Lassing and Lindberg, 1990, Yorek et al., 1994, Xu et al., 2003, Winks et al., 2005). This may effectively limit the PI(4,5)P₂ depletion during GPCR activation and keeps channels with high PI(4,5)P₂ affinity open. As no I(1,4,5)P₃ is produced and subsequently less PI(4,5)P₂ is regenerated during 5' phosphatase activity, the net effect of Ci-VSP on ion channels with high PI(4,5)P₂ affinity may be greater than that of PLC. Again, the differential response KCNQ3 versus Kir2.1228Q (same sensitivity to Ci-VSP) to GPCR stimulation (Shapiro et al., 2000) cannot be explained by this model.

Finally, it is possible that channels and receptors or phosphatases are differentially associated with different PI(4,5)P₂ pools. Distinct pools may either correspond to different subcellular compartments as shown, e.g., for phagosomal cups (see paragraph 2.2.3, (Botelho et al., 2000)) or to lipid raft versus non-lipid raft domains (Figure 32). Many GPCRs such as β1 and β2 adrenoceptors, M1 and M2 receptors, and metabotropic glutamate receptors, the G protein subunits G_{αq} and G_{αs} as well as PLC have been shown to be associated with rafts (Allen et al., 2007). In addition, many ion channels such as voltage gated Ca²⁺ (Cav2.1) channels (Davies et al., 2006) and K⁺ channels (Kv2.1 (Martens et al., 2000), Kv1.5 (Martens et al., 2001)) also seem to be localized to rafts. (Cooper et al., 2000) and (Oldfield et al., 2009) found that muscarinic receptors and KCNQ channels co-localize in lipid rafts, thereby specifying the coupling between receptors and channels and enabling receptor-mediated suppression of the channel activity by PI(4,5)P₂ hydrolysis (Figure 32 left). The spatial separation of Kir channels in non-lipid raft domains might explain the lack of response to GPCR activation (Figure 32 right). In this model, 5' phosphatases such as Ci-VSP and Inp54p, however, should be localized ubiquitously, because Kir channels (Figure 13, Figure 15, Figure 26) as well as

KCNQ (Figure 14) (Suh et al., 2006)) channels are inhibited by 5' phosphatase activity.

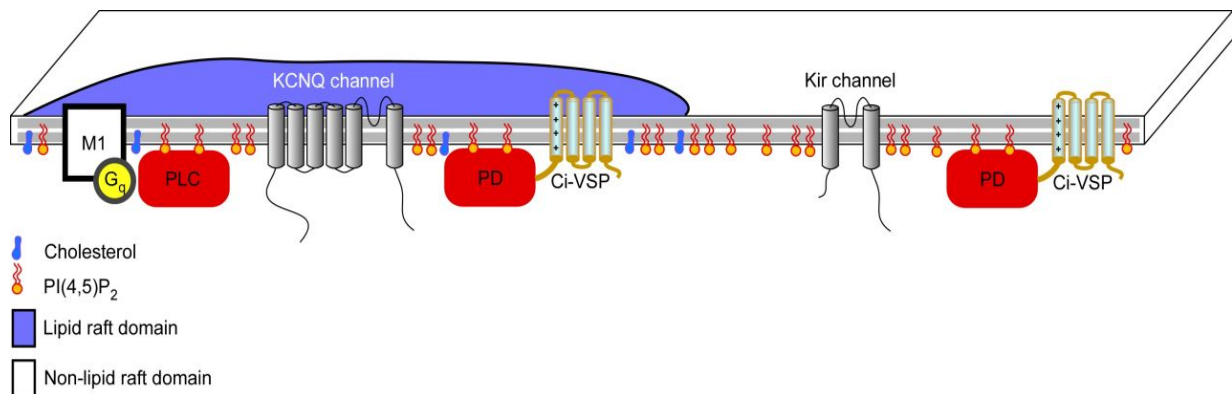


Figure 32: Hypothetical model for the distribution of ion channels, M1 receptors and Ci-VSP in lipid raft domains or non-lipid raft domains.

KCNQ channels co-localize together with M1 receptors and Ci-VSP in lipid raft domains (left). Kir channels co-localize only with Ci-VSP in non-lipid raft domains (right).

5.3 PLC δ 1-PH and tubby-CT may detect distinct PI(4,5)P₂ pools

After establishing Ci-VSP as a convenient tool to quantify the PI(4,5)P₂ affinity of effector proteins (ion channels), its properties were utilized to quantify the affinity of biosensors (PLC δ 1-PH and tubby-CT) in order to investigate their suitability for PI(4,5)P₂ live-cell-imaging. Both domains reversibly dissociated from the membrane upon Ci-VSP activation in CHO cells. Membrane dissociation of tubby-CT was faster and re-binding was slower in comparison to PLC δ 1-PH domain, indicating a lower PI(4,5)P₂ affinity of tubby-CT. These findings corroborate preliminary conclusions (Halaszovich et al., 2008), where dissociation of tubby-CT upon Ci-VSP activation has been shown to occur at a lower level of depolarization and therefore at less complete PI(4,5)P₂ depletion. Furthermore, the almost linear current-TIRF relationship of tubby-CT gave some indication that the operation range as well as the PI(4,5)P₂ affinity of tubby-CT is, in contrast to PLC δ 1-PH domain, similar to the previously reported low affinity of KCNQ2 channels (Li et al., 2004).

Different studies reported that tubby-CT dissociated from the membrane upon G_{αq} activation and following PLC- β -triggered PI(4,5)P₂ hydrolysis (Santagata et al., 2001), as well as after Inp54p- (Szentpetery et al., 2009) or Ci-VSP-induced PI(4,5)P₂ depletion (see Figure 28). These observations reveal that PLC as well as 5' phosphatases are sufficient to induce tubby-CT membrane dissociation.

Contradictory to the dissociation of tubby-CT reported during PLC-triggered PI(4,5)P₂ hydrolysis (Santagata et al., 2001), my recordings showed that following PLC activation, only PLCδ1-PH domain dissociated from the membrane (see Figure 30). Tubby-CT, however, did not translocate when PI(4,5)P₂ levels were decreased by PLC activation.

There are different possibilities to explain the discrepancy why tubby domain dissociated upon 5' phosphatase-induced PI(4,5)P₂ depletion, but not when PI(4,5)P₂ hydrolysis was triggered by PLC.

First, tubby-CT may exhibit a higher PI(4,5)P₂ affinity than PLCδ1-PH domain. This was suggested by (Nelson et al., 2008, Szentpetery et al., 2009) based on the finding that tubby-CT did not dissociate during PLC-triggered PI(4,5)P₂ hydrolysis. (Nelson et al., 2008) discussed the possibility that tubby migration between highly abundant PI(4,5)P₂ molecules competes with translocation of the probe into the cytosol. (Szentpetery et al., 2009) used fluorescence recovery after photobleaching (FRAP) studies, to investigate the affinities of PLCδ1-PH and tubby-CT domain. The time needed to reach half maximal fluorescent recovery after photobleaching selected areas of the plasma membrane was significantly shorter for tubby-CT than for PLCδ1-PH. This shorter time was thought to reflect a higher PI(4,5)P₂ affinity and subsequently a slower dissociation rate.

However, using Ci-VSP to quantify the PI(4,5)P₂ affinities of the probes showed a higher affinity for PLCδ1-PH domain than for tubby-CT (Halaszovich et al., 2008) (see Figure 28). Therefore, it was expected that tubby-CT easily dissociates upon PLC-triggered PI(4,5)P₂ depletion. The lacking tubby-CT response during GPCR activation may be caused by a lower level of PI(4,5)P₂ hydrolysis upon PLC activation than during Ci-VSP activation. As discussed above (see paragraph 5.2), this can occur when the turnover rate of PLC is lower than that of Ci-VSP (Falkenburger et al., 2010) or when PI(4,5)P₂ is resynthesized during GPCR activation. This would imply a more or less constant PI(4,5)P₂ concentration remaining during PLC activity. Thus, the dissociation of high-affinity PLCδ1-PH domain is likely to occur due to a 'pull' towards the elevated I(1,4,5)P₃ concentration in the cytoplasm (Nelson et al., 2008). This finding could be misinterpreted as low affinity for PLCδ1-PH.

However, the observation that KCNQ2 channels deactivated during PLC-induced PI(4,5)P₂ hydrolysis invalidates this argument, because resynthesis of a

PI(4,5)P₂ concentration that is sufficient preventing tubby-CT from translocation should also prevent channel deactivation, when the proteins have similar PI(4,5)P₂ affinities.

Finally, the sensors might detect spatially separated PI(4,5)P₂ pools that are sorted either into distinct compartments (see paragraph 2.2.3, (Botelho et al., 2000)) or into lipid raft or non-raft domains. Taking the hypothesis described in paragraph 5.2 as a basis, tubby-CT might exclusively target PI(4,5)P₂ located in non-raft domains (Figure 33 right), because it is insensitive to PI(4,5)P₂ changes induced by PLC activation. As described above, M1 receptors, G proteins as well as PLC have been shown to be associated with lipid raft domains (Allen et al., 2007). PLCδ1-PH, however, either targets PI(4,5)P₂ residing in the lipid raft domain (Figure 33 left) or it nonspecifically targets PI(4,5)P₂ within both domains.

In a simplistic model PI(4,5)P₂ molecules and Ci-VSP are equally distributed to raft and non-raft domains, each domain occupies 50% of the total cell membrane, and all PI(4,5)P₂ molecules are targeted by PLCδ1-PH. If PLCδ1-PH targets PI(4,5)P₂ residing in both domains, PI(4,5)P₂ depletion by Ci-VSP would induce a decrease in the fluorescent signal that is two times higher than that induced by PLC activation. A modification of this simplified case, e.g. not all PI(4,5)P₂ molecules are targeted by PLCδ1-PH, would induce a change in the fluorescent signal observed. In that case the hydrolysis of raft associated PI(4,5)P₂ might induce a transfer of PLCδ1-PH domains towards unsaturated PI(4,5)P₂ molecules associated with non-raft domains. The resulting fluorescent signal would be expected to be much lower or hardly detectable. Coming back to the simplified model, where PLCδ1-PH targets PI(4,5)P₂ that is only associated with lipid-rafts, a similar decrease of the fluorescent signal for PLC or Ci-VSP activation would be expected. Taken this as a basis allows the suggestion that PLCδ1-PH very likely targets PI(4,5)P₂ residing in lipid-raft domains (Figure 33), because the fluorescent signal observed for both approaches was similar (Figure 28, Figure 30).

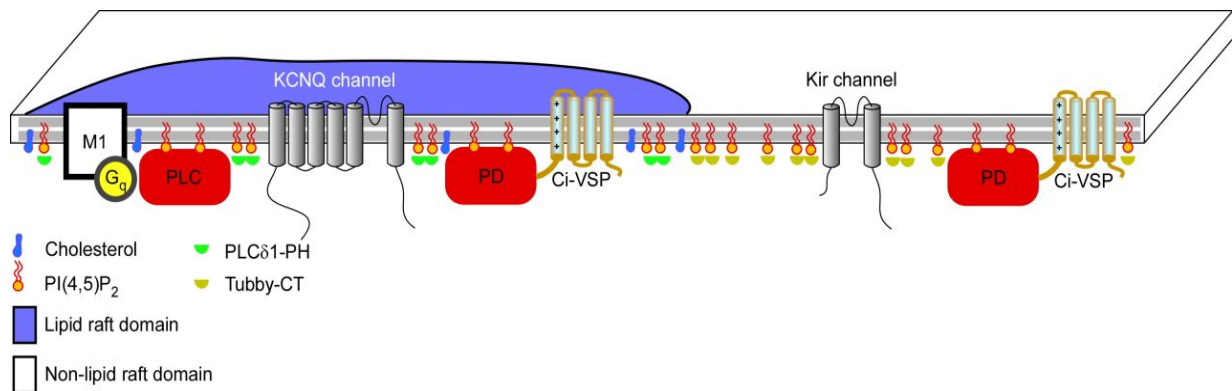


Figure 33: Hypothetical model for the distribution of the sensors PLC δ 1-PH domain and tubby-CT in lipid raft domains or non-raft domains.

PLC δ 1-PH domain (green semicircles) targets PI(4,5)P₂ molecules that are assembled in lipid raft domains. Tubby-CT (yellow semicircles) targets PI(4,5)P₂ within non-lipid raft domains (right).

5.4 Future prospects

My experiments show that Ci-VSP is a useful and reliable tool for rapid, reversible, and gradual manipulation of PIs in living cells. Ci-VSP allows for the quantitative examination of PI(4,5)P₂ sensitivities of targets (or effectors) of PI(4,5)P₂ signaling and of genetically encoded fluorescent sensors for PI(4,5)P₂ dynamics. In future studies it can be used to define the regulation of various proteins, including ion channels, by PI(4,5)P₂. For example, there is ongoing discussion whether two-pore-domain potassium (K2P) channels such as TASK channels (Lopes et al., 2005, Mathie, 2007) or transient receptor potential (TRP) channels (Estacion et al., 2001, Hilgemann et al., 2001) are regulated by PI(4,5)P₂. Ci-VSP activation now provides a novel approach to unequivocally clarify the controversial role of PI(4,5)P₂. Furthermore, during Ci-VSP activation no second messengers are generated that might influence channel activity. The same feature of Ci-VSP can be utilized to study the impact of PI(4,5)P₂ depletion on ion channels during different cellular processes, e.g. neuronal activity. However, it should be noticed that Ci-VSP is not entirely selective for PI(4,5)P₂. Therefore, verification of the data obtained with Ci-VSP by an independent method, e.g. Inp54p translocation, should be performed routinely. Finally, Ci-VSP can be used to study the PI(4,5)P₂ affinity of other PI(4,5)P₂ sensors for studying PI(4,5)P₂ dynamics. Ideally, these sensors would be perfectly selective for PI(4,5)P₂ and target PI(4,5)P₂ in both lipid raft or non-lipid raft domains.

There are a couple of questions that arose out of this study. They deal with the separation of the proteins described (channels, receptors, enzymes, sensors) into lipid raft or non-lipid raft domains.

First, the differential regulation of K^+ channels or translocation of $PI(4,5)P_2$ sensors by Ci-VSP activation versus M1 receptor activation discussed in paragraphs 5.2 and 5.3 might be explained by an association of the distinct proteins to lipid rafts (KCNQ channels, M1 receptors, PLC δ 1-PH domain), to non-raft membranes (Kir channels, tubby-CT) or to both domains (Ci-VSP). Therefore it might be interesting to investigate their actual localization, e.g. with biochemical approaches, in order to corroborate the hypotheses.

Second, the question should be addressed whether $PI(4,5)P_2$ pools that are hypothetically associated with lipid-raft or non-lipid raft domains are able to separately affect effector and sensor proteins. Therefore it would be necessary to deplete both pools separately. This may be achieved by the use of the heterodimerization assay where Inp54p is translocated to a membrane anchor. Modulation of the membrane anchor in such a way that it is either associated to raft or non-raft domains may target the translocation of the phosphatase selectively to the one of the membrane domains. This may allow for selective depletion of the $PI(4,5)P_2$ pools putatively associated with both compartments. There are two modified Inp54ps described: L10-Inp54p (N-terminal 10 residues of Lck), that associates to rafts, and S15-Inp54p (N-terminal 15 residue of Scr), that associates to non-raft domains (Johnson et al., 2008b). These constitutive phosphatases have been described to induce differential but barely comprehensible cell responses (Johnson et al., 2008b). However, the responses observed reinforce the hypothesis of compartmentalization of $PI(4,5)P_2$ -dependent signalling in cell membranes. Using the L10 and S15 residues as individual membrane anchors in the heterodimerization assay may provide a dynamical tool for the individual depletion of raft associated or non-raft associated $PI(4,5)P_2$ molecules and the investigation of possible differential effects on ion channels.

6 References

- Aguilar-Bryan L, Clement JPt, Gonzalez G, Kunjilwar K, Babenko A, Bryan J (1998) Toward understanding the assembly and structure of KATP channels. *Physiol Rev* 78:227-245.
- Aharonovitz O, Zaun HC, Balla T, York JD, Orlowski J, Grinstein S (2000) Intracellular pH regulation by Na(+)/H(+) exchange requires phosphatidylinositol 4,5-bisphosphate. *J Cell Biol* 150:213-224.
- Ahn JY, Rong R, Liu X, Ye K (2004) PIKE/nuclear PI 3-kinase signaling mediates the antiapoptotic actions of NGF in the nucleus. *Embo J* 23:3995-4006.
- Allen JA, Halverson-Tamboli RA, Rasenick MM (2007) Lipid raft microdomains and neurotransmitter signalling. *Nat Rev Neurosci* 8:128-140.
- Aman MJ, Lamkin TD, Okada H, Kurosaki T, Ravichandran KS (1998) The inositol phosphatase SHIP inhibits Akt/PKB activation in B cells. *J Biol Chem* 273:33922-33928.
- Andrews S, Stephens LR, Hawkins PT (2007) PI3K class IB pathway in neutrophils. *Sci STKE* 2007:cm3.
- Antcliff JF, Haider S, Proks P, Sansom MS, Ashcroft FM (2005) Functional analysis of a structural model of the ATP-binding site of the KATP channel Kir6.2 subunit. *Embo J* 24:229-239.
- Aoki K, Nakamura T, Inoue T, Meyer T, Matsuda M (2007) An essential role for the SHIP2-dependent negative feedback loop in neuritogenesis of nerve growth factor-stimulated PC12 cells. *J Cell Biol* 177:817-827.
- Attali B (1996) Ion channels. A new wave for heart rhythms. *Nature* 384:24-25.
- Baukrowitz T, Schulte U, Oliver D, Herlitze S, Krauter T, Tucker SJ, Ruppersberg JP, Fakler B (1998) PIP2 and PIP as determinants for ATP inhibition of KATP channels. *Science* 282:1141-1144.
- Beauge L, Asteggiano C, Berberian G (2002) Regulation of phosphatidylinositol-4,5-bisphosphate bound to the bovine cardiac Na⁺/Ca²⁺ exchanger. *Ann N Y Acad Sci* 976:288-299.
- Bernier LP, Ase AR, Chevallier S, Blais D, Zhao Q, Boue-Grabot E, Logothetis D, Seguela P (2008) Phosphoinositides regulate P2X4 ATP-gated channels through direct interactions. *J Neurosci* 28:12938-12945.
- Bian J, Cui J, McDonald TV (2001) HERG K(+) channel activity is regulated by changes in phosphatidyl inositol 4,5-bisphosphate. *Circ Res* 89:1168-1176.

- Bond CT, Pessia M, Xia XM, Lagrutta A, Kavanaugh MP, Adelman JP (1994) Cloning and expression of a family of inward rectifier potassium channels. *Receptors Channels* 2:183-191.
- Botelho RJ, Teruel M, Dierckman R, Anderson R, Wells A, York JD, Meyer T, Grinstein S (2000) Localized biphasic changes in phosphatidylinositol-4,5-bisphosphate at sites of phagocytosis. *J Cell Biol* 151:1353-1368.
- Bradley KK, Jaggar JH, Bonev AD, Heppner TJ, Flynn ER, Nelson MT, Horowitz B (1999) Kir2.1 encodes the inward rectifier potassium channel in rat arterial smooth muscle cells. *J Physiol* 515 (Pt 3):639-651.
- Brown DA, London E (2000) Structure and function of sphingolipid- and cholesterol-rich membrane rafts. *J Biol Chem* 275:17221-17224.
- Carney DH, Scott DL, Gordon EA, LaBelle EF (1985) Phosphoinositides in mitogenesis: neomycin inhibits thrombin-stimulated phosphoinositide turnover and initiation of cell proliferation. *Cell* 42:479-488.
- Carr DB, Surmeier DJ (2007) M1 muscarinic receptor modulation of Kir2 channels enhances temporal summation of excitatory synaptic potentials in prefrontal cortex pyramidal neurons. *J Neurophysiol* 97:3432-3438.
- Catimel B, Schieber C, Condrón M, Patsiouras H, Connolly L, Catimel J, Nice EC, Burgess AW, Holmes AB (2008) The PI(3,5)P2 and PI(4,5)P2 Interactomes. *J Proteome Res*.
- Cho H, Lee D, Lee SH, Ho WK (2005) Receptor-induced depletion of phosphatidylinositol 4,5-bisphosphate inhibits inwardly rectifying K⁺ channels in a receptor-specific manner. *Proc Natl Acad Sci U S A* 102:4643-4648.
- Chuang H, Jan YN, Jan LY (1997) Regulation of IRK3 inward rectifier K⁺ channel by m1 acetylcholine receptor and intracellular magnesium. *Cell* 89:1121-1132.
- Coburn RF (2009) Polyamine effects on cell function: Possible central role of plasma membrane PI(4,5)P2. *J Cell Physiol* 221:544-551.
- Collins A, Somlyo AV, Hilgemann DW (1992) The giant cardiac membrane patch method: stimulation of outward Na⁽⁺⁾-Ca²⁺ exchange current by MgATP. *J Physiol* 454:27-57.
- Cooper EC, Aldape KD, Abosch A, Barbaro NM, Berger MS, Peacock WS, Jan YN, Jan LY (2000) Colocalization and coassembly of two human brain M-type potassium channel subunits that are mutated in epilepsy. *Proc Natl Acad Sci U S A* 97:4914-4919.
- Coulter KL, Perier F, Radeke CM, Vandenberg CA (1995) Identification and molecular localization of a pH-sensing domain for the inward rectifier potassium channel HIR. *Neuron* 15:1157-1168.

- Cukras CA, Jeliaskova I, Nichols CG (2002) The role of NH₂-terminal positive charges in the activity of inward rectifier KATP channels. *J Gen Physiol* 120:437-446.
- Czech MP (2003) Dynamics of phosphoinositides in membrane retrieval and insertion. *Annu Rev Physiol* 65:791-815.
- D'Avanzo N, Cheng WW, Doyle DA, Nichols CG (2010) Direct and specific activation Of human inward rectifier K⁺ channels by membrane phosphatidylinositol 4,5-bisphosphate. *J Biol Chem*.
- Dahlmann A, Li M, Gao Z, McGarrigle D, Sackin H, Palmer LG (2004) Regulation of Kir channels by intracellular pH and extracellular K⁽⁺⁾: mechanisms of coupling. *J Gen Physiol* 123:441-454.
- Damen JE, Liu L, Rosten P, Humphries RK, Jefferson AB, Majerus PW, Krystal G (1996) The 145-kDa protein induced to associate with Shc by multiple cytokines is an inositol tetrakisphosphate and phosphatidylinositol 3,4,5-triphosphate 5-phosphatase. *Proc Natl Acad Sci U S A* 93:1689-1693.
- Dascal N (1997) Signalling via the G protein-activated K⁺ channels. *Cell Signal* 9:551-573.
- Dascal N (2001) Ion-channel regulation by G proteins. *Trends Endocrinol Metab* 12:391-398.
- Davies A, Douglas L, Hendrich J, Wratten J, Tran Van Minh A, Foucault I, Koch D, Pratt WS, Saibil HR, Dolphin AC (2006) The calcium channel α 2delta-2 subunit partitions with CaV2.1 into lipid rafts in cerebellum: implications for localization and function. *J Neurosci* 26:8748-8757.
- Di Paolo G, De Camilli P (2006) Phosphoinositides in cell regulation and membrane dynamics. *Nature* 443:651-657.
- Di Paolo G, Moskowitz HS, Gipson K, Wenk MR, Voronov S, Obayashi M, Flavell R, Fitzsimonds RM, Ryan TA, De Camilli P (2004) Impaired PtdIns(4,5)P₂ synthesis in nerve terminals produces defects in synaptic vesicle trafficking. *Nature* 431:415-422.
- Doi T, Fakler B, Schultz JH, Schulte U, Brandle U, Weidemann S, Zenner HP, Lang F, Ruppersberg JP (1996) Extracellular K⁺ and intracellular pH allosterically regulate renal Kir1.1 channels. *J Biol Chem* 271:17261-17266.
- Doring F, Derst C, Wischmeyer E, Karschin C, Schneggenburger R, Daut J, Karschin A (1998) The epithelial inward rectifier channel Kir7.1 displays unusual K⁺ permeation properties. *J Neurosci* 18:8625-8636.
- Drain P, Li L, Wang J (1998) KATP channel inhibition by ATP requires distinct functional domains of the cytoplasmic C terminus of the pore-forming subunit. *Proc Natl Acad Sci U S A* 95:13953-13958.

- Du X, Zhang H, Lopes C, Mirshahi T, Rohacs T, Logothetis DE (2004) Characteristic interactions with phosphatidylinositol 4,5-bisphosphate determine regulation of Kir channels by diverse modulators. *J Biol Chem* 279:37271-37281.
- Enkvetchakul D, Nichols CG (2003) Gating mechanism of KATP channels: function fits form. *J Gen Physiol* 122:471-480.
- Estacion M, Sinkins WG, Schilling WP (2001) Regulation of *Drosophila* transient receptor potential-like (TrpL) channels by phospholipase C-dependent mechanisms. *J Physiol* 530:1-19.
- Falkenburger BH, Jensen JB, Hille B (2010) Kinetics of PIP₂ metabolism and KCNQ2/3 channel regulation studied with a voltage-sensitive phosphatase in living cells. *J Gen Physiol* 135:99-114.
- Fan Z, Makielski JC (1997) Anionic phospholipids activate ATP-sensitive potassium channels. *J Biol Chem* 272:5388-5395.
- Finley M, Arrabit C, Fowler C, Suen KF, Slesinger PA (2004) betaL-betaM loop in the C-terminal domain of G protein-activated inwardly rectifying K(+) channels is important for G(beta gamma) subunit activation. *J Physiol* 555:643-657.
- Franke TF, Kaplan DR, Cantley LC, Toker A (1997) Direct regulation of the Akt proto-oncogene product by phosphatidylinositol-3,4-bisphosphate. *Science* 275:665-668.
- Frech M, Andjelkovic M, Ingley E, Reddy KK, Falck JR, Hemmings BA (1997) High affinity binding of inositol phosphates and phosphoinositides to the pleckstrin homology domain of RAC/protein kinase B and their influence on kinase activity. *J Biol Chem* 272:8474-8481.
- Gamper N, Shapiro MS (2007) Regulation of ion transport proteins by membrane phosphoinositides. *Nat Rev Neurosci* 8:921-934.
- Golub T, Caroni P (2005) PI(4,5)P₂-dependent microdomain assemblies capture microtubules to promote and control leading edge motility. *J Cell Biol* 169:151-165.
- Halaszovich CR, Schreiber DN, Oliver D (2008) Ci-VSP is a depolarization-activated PI(4,5)P₂ and PI(3,4,5)P₃ 5'-phosphatase. *J Biol Chem*.
- Halstead JR, Jalink K, Divecha N (2005) An emerging role for PtdIns(4,5)P₂-mediated signalling in human disease. *Trends Pharmacol Sci* 26:654-660.
- Hamill OP, Marty A, Neher E, Sakmann B, Sigworth FJ (1981) Improved patch-clamp techniques for high-resolution current recording from cells and cell-free membrane patches. *Pflugers Arch* 391:85-100.
- Haucke V (2005) Phosphoinositide regulation of clathrin-mediated endocytosis. *Biochem Soc Trans* 33:1285-1289.

- Haugh JM, Codazzi F, Teruel M, Meyer T (2000) Spatial sensing in fibroblasts mediated by 3' phosphoinositides. *J Cell Biol* 151:1269-1280.
- He Z, Feng S, Tong Q, Hilgemann DW, Philipson KD (2000) Interaction of PIP(2) with the XIP region of the cardiac Na/Ca exchanger. *Am J Physiol Cell Physiol* 278:C661-666.
- Hernandez CC, Zaika O, Shapiro MS (2008) A carboxy-terminal inter-helix linker as the site of phosphatidylinositol 4,5-bisphosphate action on Kv7 (M-type) K⁺ channels. *J Gen Physiol* 132:361-381.
- Hibino H, Inanobe A, Furutani K, Murakami S, Findlay I, Kurachi Y (2010) Inwardly rectifying potassium channels: their structure, function, and physiological roles. *Physiol Rev* 90:291-366.
- Hilgemann DW, Feng S, Nasuhoglu C (2001) The complex and intriguing lives of PIP2 with ion channels and transporters. *Sci STKE* 2001:RE19.
- Hirose K, Kadowaki S, Tanabe M, Takeshima H, Iino M (1999) Spatiotemporal dynamics of inositol 1,4,5-trisphosphate that underlies complex Ca²⁺ mobilization patterns. *Science* 284:1527-1530.
- Ho IH, Murrell-Lagnado RD (1999) Molecular mechanism for sodium-dependent activation of G protein-gated K⁺ channels. *J Physiol* 520 Pt 3:645-651.
- Ho K, Nichols CG, Lederer WJ, Lytton J, Vassilev PM, Kanazirska MV, Hebert SC (1993) Cloning and expression of an inwardly rectifying ATP-regulated potassium channel. *Nature* 362:31-38.
- Hokin LE (1985) Receptors and phosphoinositide-generated second messengers. *Annu Rev Biochem* 54:205-235.
- Hossain MI, Iwasaki H, Okochi Y, Chahine M, Higashijima S, Nagayama K, Okamura Y (2008) Enzyme domain affects the movement of the voltage sensor in ascidian and zebrafish VSPs. *J Biol Chem*.
- Huang CL, Feng S, Hilgemann DW (1998) Direct activation of inward rectifier potassium channels by PIP2 and its stabilization by Gbetagamma. *Nature* 391:803-806.
- Hughes BA, Swaminathan A (2008) Modulation of the Kir7.1 potassium channel by extracellular and intracellular pH. *Am J Physiol Cell Physiol* 294:C423-431.
- Ivanina T, Varon D, Peleg S, Rishal I, Porozov Y, Dessauer CW, Keren-Raifman T, Dascal N (2004) Galphai1 and Galphai3 differentially interact with, and regulate, the G protein-activated K⁺ channel. *J Biol Chem* 279:17260-17268.
- Iwasaki H, Murata Y, Kim Y, Hossain MI, Worby CA, Dixon JE, McCormack T, Sasaki T, Okamura Y (2008) A voltage-sensing phosphatase, Ci-VSP, which shares sequence identity with PTEN, dephosphorylates phosphatidylinositol 4,5-bisphosphate. *Proc Natl Acad Sci U S A* 105:7970-7975.

- Jin W, Lu Z (1998) A novel high-affinity inhibitor for inward-rectifier K⁺ channels. *Biochemistry* 37:13291-13299.
- Johnson CM, Chichili GR, Rodgers W (2008a) Compartmentalization of phosphatidylinositol 4,5-bisphosphate (PIP₂) signaling evidenced using targeted phosphatases. *J Biol Chem*.
- Johnson CM, Chichili GR, Rodgers W (2008b) Compartmentalization of phosphatidylinositol 4,5-bisphosphate signaling evidenced using targeted phosphatases. *J Biol Chem* 283:29920-29928.
- Jones S, Brown DA, Milligan G, Willer E, Buckley NJ, Caulfield MP (1995) Bradykinin excites rat sympathetic neurons by inhibition of M current through a mechanism involving B₂ receptors and G_{αq/11}. *Neuron* 14:399-405.
- Jones SV (1996) Modulation of the inwardly rectifying potassium channel IRK1 by the m₁ muscarinic receptor. *Mol Pharmacol* 49:662-667.
- Kimber WA, Trinkle-Mulcahy L, Cheung PC, Deak M, Marsden LJ, Kieloch A, Watt S, Javier RT, Gray A, Downes CP, Lucocq JM, Alessi DR (2002) Evidence that the tandem-pleckstrin-homology-domain-containing protein TAPP1 interacts with Ptd(3,4)P₂ and the multi-PDZ-domain-containing protein MUPP1 in vivo. *Biochem J* 361:525-536.
- Kobrinsky E, Mirshahi T, Zhang H, Jin T, Logothetis DE (2000) Receptor-mediated hydrolysis of plasma membrane messenger PIP₂ leads to K⁺-current desensitization. *Nat Cell Biol* 2:507-514.
- Kubisch C, Schroeder BC, Friedrich T, Lutjohann B, El-Amraoui A, Marlin S, Petit C, Jentsch TJ (1999) KCNQ4, a novel potassium channel expressed in sensory outer hair cells, is mutated in dominant deafness. *Cell* 96:437-446.
- Kubista H, Kosenburger K, Mahlknecht P, Drobny H, Boehm S (2009) Inhibition of transmitter release from rat sympathetic neurons via presynaptic M(1) muscarinic acetylcholine receptors. *Br J Pharmacol* 156:1342-1352.
- Kubo Y, Baldwin TJ, Jan YN, Jan LY (1993) Primary structure and functional expression of a mouse inward rectifier potassium channel. *Nature* 362:127-133.
- Lam HD, Lemay AM, Briggs MM, Yung M, Hill CE (2006) Modulation of Kir4.2 rectification properties and pH_i-sensitive run-down by association with Kir5.1. *Biochim Biophys Acta* 1758:1837-1845.
- Lassing I, Lindberg U (1990) Polyphosphoinositide synthesis in platelets stimulated with low concentrations of thrombin is enhanced before the activation of phospholipase C. *FEBS Lett* 262:231-233.

- Lee SS, Glaunsinger B, Mantovani F, Banks L, Javier RT (2000) Multi-PDZ domain protein MUPP1 is a cellular target for both adenovirus E4-ORF1 and high-risk papillomavirus type 18 E6 oncoproteins. *J Virol* 74:9680-9693.
- Lemmon MA (2003) Phosphoinositide recognition domains. *Traffic* 4:201-213.
- Li Y, Gamper N, Hilgemann DW, Shapiro MS (2005) Regulation of Kv7 (KCNQ) K⁺ channel open probability by phosphatidylinositol 4,5-bisphosphate. *J Neurosci* 25:9825-9835.
- Li Y, Gamper N, Shapiro MS (2004) Single-channel analysis of KCNQ K⁺ channels reveals the mechanism of augmentation by a cysteine-modifying reagent. *J Neurosci* 24:5079-5090.
- Light PE, Bladen C, Winkfein RJ, Walsh MP, French RJ (2000) Molecular basis of protein kinase C-induced activation of ATP-sensitive potassium channels. *Proc Natl Acad Sci U S A* 97:9058-9063.
- Lin D, Sterling H, Lerea KM, Giebisch G, Wang WH (2002) Protein kinase C (PKC)-induced phosphorylation of ROMK1 is essential for the surface expression of ROMK1 channels. *J Biol Chem* 277:44278-44284.
- Lin YW, MacMullen C, Ganguly A, Stanley CA, Shyng SL (2006) A novel KCNJ11 mutation associated with congenital hyperinsulinism reduces the intrinsic open probability of beta-cell ATP-sensitive potassium channels. *J Biol Chem* 281:3006-3012.
- Liou HH, Zhou SS, Huang CL (1999) Regulation of ROMK1 channel by protein kinase A via a phosphatidylinositol 4,5-bisphosphate-dependent mechanism. *Proc Natl Acad Sci U S A* 96:5820-5825.
- Logothetis DE, Jin T, Lupyán D, Rosenhouse-Dantsker A (2007a) Phosphoinositide-mediated gating of inwardly rectifying K(+) channels. *Pflugers Arch* 455:83-95.
- Logothetis DE, Lupyán D, Rosenhouse-Dantsker A (2007b) Diverse Kir modulators act in close proximity to residues implicated in phosphoinositide binding. *J Physiol* 582:953-965.
- Lopatin AN, Makhina EN, Nichols CG (1994) Potassium channel block by cytoplasmic polyamines as the mechanism of intrinsic rectification. *Nature* 372:366-369.
- Lopatin AN, Nichols CG (2001) Inward rectifiers in the heart: an update on I(K1). *J Mol Cell Cardiol* 33:625-638.
- Lopes CM, Rohacs T, Czirjak G, Balla T, Enyedi P, Logothetis DE (2005) PIP2 hydrolysis underlies agonist-induced inhibition and regulates voltage gating of two-pore domain K⁺ channels. *J Physiol* 564:117-129.

- Lopes CM, Zhang H, Rohacs T, Jin T, Yang J, Logothetis DE (2002) Alterations in conserved Kir channel-PIP2 interactions underlie channelopathies. *Neuron* 34:933-944.
- Loussouarn G, Makhina EN, Rose T, Nichols CG (2000) Structure and dynamics of the pore of inwardly rectifying K(ATP) channels. *J Biol Chem* 275:1137-1144.
- Mao J, Wu J, Chen F, Wang X, Jiang C (2003) Inhibition of G-protein-coupled inward rectifying K⁺ channels by intracellular acidosis. *J Biol Chem* 278:7091-7098.
- Martens JR, Navarro-Polanco R, Coppock EA, Nishiyama A, Parshley L, Grobaski TD, Tamkun MM (2000) Differential targeting of Shaker-like potassium channels to lipid rafts. *J Biol Chem* 275:7443-7446.
- Martens JR, Sakamoto N, Sullivan SA, Grobaski TD, Tamkun MM (2001) Isoform-specific localization of voltage-gated K⁺ channels to distinct lipid raft populations. Targeting of Kv1.5 to caveolae. *J Biol Chem* 276:8409-8414.
- Matavel A, Medei E, Lopes CM (2010) PKA and PKC partially rescue long QT type 1 phenotype by restoring channel-PIP2 interactions. *Channels (Austin)* 4:3-11.
- Mathie A (2007) Neuronal two-pore-domain potassium channels and their regulation by G protein-coupled receptors. *J Physiol* 578:377-385.
- McLaughlin S, Wang J, Gambhir A, Murray D (2002) PIP(2) and proteins: interactions, organization, and information flow. *Annu Rev Biophys Biomol Struct* 31:151-175.
- McNicholas CM, Wang W, Ho K, Hebert SC, Giebisch G (1994) Regulation of ROMK1 K⁺ channel activity involves phosphorylation processes. *Proc Natl Acad Sci U S A* 91:8077-8081.
- Milosevic I, Sorensen JB, Lang T, Krauss M, Nagy G, Haucke V, Jahn R, Neher E (2005) Plasmalemmal phosphatidylinositol-4,5-bisphosphate level regulates the releasable vesicle pool size in chromaffin cells. *J Neurosci* 25:2557-2565.
- Murata Y, Iwasaki H, Sasaki M, Inaba K, Okamura Y (2005) Phosphoinositide phosphatase activity coupled to an intrinsic voltage sensor. *Nature* 435:1239-1243.
- Murata Y, Okamura Y (2007) Depolarization activates the phosphoinositide phosphatase Ci-VSP, as detected in *Xenopus* oocytes coexpressing sensors of PIP2. *J Physiol* 583:875-889.
- Nelson CP, Nahorski SR, Challiss RA (2008) Temporal profiling of changes in phosphatidylinositol 4,5-bisphosphate, inositol 1,4,5-trisphosphate and diacylglycerol allows comprehensive analysis of phospholipase C-initiated signalling in single neurons. *J Neurochem* 107:602-615.
- Odorizzi G, Babst M, Emr SD (2000) Phosphoinositide signaling and the regulation of membrane trafficking in yeast. *Trends Biochem Sci* 25:229-235.

- Oldfield S, Hancock J, Mason A, Hobson SA, Wynick D, Kelly E, Randall AD, Marrion NV (2009) Receptor-mediated suppression of potassium currents requires colocalization within lipid rafts. *Mol Pharmacol* 76:1279-1289.
- Pegan S, Arrabit C, Zhou W, Kwiatkowski W, Collins A, Slesinger PA, Choe S (2005) Cytoplasmic domain structures of Kir2.1 and Kir3.1 show sites for modulating gating and rectification. *Nat Neurosci* 8:279-287.
- Pfaffinger PJ, Martin JM, Hunter DD, Nathanson NM, Hille B (1985) GTP-binding proteins couple cardiac muscarinic receptors to a K channel. *Nature* 317:536-538.
- Pizarro-Cerda J, Cossart P (2004) Subversion of phosphoinositide metabolism by intracellular bacterial pathogens. *Nat Cell Biol* 6:1026-1033.
- Proks P, Gribble FM, Adhikari R, Tucker SJ, Ashcroft FM (1999) Involvement of the N-terminus of Kir6.2 in the inhibition of the KATP channel by ATP. *J Physiol* 514 (Pt 1):19-25.
- Quinn KV, Behe P, Tinker A (2008) Monitoring changes in membrane phosphatidylinositol 4,5-bisphosphate in living cells using a domain from the transcription factor tubby. *J Physiol* 586:2855-2871.
- Rajala RV, Anderson RE (2003) Light regulation of the insulin receptor in the retina. *Mol Neurobiol* 28:123-138.
- Rapedius M, Fowler PW, Shang L, Sansom MS, Tucker SJ, Baukrowitz T (2007a) H bonding at the helix-bundle crossing controls gating in Kir potassium channels. *Neuron* 55:602-614.
- Rapedius M, Haider S, Browne KF, Shang L, Sansom MS, Baukrowitz T, Tucker SJ (2006) Structural and functional analysis of the putative pH sensor in the Kir1.1 (ROMK) potassium channel. *EMBO Rep* 7:611-616.
- Rapedius M, Paynter JJ, Fowler PW, Shang L, Sansom MS, Tucker SJ, Baukrowitz T (2007b) Control of pH and PIP2 gating in heteromeric Kir4.1/Kir5.1 channels by H-Bonding at the helix-bundle crossing. *Channels (Austin)* 1:327-330.
- Rasgado-Flores H, Gonzalez-Serratos H (2000) Plasmalemmal transport of magnesium in excitable cells. *Front Biosci* 5:D866-879.
- Rohacs T, Chen J, Prestwich GD, Logothetis DE (1999) Distinct specificities of inwardly rectifying K(+) channels for phosphoinositides. *J Biol Chem* 274:36065-36072.
- Rohacs T, Lopes CM, Jin T, Ramdya PP, Molnar Z, Logothetis DE (2003) Specificity of activation by phosphoinositides determines lipid regulation of Kir channels. *Proc Natl Acad Sci U S A* 100:745-750.

- Rosenhouse-Dantsker A, Sui JL, Zhao Q, Rusinova R, Rodriguez-Menchaca AA, Zhang Z, Logothetis DE (2008) A sodium-mediated structural switch that controls the sensitivity of Kir channels to PtdIns(4,5)P(2). *Nat Chem Biol* 4:624-631.
- Rozelle AL, Machesky LM, Yamamoto M, Driessens MH, Insall RH, Roth MG, Luby-Phelps K, Marriott G, Hall A, Yin HL (2000) Phosphatidylinositol 4,5-bisphosphate induces actin-based movement of raft-enriched vesicles through WASP-Arp2/3. *Curr Biol* 10:311-320.
- Rubinstein M, Peleg S, Berlin S, Brass D, Keren-Raifman T, Dessauer CW, Ivanina T, Dascal N (2009) Divergent regulation of GIRK1 and GIRK2 subunits of the neuronal G protein gated K⁺ channel by GalphaiGDP and Gbetagamma. *J Physiol* 587:3473-3491.
- Santagata S, Boggon TJ, Baird CL, Gomez CA, Zhao J, Shan WS, Myszka DG, Shapiro L (2001) G-protein signaling through tubby proteins. *Science* 292:2041-2050.
- Schulte U, Hahn H, Konrad M, Jeck N, Derst C, Wild K, Weidemann S, Ruppertsberg JP, Fakler B, Ludwig J (1999) pH gating of ROMK (K(ir)1.1) channels: control by an Arg-Lys-Arg triad disrupted in antenatal Bartter syndrome. *Proc Natl Acad Sci U S A* 96:15298-15303.
- Schulte U, Weidemann S, Ludwig J, Ruppertsberg J, Fakler B (2001) K(+)-dependent gating of K(ir)1.1 channels is linked to pH gating through a conformational change in the pore. *J Physiol* 534:49-58.
- Schulze D, Krauter T, Fritzenschaft H, Soom M, Baukowitz T (2003) Phosphatidylinositol 4,5-bisphosphate (PIP₂) modulation of ATP and pH sensitivity in Kir channels. A tale of an active and a silent PIP₂ site in the N terminus. *J Biol Chem* 278:10500-10505.
- Selyanko AA, Hadley JK, Wood IC, Abogadie FC, Jentsch TJ, Brown DA (2000) Inhibition of KCNQ1-4 potassium channels expressed in mammalian cells via M1 muscarinic acetylcholine receptors. *J Physiol* 522 Pt 3:349-355.
- Shapiro MS, Roche JP, Kaftan EJ, Cruzblanca H, Mackie K, Hille B (2000) Reconstitution of muscarinic modulation of the KCNQ2/KCNQ3 K(+) channels that underlie the neuronal M current. *J Neurosci* 20:1710-1721.
- Shen W, Tian X, Day M, Ulrich S, Tkatch T, Nathanson NM, Surmeier DJ (2007) Cholinergic modulation of Kir2 channels selectively elevates dendritic excitability in striatopallidal neurons. *Nat Neurosci* 10:1458-1466.
- Shyng S, Nichols CG (1997) Octameric stoichiometry of the KATP channel complex. *J Gen Physiol* 110:655-664.
- Shyng SL, Cukras CA, Harwood J, Nichols CG (2000) Structural determinants of PIP₂ regulation of inward rectifier K(ATP) channels. *J Gen Physiol* 116:599-608.

- Shyng SL, Nichols CG (1998) Membrane phospholipid control of nucleotide sensitivity of KATP channels. *Science* 282:1138-1141.
- Soom M, Schonherr R, Kubo Y, Kirsch C, Klinger R, Heinemann SH (2001) Multiple PIP2 binding sites in Kir2.1 inwardly rectifying potassium channels. *FEBS Lett* 490:49-53.
- Stauffer TP, Ahn S, Meyer T (1998) Receptor-induced transient reduction in plasma membrane PtdIns(4,5)P2 concentration monitored in living cells. *Curr Biol* 8:343-346.
- Stoffel M, Tokuyama Y, Trabb JB, German MS, Tsarr ML, Jan LY, Polonsky KS, Bell GI (1995) Cloning of rat KATP-2 channel and decreased expression in pancreatic islets of male Zucker diabetic fatty rats. *Biochem Biophys Res Commun* 212:894-899.
- Suh BC, Hille B (2002) Recovery from muscarinic modulation of M current channels requires phosphatidylinositol 4,5-bisphosphate synthesis. *Neuron* 35:507-520.
- Suh BC, Inoue T, Meyer T, Hille B (2006) Rapid chemically induced changes of PtdIns(4,5)P2 gate KCNQ ion channels. *Science* 314:1454-1457.
- Suh BC, Leal K, Hille B (2010) Modulation of high-voltage activated Ca(2+) channels by membrane phosphatidylinositol 4,5-bisphosphate. *Neuron* 67:224-238.
- Szentpetery Z, Balla A, Kim YJ, Lemmon MA, Balla T (2009) Live cell imaging with protein domains capable of recognizing phosphatidylinositol 4,5-bisphosphate; a comparative study. *BMC Cell Biol* 10:67.
- Tanemoto M, Kittaka N, Inanobe A, Kurachi Y (2000) In vivo formation of a proton-sensitive K⁺ channel by heteromeric subunit assembly of Kir5.1 with Kir4.1. *J Physiol* 525 Pt 3:587-592.
- Terebiznik MR, Vieira OV, Marcus SL, Slade A, Yip CM, Trimble WS, Meyer T, Finlay BB, Grinstein S (2002) Elimination of host cell PtdIns(4,5)P(2) by bacterial SigD promotes membrane fission during invasion by Salmonella. *Nat Cell Biol* 4:766-773.
- Thomas AM, Brown SG, Leaney JL, Tinker A (2006) Differential phosphoinositide binding to components of the G protein-gated K⁺ channel. *J Membr Biol* 211:43-53.
- Toker A (2002) Phosphoinositides and signal transduction. *Cell Mol Life Sci* 59:761-779.
- Trapp S, Haider S, Jones P, Sansom MS, Ashcroft FM (2003) Identification of residues contributing to the ATP binding site of Kir6.2. *Embo J* 22:2903-2912.

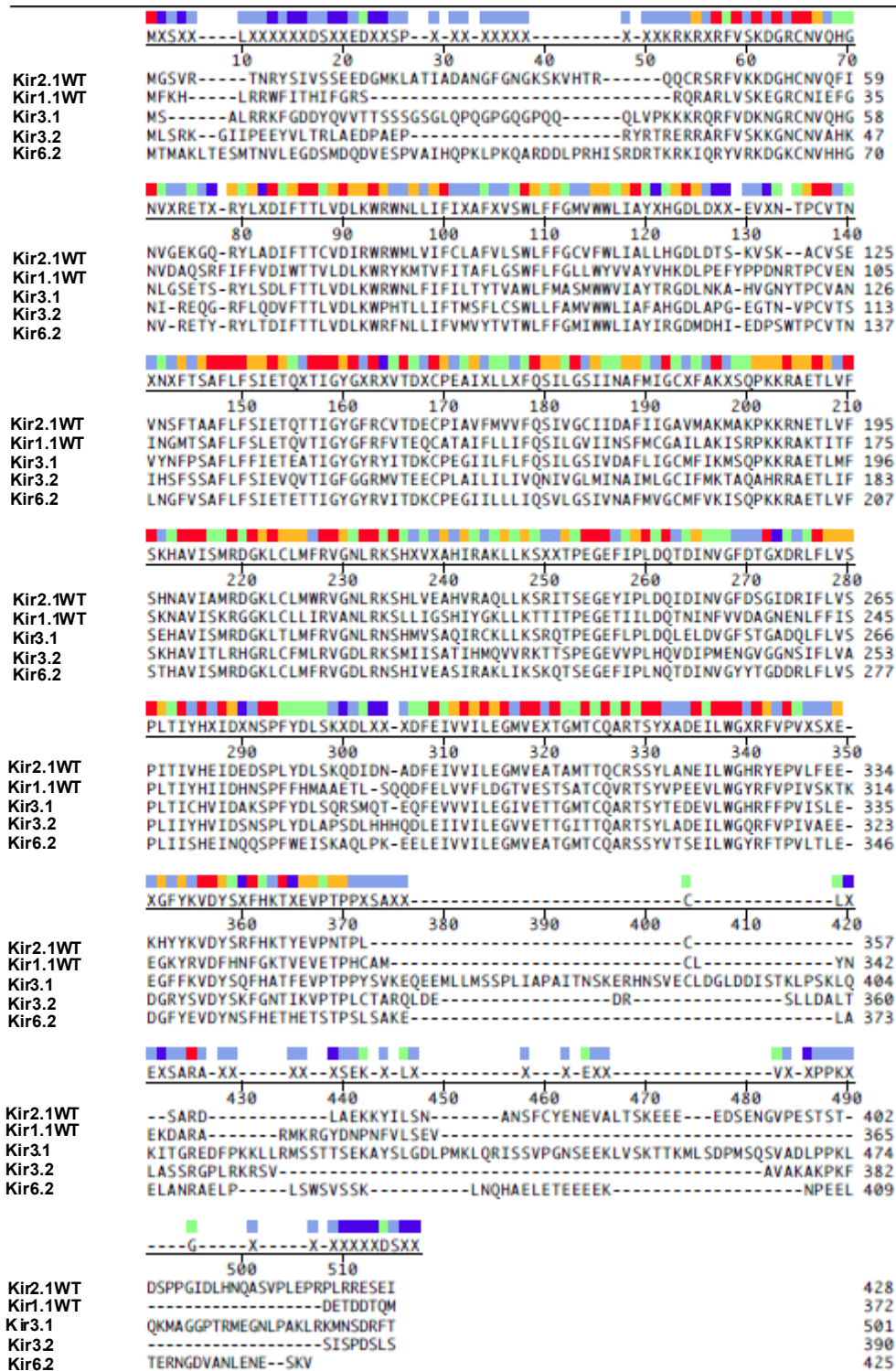
- Trapp S, Proks P, Tucker SJ, Ashcroft FM (1998) Molecular analysis of ATP-sensitive K channel gating and implications for channel inhibition by ATP. *J Gen Physiol* 112:333-349.
- Traynor-Kaplan AE, Thompson BL, Harris AL, Taylor P, Omann GM, Sklar LA (1989) Transient increase in phosphatidylinositol 3,4-bisphosphate and phosphatidylinositol trisphosphate during activation of human neutrophils. *J Biol Chem* 264:15668-15673.
- Tucker SJ, Baukowitz T (2008) How highly charged anionic lipids bind and regulate ion channels. *J Gen Physiol* 131:431-438.
- Tucker SJ, Gribble FM, Proks P, Trapp S, Ryder TJ, Haug T, Reimann F, Ashcroft FM (1998) Molecular determinants of KATP channel inhibition by ATP. *Embo J* 17:3290-3296.
- Tung RT, Kurachi Y (1991) On the mechanism of nucleotide diphosphate activation of the ATP-sensitive K⁺ channel in ventricular cell of guinea-pig. *J Physiol* 437:239-256.
- Ueda K, Inagaki N, Seino S (1997) MgADP antagonism to Mg²⁺-independent ATP binding of the sulfonylurea receptor SUR1. *J Biol Chem* 272:22983-22986.
- Vanhaesebroeck B, Leever SJ, Ahmadi K, Timms J, Katso R, Driscoll PC, Woscholski R, Parker PJ, Waterfield MD (2001) Synthesis and function of 3-phosphorylated inositol lipids. *Annu Rev Biochem* 70:535-602.
- Varnai P, Balla T (2006) Live cell imaging of phosphoinositide dynamics with fluorescent protein domains. *Biochim Biophys Acta* 1761:957-967.
- Varnai P, Thyagarajan B, Rohacs T, Balla T (2006) Rapidly inducible changes in phosphatidylinositol 4,5-bisphosphate levels influence multiple regulatory functions of the lipid in intact living cells. *J Cell Biol* 175:377-382.
- Vasudevan L, Jeromin A, Volpicelli-Daley L, De Camilli P, Holowka D, Baird B (2009) The beta- and gamma-isoforms of type I PIP5K regulate distinct stages of Ca²⁺ signaling in mast cells. *J Cell Sci* 122:2567-2574.
- Venkateswarlu K, Oatey PB, Tavaré JM, Cullen PJ (1998) Insulin-dependent translocation of ARNO to the plasma membrane of adipocytes requires phosphatidylinositol 3-kinase. *Curr Biol* 8:463-466.
- Wang F, Herzmark P, Weiner OD, Srinivasan S, Servant G, Bourne HR (2002) Lipid products of PI(3)Ks maintain persistent cell polarity and directed motility in neutrophils. *Nat Cell Biol* 4:513-518.
- Wang HS, Pan Z, Shi W, Brown BS, Wymore RS, Cohen IS, Dixon JE, McKinnon D (1998) KCNQ2 and KCNQ3 potassium channel subunits: molecular correlates of the M-channel. *Science* 282:1890-1893.

- Winks JS, Hughes S, Filippov AK, Tatulian L, Abogadie FC, Brown DA, Marsh SJ (2005) Relationship between membrane phosphatidylinositol-4,5-bisphosphate and receptor-mediated inhibition of native neuronal M channels. *J Neurosci* 25:3400-3413.
- Xie LH, John SA, Ribalet B, Weiss JN (2005) Long polyamines act as cofactors in PIP2 activation of inward rectifier potassium (Kir2.1) channels. *J Gen Physiol* 126:541-549.
- Xu C, Watras J, Loew LM (2003) Kinetic analysis of receptor-activated phosphoinositide turnover. *J Cell Biol* 161:779-791.
- Xu ZC, Yang Y, Hebert SC (1996) Phosphorylation of the ATP-sensitive, inwardly rectifying K⁺ channel, ROMK, by cyclic AMP-dependent protein kinase. *J Biol Chem* 271:9313-9319.
- Yamada M, Kurachi Y (2004) The nucleotide-binding domains of sulfonylurea receptor 2A and 2B play different functional roles in nicorandil-induced activation of ATP-sensitive K⁺ channels. *Mol Pharmacol* 65:1198-1207.
- Yang WP, Levesque PC, Little WA, Conder ML, Ramakrishnan P, Neubauer MG, Blonar MA (1998) Functional expression of two KvLQT1-related potassium channels responsible for an inherited idiopathic epilepsy. *J Biol Chem* 273:19419-19423.
- Yorek MA, Dunlap JA, Stefani MR, Davidson EP, Zhu X, Eichberg J (1994) Decreased myo-inositol uptake is associated with reduced bradykinin-stimulated phosphatidylinositol synthesis and diacylglycerol content in cultured neuroblastoma cells exposed to L-fucose. *J Neurochem* 62:147-158.
- Zeng WZ, Liou HH, Krishna UM, Falck JR, Huang CL (2002) Structural determinants and specificities for ROMK1-phosphoinositide interaction. *Am J Physiol Renal Physiol* 282:F826-834.
- Zhang H, Craciun LC, Mirshahi T, Rohacs T, Lopes CM, Jin T, Logothetis DE (2003) PIP(2) activates KCNQ channels, and its hydrolysis underlies receptor-mediated inhibition of M currents. *Neuron* 37:963-975.
- Zhang H, He C, Yan X, Mirshahi T, Logothetis DE (1999) Activation of inwardly rectifying K⁺ channels by distinct PtdIns(4,5)P₂ interactions. *Nat Cell Biol* 1:183-188.
- Zhu G, Qu Z, Cui N, Jiang C (1999) Suppression of Kir2.3 activity by protein kinase C phosphorylation of the channel protein at threonine 53. *J Biol Chem* 274:11643-11646.
- Zolles G, Klocker N, Wenzel D, Weisser-Thomas J, Fleischmann BK, Roeper J, Fakler B (2006) Pacemaking by HCN channels requires interaction with phosphoinositides. *Neuron* 52:1027-1036.

<http://en.wikipedia.org/wiki/PIP2>

7 Attachments

Alignment of the protein sequences of Kir2.1WT (*Mus musculus*), Kir1.1WT (*Rattus norvegicus*), Kir3.1 (*Mus musculus*), Kir3.2 (*Homo sapiens*), and Kir6.2 channels (*Mus musculus*).



Curriculum Vitae

Alexandra Rjasanow



Persönliche Daten

Private Adresse: Weddigenstraße 10
79100 Freiburg
Deutschland
Tel: 0761-5902795
Mobil: 0176-24202760
E-mail: alexandra.rjasanow@physiologie.uni-freiburg.de

Geburtsdatum und -ort: 01.01.1983, Karl-Marx-Stadt (Deutschland)
Staatsangehörigkeit: Deutsch

Ausbildung

09/1989 – 09/1990 Grundschule: Wilhelm-Firl-Oberschule in Karl-Marx-Stadt

10/1990 – 06/1993 Grundschule: Pestalozzischule in Kaiserslautern

07/1993 – 03/2002 Weiterführende Schule: Hohenstaufen-Gymnasium
in Kaiserslautern

10/2003 – 02/2007 Studium der Biologie an der Technischen Universität
Kaiserslautern

Hauptfächer: Tierphysiologie, Molekulare Zellbiologie,
Biophysik

Zertifikate, Diplom

03/2002 Abitur (Kaiserslautern)

02/2007 Diplom in Biology (Kaiserslautern)

Thema: "Elektrophysiologische und pharmakologische Charakterisierung von Neuroblastoma and HEK293 Zellen"

Betreuung durch Prof. Dr. E. Friauf

Seit 03/2007:

Doktorarbeit im Physiologischen Institut II der Albert-Ludwigs-Universität Freiburg

Thema: "Quantifizierung der in-vivo Affinität von PI(4,5)P₂-Effektoren und Sensoren mit Hilfe der Phosphoinositidphosphatase Ci-VSP"

Betreuung durch Prof. Dr. D. Oliver und Prof. Dr. B. Fakler

Qualifikationen

06/1998 – 07/1998

Berufspraktikum im Fachbereichsgarten der TU Kaiserslautern

02/1999 – 12/2001

Wissenschaftliche Hilfskraft am Institut für Biotechnologie und Wirkstoffforschung an der TU Kaiserslautern

04/2005 – 12/2005

Wissenschaftliche Hilfskraft im Fachbereich Tierphysiologie: Pheromone

Unterrichtserfahrung

11/2006 – 12/2006

Unterrichten von Studenten in Forschungspraktika (Patch-Clamp-Technik and Grundlagen der Pharmakologie in akuten Hirnschnitten)

seit 03/2007

Unterrichten der Medizinstudenten im physiologischen Praktikum (Vestibularsystem, Hämostatik und Elektro- und Vektorkardiographie)

Liste der Publikationen

Rjasanow, A., Fakler, B., Oliver, D. (Manuskript in Vorbereitung) Affinity of inward rectifier potassium channels for endogenous phosphoinositides determined with voltage-sensitive phosphatases.

Rjasanow, A., Leitner, M., Ivanova, O., Schreiber, D.N., Halaszovich, C.R., Oliver, D. (Manuskript in Vorbereitung) Quantitative characterization of tubbyC as a genetically encoded optical probe for plasma membrane PIP₂ concentration.

Liste der Vorträge und Poster Präsentationen

03/2008 Deutsche Physiologische Gesellschaft; Congress 2008 in Köln, Deutschland;
Vortrag: "Measuring PI(4,5)P₂ affinity of ion channels with a switchable PI(4,5)P₂ phosphatase"; A Rjasanow, CR Halaszovich, B Fakler, D Oliver

09/2010 International Meeting "Functional compartmentalization of PIP₂-signalling", Günzburg, Deutschland
Poster: "Quantifying PI(4,5)P₂ affinities of ion channels with the phosphoinositide phosphatase Ci-VSP" A Rjasanow, CR Halaszovich, B Fakler, D Oliver

Zusätzliche Kurse

12/2007 – 03/2010 Graduiertenkolleg-Oberseminar: "Mechanisms of Neuronal Signal Transduction"

03/2008 SMP-Kurs des Freiburger Brain Imaging Labs

10/2008 Kurs: „Akademisches Schreiben“ der Internationalen Graduiertenakademie (IGA) der Universität Feiburg

01/2009 Kurs: „Hochschuldidaktische Grundlagen für Doktorandinnen und Doktoranden“ der IGA der Universität Freiburg

Sprachen

Deutsch (Muttersprache)
Englisch (fließend in Wort und Schrift)
Russisch
Französisch
Latein

Stipendien

12/2007 – 03/2010 Stipendium des Graduiertenkollegs: "Mechanisms of Neuronal Signal Transduction" der Universität Freiburg

Verzeichnis der akademischen Lehrer

Meine akademischen Lehrer waren folgende Damen und Herren in Kaiserslautern:

Anke, Blau, Brüne, Büdel, Cullum, Deitmer, Diller, Friauf, Güttinger, Hahn, Hakenbeck, Henrich, Koch, Krüger, Löhrke, Neuhaus, Nothwang, Philipp, Schmidt, Sültemeyer, Trommer, Türk, Zankl, Ziegler, Wirth

Freiburg

Aertsen, Baumeister, Bentrop, Bischofberger, Driever, Fakler, Fischbach, Frotscher, Häusser, Jonas, Klöcker, Meyer, Nikkah, Pedarzani, Schulze-Bonnhage, Weiller

Marburg

Oliver

Danksagung

Mein besonderer Dank gilt Herrn Prof. Dr. Dominik Oliver, Direktor des Instituts für Physiologie und Pathophysiologie der Philipps-Universität Marburg für die Bereitstellung des Forschungsthemas, die Möglichkeit zur Durchführung eines Teils der Experimente in seinem Labor und die wissenschaftlichen Diskussionen, die zum erfolgreichen Abschluss dieser Arbeit geführt haben.

Mein weiterer besonderer Dank gilt Herrn Prof. Dr. Bernd Fakler, Direktor des Physiologischen Instituts II der Albert-Ludwigs-Universität Freiburg für die Bereitstellung des Arbeitsplatzes und aller benötigter Materialien, für die großzügige finanzielle Unterstützung während meiner Forschungsarbeiten in Freiburg und für die vielen Dienstreisen, sowie für die wissenschaftlichen Diskussionen, die zum erfolgreichen Abschluss dieser Arbeit geführt haben.

Danken möchte ich auch den Mitarbeitern Gerd Zolles, Cristina Constantin, Thorsten Schächinger, Michael Leitner und Christian Halaszovich für die vielen wissenschaftlichen Diskussionen sowie die Einarbeitung in die Messgeräte.

Den Technischen Assistentinnen Silke Eble, Maria Oberle, Sandra Urbaniak, Gerlinde Kummer, Monika Mack-Vetter, Olga Ebers und Sigrid Petzold möchte ich herzlich für die technische Unterstützung in der Molekularbiologie, Elektrophysiologie und Zellbiologie danken.

Allen weiteren Mitarbeitern und ins besondere Irene Schaber, Monika Mack-Vetter, Anna Shnyder und Michael Leitner möchte ich für die angenehme Arbeitsatmosphäre und für die Unterstützung beim Gelingen dieser Arbeit danken.

Von ganzem Herzen danke ich meinen Eltern, Geschwistern, meinem Opa, Ruth, meinen Freunden und meinem Freund Marcus Illy, die mir durch ihre intensive seelisch-moralische Unterstützung und Liebe die Kraft für diesen Lebensabschnitt gegeben haben.

Ehrenwörtliche Erklärung

Ich erkläre ehrenwörtlich, dass ich die dem Fachbereich Medizin in Marburg zur Promotionsprüfung eingereichte Arbeit mit dem Titel "Quantification of the in-vivo affinity of PI(4,5)P₂ effectors and sensors with the phosphoinositide phosphatase Ci-VSP" am Institut für Physiologie und Pathophysiologie der Philipps-Universität Marburg und am Physiologischen Institut II der Albert-Ludwigs-Universität Freiburg mit Unterstützung von Herrn Prof. Dr. Dominik Oliver und Herrn Prof. Dr. Bernd Fakler ohne sonstige Hilfe selbst durchgeführt und bei der Abfassung der Arbeit keine anderen als die in der Dissertation aufgeführten Hilfsmittel benutzt habe. Ich habe bisher an keinem in- oder ausländischen Medizinischen Fachbereich ein Gesuch um Zulassung zur Promotion eingereicht, noch die vorliegende Arbeit oder eine andere Arbeit als Dissertation vorgelegt.

Freiburg den,